OXIDATION OF METALS

A thesis in fulfilment of the requirements

of the degree of M.Sc.

by

NAZIHA PROUFF

Faculty of Science

Department of Chemistry

The University of Glasgow

December 1986

I would like to dedicate this work

to my Husband

and my Parents

Acknowledgement

I would like to express my thanks and deep respect to my supervisor, Dr. J.M. Winfield. I should also like to express my gratitude to Professor D.W.A. Sharp, to Dr. G. Webb and Dr. C. Campbell for their helpful discussions.

I am also grateful to my colleagues and the technical staff in the department for their assistance, and to my friends for their kindness and encouragement, in particular, Miss E. Forbes, Mr. A. Refai, Miss A.S. El Mahrezi, Miss A. Yaroub, Mrs. F.Z. Hadji and Miss S.S. Toubar.

Finally, I would like to thank the Algerian Government for the scholarship awarded to me.

CONTENTS

SUMMARY

This thesis is concerned with the study the behaviour of UF_6, MoF_6, WF_6 and NO^+ towards the metals Co, Ni and Zn in CH_3CN medium, and thus give a better insight into the reactivity of these hexafluorides towards first row transition elements.

Solvated Co(II) has been prepared by the oxidation reactions of the metal by MoF_6, WF_6 and NO^+. The solvated salt $[Co(NCMe)_6][PF_6]_2$ is stable in absence of moisture and oxygen and can be stored in an argon-atmosphere glove box. $[Co(NCMe)_6][WF_6]_2$ and $[Co(NCMe)_6][MoF_6]_2$ are very prone to hydrolysis and can be kept in liquid nitrogen for only one or two days. The spectra of the salts are consistent with octahedrally coordinated Co(II). Values of the ligand field splitting parameters (Δ) and electronic repulsion parameter (B') have been calculated and compared with those of some relevant CoL_6^{2+} cations. They were found to fit the theoretical expectations and showed that acetonitrile is a good coordinating agent though not the strongest in the spectrochemical series.

Co(II) can be electrochemically oxidised to Co(III) in cases where the counter anion is PF_6^-. This is not observed when WF_6^- is the counter anion, which is probably due to the oxidation potentials of the Co^{2+}/Co^{3+} and WF_7^-/W^V couples, which occur in the same range, hence the wave assigned to Co^{2+}/Co^{3+} could not be observed.

MoF_6 oxidises cobalt metal to Co(II). Further oxidation, as would be predicted from the electrochemistry of $[Co(NCMe)_6][PF_6]_2$ was

not observed, probably for kinetic reasons. UF_6 did not react with cobalt metal. Polymerisation of acetonitrile and reduction of UF_6 took place instead.

Zinc is not a transition metal but its behaviour towards the hexafluorides of uranium, molybdenum and tungsten, is similar to that of most of the first row transition elements. The metal is oxidized by MoF_6, NO^+ and WF_6 and the salt $[Zn(NCMe)_6][MF_6]_2$ (M=Mo,P,W) is generated in solution. Coordination of acetonitrile and the presence of the anion, MF_6^- (M=Mo,P,W), has been established from the study of its infrared and Raman spectra. UF_6 does not oxidize zinc metal.

Nickel metal is not oxidized by MoF_6 and UF_6 but it is relatively easily oxidized by NO^+ and WF_6 at room temperature.

The solid $[Ni(NCMe)_6][PF_6]_2$ is stable at room temperature but $[Ni(NCMe)_6][WF_6]_2$ hydrolyses easily.

A purple salt, $[Ni(NCMe)_6][WF_6]_2$, is formed when the oxidation of the metal is performed in acetonitrile solution. A fluoride ion transfer occurs in parallel, in which the hexafluorotungstate(V) anion behaves as a fluoride ion donor in acetonitrile. It reacts with WF_6 to give WF_7^- anion as a product.

When the reaction is performed in the gas phase $[Ni(NCMe)_5][WF_6]_2$, a white solid the is formed.

Neither MoF_6 nor UF_6 is able to oxidize massive nickel. MoF_6 can, however, oxidize chemically cleaned nickel metal or vacuum evaporated nickel film. A purple salt is formed; it is identified as $[Ni(NCMe)_6][MoF_6]_2$. If the nickel film is exposed to air before reaction, MoF_6 does not oxidize it. This clearly shows that it is the

oxide film that inhibits the reaction. On the other hand WF_6, which reacts easily with massive nickel, is inert towards a nickel film free from its oxide layer. The reaction of an evaporated nickel film with WF_5-^{18}F shows that tungsten hexafluoride is adsorbed on the surface of the metal but this reaction could not be observed for kinetic reasons.

Although previous workers did not take into account the role of the oxide film during the oxidation of metals, the series of reactions described above shows clearly its importance in the oxidation process. On this basis it seems reasonable to assume that an electron transfer takes place between the oxide film and the oxidizing agent. Nickel oxide being stable, the electron transfer does not occur with MoF_6. WF_6 being a strong Lewis acid, it is able to form a Lewis Acid-Lewis-Base adduct which catalyses the oxidation reaction of nickel metal.

Addition of pyridine to a solution mixture of nickel and MoF_6 in MeCN produced a yellow solid. Its microanalysis revealed that it is in fact a MoF_5.2py adduct which is formed. The reaction was also performed in absence of nickel, yielding the same product, identified by microanalysis, atomic absorption and vibrational spectroscopy.

Uranium hexafluoride is reported to be the strongest oxidizing agent of the series considered in this study. There was, however, no evidence of any reaction occurring between the metals, cobalt, nickel and zinc and UF_6. In all cases, reduction of the hexafluoride occurred before reaction with the metal could be detected. This was followed by polymerisation of the solvent. UF_6 was also reacted with a vacuum evaporated nickel film. In this case also, no reaction was observed.

INTRODUCTION

The chemistry of transition elements is concerned with the chemistry of coordination compounds, in other words, complex formation. A coordination compound is formed when the number of ligands attached to the central metal is greater than its oxidation state. The mechanism of complex formation is based on the donation of an electron pair from the ligand to the central metal. This electron pair is not completely transferred to the central metal, but is used to form covalent bonds. So complex formation is basically a Lewis acid-Lewis base interaction.

Transition elements can be briefly described as elements with partly filled d or f shells. Although copper has the electronic configuration $3d^{10}s^{1}$, it is also included in the definition, as in its commonly occurring oxidation state it has the configuration $3d^{9}$. Zinc is not normally considered a transition element, because both the element and its compounds have a filled 3d shell. In addition, zinc does not show the same characteristics as the rest of the transition elements.

The aqueous chemistry of the transition elements has been extensively reviewed. A number of compounds have stable oxidation states (towards disproportionation) in aqueous solution. However, there are known cases where the metal cation disproportionates in aqueous medium, and addition of π-acceptor, for instance, becomes necessary in order to stabilise low oxidation states.[1,2]

Previous work has shown that metal cations can be generated in acetonitrile either by oxidation of the metals using covalent high oxidation state fluorides, or by Lewis acid-Lewis base reactions between

metal fluorides and covalent high oxidation state fluorides.[3,4] Solvated Cu^{II} and Fe^{II} cations can be generated by the reaction of their binary fluorides with PF_5. Co metal can be easily oxidized by WF_6 and MoF_6 to give Co^{2+}. Ni metal is oxidized to Ni^{2+} by WF_6. The complex fluoroanions formed can be easily detected by spectroscopic methods.

Acetonitrile was chosen as the reaction medium because it is a very mild solvent and also very easy to handle.[5] In addition, the high volatility of acetonitrile makes it ideal for vacuum line work (m.p.=-45.7°C, b.p.=81.6°C). Acetonitrile is a neutral aprotic dipolar solvent with a dielectric constant of 35.5 at 20°C. CH_3CN is a good σ-donor and π-acceptor towards transition metals and thus favours low oxidation states. It possesses both lone-pair electrons, localised on its nitrogen atom, and vacant π-orbitals of π symmetry.[6,7] In the coordination process the electrons are donated from the ligand acetonitrile through its σ-bond, to empty orbitals of the metal. Because of, probably, a build-up of a negative charge on the metal, the electrons are donated back to the ligand by π-bonding.

Commercial acetonitrile usually contains impurities such as acetamide, ammonia and, in some cases, ammonium acetates. Besides this, acetonitrile is highly hygroscopic. It must thus be carefully purified before use. The method of purification used was developed in this department and is an extension of the method of Walter and Ramaley. A detailed account of the purification process used is given in the chapter concerned with the experimental techniques.

During the course of this work, high oxidation fluorides, i.e. UF_6, MoF_6 and WF_6 were used as oxidizing agents. UF_6 and MoF_6 are considered to be the stronger oxidizing agents. However, oxidation of nickel metal was straightforward only with WF_6.

1.2 Lewis Acid-Lewis Base Reactions

Work previously carried out in acetonitrile showed that ionic metal chlorides react with Lewis acid covalent chlorides in acetonitrile, giving solvated metal salts.[4] In this way, solvated salts of Fe(II), Co(II), Ni(II) and Cu(II) were generated from the reaction of MCl_2 with MCl_x (x = 3, 4 or 5), the anions being $FeCl_4^-$, $TlCl_4^-$, $SnCl_6^{2-}$ or $SbCl_6^-$.[8] Similarly, Cu(II) and Tl(II) heptafluorotungstates(VI) have been prepared by reaction of anhydrous CuF_2 with MF_5 (M=Ta,P, As). TaF_5 and AsF_5 are generally regarded as stronger Lewis acids than PF_5. They exist in acetonitrile as the monomeric complexes MF_5NCMe.

Although the solvated cations of nickel and cobalt are known to exist in acetonitrile, neither of them reacts with the pentafluorides. It was assumed that this difference in behaviour is due to kinetic factors. Ag(I) and Tl(I) fluorides react with AsF_5 to give AsF_6^- salts. In contrast to the chloroanion complexes, fluoroanion complexes show little tendency to coordinate with the metal ion leaving only the solvent in its primary coordination sphere. Thus it may be argued that the use of a Lewis acid fluoride as opposed to a Lewis acid chloride is more likely to lead to the formation of a solvated metal cation or, at the very least, a solvent separation ion pair.

1.3 Preparation of Uranium, Molybdenum and Tungsten Hexafluorides

All three hexafluorides can be prepared by direct fluorination of the respective metals. UF_6, MoF_6 and WF_6 produced must be purified by at least three successive distillations over anhydrous sodium fluoride.[9]

Uranium hexafluoride is prepared industrially by the following three-step process. The trioxide UO_3, prepared from U_3O_8, is reduced to UO_2. UO_2 is fluorinated by HF to give UF_4. Finally fluorination of UF_4 by elemental fluorine produces UF_6. In step 3 uranium tetrafluoride can be oxidized by oxygen producing UF_6 and UO_2F_2 (equation 1). UO_2F_2 is in turn recycled by reaction with HF to give UF_4. In this method it is not necessary to handle elemental fluorine.[10]

$$UF_4 + O_2 \xrightarrow{1073K} UF_6\,(g) + UO_2F_2 \qquad (1)$$

Molybdenum hexafluoride can be easily prepared in the laboratory by reaction of fluorine with metallic molybdenum, which has been previously heated in hydrogen to remove surface oxide, and cooled in nitrogen. The product of the reaction is collected in a Pyrex trap containing activated sodium fluoride. NaF retains traces of HF present and thus oxyfluoride formation is minimised. MoF_6 is transferred by vacuum distillation to a breakseal flask for storage. For purification the breakseal flask is resealed to a vacuum manifold and connected in series with three other breakseal traps containing

previously dried sodium fluoride. Purification of molybdenum hexafluoride is performed by vacuum distillation of the hexafluoride from one trap to another, adjusting the temperatures of the traps to give a slow distillation. Any SiF_4 present is removed at -78°C and MoF_6 is finally collected at -190°C. WF_6 can be prepared on a laboratory scale in a similar manner.

Both molybdenum and tungsten hexafluorides have been prepared by reaction of molybdenum or tungsten dibromides with anhydrous hydrogen fluoride at a temperature above 500°C,[11] (equations 2 and 3)

$$3\ MBr_2 + 6\ HF \rightleftharpoons 3\ MF_2 + 6\ HBr \qquad (2)$$

$$3\ MF_2 \xrightarrow{600°C} 2\ M + MF_6 \qquad (M=Mo,W) \qquad (3)$$

Preparation of tungsten hexafluoride can also be achieved by halogen exchange between tungsten hexachloride and fluorinating agents such as hydrogen fluoride (eqn. 4), arsenic trifluoride (eqn. 5) or antimony pentafluoride (eqn. 6).[12]

$$WC\ell_6 + 6\ HF \longrightarrow WF_6 + 6\ HC\ell \qquad (4)$$

$$WC\ell_6 + 2\ As_3F_3 \longrightarrow WF_6 + 2\ AsC\ell_3 \qquad (5)$$

$$WC\ell_6 + 3\ SbF_5 \longrightarrow WF_6 + 3\ SbF_3C\ell_2 \qquad (6)$$

Uranium hexafluoride can be prepared by fluorination of uranium tetrafluoride with elemental fluorine at high temperature,[13] (eqn. 7)

$$UF_4 + F_2 \xrightarrow{220\text{-}400^{\circ}C} UF_6 \qquad (7)$$

UF_6 can also be prepared by fluorination of uranium carbide with fluorine,[10] (eqn. 8)

$$UC_2 + 7F_2 \longrightarrow UF_6 + 2CF_4 \qquad (8)$$

1.4 Physical Properties of UF_6, MoF_6 and WF_6

Uranium, molybdenum and tungsten hexafluorides are colourless compounds in their gaseous, liquid and solid states.[14] They have short liquid ranges, MoF_6 (m.p. 17.4°, b.p. 34°C), WF_6 (m.p. 2.0°, b.p. 17.1°C), UF_6 (b.p. 56°C).

The hexafluorides of uranium, molybdenum and tungsten undergo a solid phase transition from a low temperature orthorhombic form to a high temperature cubic form.[15] The transition temperatures and the heats of transition are:

Compound	Transition T°C	ΔH trans. kJ mol^{-1}
MoF_6	- 8.7	4.685 10^{-5}
WF_6	- 8.2	3.346 10^{-5}

The structure of UF_6 has been shown to be octahedral in the gas phase with a small tetragonal distortion in the molecular structure.

Special precautions are necessary when allowing the solid hexafluorides to warm up from low temperature. The volume change associated with the solid phase transition is quite large and there have been occasions when the hexafluorides collected in cooled conventional glass traps have shattered the apparatus on warming up.

1.5 Structure and Bonding

UF_6, MoF_6 and WF_6 are monomeric and octahedral but they undergo a solid phase transition to a cubic form at higher temperatures. This change in the crystal structure has been studied by powder diffraction at -196°C.[15] Comparison of the results with those obtained at -80°C suggests that the octahedra are packing more efficiently, but no significant decrease in the metal-fluorine bond length was observed. The Mo-F and W-F bonds have approximately the same length ($\approx$ 2.00Å). From available data, the values of the fluorine to metal bond are respectively, 2.50 kJ in MoF_6 and 2.89 kJ in WF_6.[51,52] These values indicate a stronger bonding in tungsten hexafluoride than in molybdenum hexafluoride. Another piece of evidence for this is provided by the bond stretching force constants calculated from spectral data. The values are 5.13 for WF_6 and 4.73 in MoF_6.[53] Seemingly, volatilities and reactivities of transition metal hexafluorides are related functions. It is noteworthy that the less volatile hexafluorides are the most reactive.[54] The relative inertness of tungsten hexafluoride is an example to support this. A possible explanation for the trend of

decreasing bond strength with increasing atomic number in a row of transition metal hexafluorides is the transfer of electrons from the p-orbitals of the fluorine atoms and the d-orbitals of the central metal, as well as a σ-donation. The π-bonding effect decreases with increase of the number of electrons in the t_{2g} orbitals. Therefore π-bonding should decrease from tungsten hexafluoride to platinum hexafluoride. A decrease in the Van der Waals' radius should also be observed as a result of the diminution of the number of electrons outside the fluorine ligands. This explains in part the readiness with which RuF_6, RhF_6 and PtF_6 lose fluorine ligands.[55]

$$MF_6 \longrightarrow MF_{(6-x)} + 1/2_x F_2$$

Values of ν_1 for the second and third row transition elements all lie between 628-771 cm^{-1} and the value of ν_1 falls with increasing atomic number in a given row.[55]

1.6 Electron Affinities of WF_6, MoF_6 and UF_6

The electron affinity of a molecule or atom is defined by the difference in energy between the neutral molecule or atom in its ground state (E°) and the ion in its ground state (E^-),[14] (eqn. 9)

$$-EA = E^\circ - E^- \qquad (9)$$

Because of the difficulties encountered when measuring electron affinities, they are known with accuracy only for a few elements. In

Table 1-2 : Electron affinity of UF_6, MoF_6, WF_6 ($KJ.mol^{-1}$)

Technique	UF_6	MoF_6	WF_6	Ref
Absorption spectra of XeMF complexes (M=U,Mo,W)	558	554	432	15 (1978)
Effusion mass spectroscopy		345±19		(1982)
Molecular beam reaction with alkali metals	413	432	471	18 (1978) 19 (1977)
Ion cyclotron resonnance spectroscopy	470±48		331±10	20 (1979)
Gase phase reaction of NO with 3 transition metal hexafluorides			292	
Reaction with graphite			367	56 (1982)
Termochemistry of MF_6^- salts		517±6	490±5	23 (1974)
Ion molecular equilibrium	471±24 528±29 539±25			(1980) (1982)

most cases an estimated value is given using indirect methods.

Electron affinities of second and third row transition metal and actinide hexafluorides have been calculated by different means. Different values were obtained for each method used, but all results show the same trend in increasing electron affinity. The values are summarised in Table 1.

Electron affinities of molybdenum and tungsten hexafluoride have been collected using charge transfer spectra of these hexafluorides with xenon. The data obtained from the band position indicate that $EA(MoF_6) > EA(WF_6)$. During the calculation value of $EA(WF_6)$ was taken from the collisional ionization method. The error in the values is probably due to neglect of the interaction of the $MF_6^-Xe^+$ electronic configuration with the ground (MF_6Xe) and excited (MF_6^*Xe) configuration. Values determined for both $EA(WF_6)$ and $EA(MoF_6)$ are the following; $EA(WF_6) = 432$ kJ mol^{-1}, $EA(MoF_6) = 554$ kJ mol^{-1}.[15]

Electron affinities of both hexafluorides were also calculated by Sidorov et al., by an effusion technique. The values obtained are very low compared to those of other methods. In their calculation, it was assumed that alkali metals ionise with molybdenum and tungsten hexafluorides. The value of the bond dissociation energy $D(MoF_5\text{-}F)$ was determined experimentally from the equilibrium constant of the ion molecular reaction, (eqn. 10)

$$MoF_5 + 2BeF_3^- \rightleftharpoons MoF_6^- + Be_2F_5^- \qquad (10)$$

$D(MoF_5\text{-}F)$ = 397 ± 3 kJ mol^{-1} and EA(F) = 259 ± 2 kJ mol^{-1}, are literature values that were used to determine the electron affinity of MoF_6, which was estimated as 345 ± 19 kJ mol^{-1}.

Mathur et al., determined the electron affinities of WF_6, MoF_6, and UF_6 by the method of ionization reactions of the hexafluorides MF_6 (M = U, Mo, W) with alkali metals in crossed molecular beams.[18,19] In this method the ionization of the alkali metals was supposed to occur from the interaction with WF_6, MoF_6 and UF_6 according to reaction (11) even at thermal velocities of the atoms.

$$Na + MF_6 \longrightarrow Na^+ + MF_6^- \qquad (11)$$

Thus the magnitude of the electron affinities of the MF_6 must be greater or equal to the magnitude of the ionization potential (IP) of Na, (eqn. 12)

$$| EA(MF_6) | \geq | IP(Na) | \qquad (12)$$

Mathur et al., assumed that the observation of MF_6^- was probably due to the presence of dimers A_2 in the alkali beam, (eqn. 13)

$$A_2 + 2MF_6 \longrightarrow 2A^+ + 2MF_6^- \qquad (13)$$

A : alkali metal

M : W, Mo, U

Hence $|EA(MF_6)| > |IP(A)| + |D(A_2)|$

where $D(A_2)$ is the dissociation energy of the dimer.
The values reported were $EA(WF_6) \geqslant 471$ kJ mol^{-1}; $EA(MoF_6) \geqslant 432$ kJ mol^{-1} and $EA(UF_6) \geqslant 413$ kJ mol^{-1}. If the assumption in (eqn. 12) is right, then the potential surface of MF_6^- anion and Na^+ ion must be smaller than that of MF_6 and Na particles and does not cross it. This then rules out reaction (11). Sidorov et al., assumed that the reaction products are in their excited states and the electron affinity of MF_6 is given in an excited state rather than in the ground state. In this case correlation (12) is still possible.

Electron affinities of both WF_6 and UF_6 were also determined by George and Beauchamp.[20] $EA(WF_6)$ was determined from ion molecular reactions using the method of ion cyclotron resonance spectroscopy. F^- formed from NF_3 by dissociation attachment was found to react with WF_6 by an electron transfer reaction, (eqn. 14), as well as the fluoride attachment reactions, (eqn. 15).[21,22]

$$WF_6 + F^- \longrightarrow WF_6^- + F \qquad (14)$$

$$WF_6 + F^- \longrightarrow WF_7^- \qquad (15)$$

The electron transfer reaction, (eqn. 14), has a decreasing rate constant with increasing ion energy and is thus exothermic. Reaction of $C\ell^-$ formed from $CC\ell_4$ by a dissociative electron attachment with WF_6 was not observed, therefore the electron affinity of WF_6 must be smaller than that of $C\ell$ and hence,

$$EA(F) < EA(WF_6) < EA(C\ell)$$

$EA(WF_6)$ is probably equal to 331 ± 10 kJ mol^{-1}, as EA(F) = 327 kJ mol^{-1} and $EA(C\ell)$ = 341 kJ mol^{-1}.

$EA(UF_6)$ was determined by ion cyclotron resonance technique. A threshold value was measured for the reaction, (eqn. 15)

$$UF_6^- + BF_3 \longrightarrow BF_4^- + UF_5 \qquad (16)$$

As $AP(BF_4^-)$ and on the basis of the bond dissociation energy $D(BF_3\text{-}F^-)$ = 297 ± 21 kJ mol^{-1} and $DH_f^\circ(UF_6)$ = -2136, $\Delta H_f^\circ(UF_5)$ = -1902 and ΔH_f° = 255 kJ mol^{-1}. $EA(UF_6)$ was deduced as approximately 470 ± 48 kJ mol^{-1}.

From the study of the redox reactions of NO and FNO with third row hexafluorides, Bartlett found that the electron affinity increases by approximately 84 kJ mol^{-1}, with increase of atomic number. The electron affinity of WF_6, determined by this method, was comparable to that determined by George and Beauchamp and is $EA(WF_6) \leqslant 292$ kJ mol^{-1}.[24]

From studies of the intercalation of hexafluoride in graphite it can be deduced that $EA(WF_6)$ must be lower than 451 kJ mol^{-1}, as tungsten hexafluoride does not intercalate or spontaneously oxidise pure graphite. However, C_8MoF_6 is produced when MoF_6 is reacted with graphite. This again suggests that WF_6 has the lower electron affinity. On the basis of Bartlett's work, $EA(WF_6) < 367$ kJ mol^{-1}.[56]

Electron affinities of gaseous molybdenum and tungsten hexafluorides have also been estimated from measurements of the heats of

oxidative alkaline hydrolysis of K, Rb and Cs salts of the hexafluorometallates, together with the calculation of Burgess et al. of lattice energies of $AMF_{6(c)}$, (A = K, Rb, Cs and M = Mo, W). The electron affinities of MoF_6 and WF_6 were then derived from a Born-Haber cycle. $EA(MoF_6)$ = 517 ± 6 kJ mol^{-1} and $EA(WF_6)$ = 490 ± 5 kJ mol^{-1}. The uncertainty in the results determined for thermochemical measurements is probably due to the error in the calculation of the crystal lattice energy.[23] A more recent study involving thermochemical measurements of $NaWF_6$ and $LiWF_6$ showed that $EA(WF_6)$ was approximately 447 kJ mol^{-1}.

The electron affinity of UF_6 was determined by Sidorov et al. from the equilibrium constant of the following reaction[25]

$$UF_6^- + UF_4 \rightleftharpoons UF_5^- + UF_5 \qquad (17)$$

The equilibrium constant of the reaction (eqn. 17) was itself derived from the measurement of $I(UF_5^-)/I(UF_6^-)$ and $P(UF_5)/P(UF_4)$. $EA(UF_6)$ was found equal to 471 ± 24 kJ mol^{-1}. This result was later revised and it was shown that the above ratios are cell material and time dependent. The equilibrium constant value of the reaction was again determined using a single effusion cell and by carefully measuring the time. According to this, $EA(UF_6)$ was determined as equal to 528 ± 29 kJ mol^{-1}.

Pyatenko et al., determined the electron affinity of UF_6 from the equilibrium constant of the reaction, (eqn. 18).

$$UF_6 + K \rightleftharpoons UF_5 + KF \qquad (18)$$

From measurements of the ratios $I(UF_5^-)/I(UF_6^-)$ and $P(KUF_5)/P(K)$ the value determined was $EA(UF_6) = 539 \pm 25$ kJ mol^{-1}.

Electron affinity values of UF_6 and WF_6 are relatively precise and the results reported from the different methods cited above are in good agreement; still $EA(MoF_6)$ needs to be investigated. Data, however indicate the following order of electron affinities $UF_6 > MoF_6 > WF_6$.

1.7 Fluoride Ion Affinity of WF_6[20]

The fluoride ion affinity of tungsten hexafluoride has been determined from the fluoride transfer reaction that occurs when SiF_4 is added to SF_6 and WF_6. SF_6^- and SF_5^- are produced by attachment of near thermal energy electrons to SF_6, and further, SiF_4 reacts with both SF_6^- and SF_5^-, producing SiF_5^-. This reacts with WF_6 to produce WF_7^-, (eqn. 19)

$$SiF_5^- + WF_6 \longrightarrow WF_7^- + SiF_4 \qquad (19)$$

So $D(WF_6\text{-}F^-)$, (the reverse of the fluoride ion affinity of WF_6), must be greater than $D(SiF_4\text{-}F^-)$. A decrease in the amount of WF_7^- produced was observed when BF_3 was added to a mixture of SF_6 and WF_6. A one-way reaction, where BF_4^- is produced, was observed. It was then concluded that $D(WF_6\text{-}F^-) < D(BF_3\text{-}F^-).D(SiF_4\text{-}F^-)$. An estimated value of $D(WF_6\text{-}F^-) = 293 \pm 21$ kJ mol^{-1} was determined from

a recently reported value of $D(BF_3\text{-}F^-) = 301 \pm 21$ kJ mol^{-1}.

1.8 Chemistry of UF_6, MoF_6 and WF_6

The traditional view of UF_6, MoF_6 and WF_6 was that their chemistries were identical.[27] This was probably based on the property of the three hexafluorides to hydrolyse rapidly in moist air, producing in all cases HF and oxide fluorides.[14]

Uranium is similar in many respects to molybdenum and tungsten and was historically considered as the 4th row group VI A transition metal. Evidence has been mounting to show that in fact WF_6 is a less powerful oxidant than either UF_6 or MoF_6 or other second and third row transition metal hexafluorides. It is in fact the least reactive hexafluoride of the third row transition metals, the reactionally order being $WF_6 < ReF_6 < OsF_6 < IrF_6 < PtF_6$.[28,29] Some of the evidence is presented and discussed below.

1.8a Gas phase chemical reactivity of UF_6, MoF_6 and WF_6.

Oxidation of lower fluorides of metals

In their work, O'Donnell and Stewart investigated the reduction of uranium, molybdenum and tungsten hexafluorides by some lower fluorides of non-metals, e.g. phosphorus, arsenic, antimony and bismuth trifluorides. UF_6 reacted readily with PF_3, whereas the reduction of MoF_6 was only partial. This is because the phosphorus pentafluoride so formed is capable of oxidizing molybdenum pentafluoride. Reduction of WF_6 by PF_3 was very slow and occurred only to a limited extent.

Addition of anhydrous hydrogen fluoride appears to be necessary to catalyse the reaction.[29] Because chromium hexafluoride is thermally unstable, chromium pentafluoride was used instead.[30] Chromium pentafluoride oxidizes readily phosphor us and arsenic trifluorides. If anhydrous hydrogen fluoride is added to the reaction, chromium pentafluoride oxidizes antimony trifluoride to antimony pentafluoride. Chromium hexafluoride is a more powerful oxidant than chromium pentafluoride. On the basis of the reactivity of CrF_5, CrF_6 is then a more reactive oxidant than UF_6. Taking into account the above behaviour of CrF_5, MoF_6, UF_6 and WF_6 towards some lower fluorides of non-metals, we can deduce the reactivity of group VI A hexafluorides.

$$CrF_6 > UF_6 > MoF_6 > WF_6$$

In the same way, the reactivity of third row transition metal hexafluorides can also be deduced. ReF_6 is readily reduced by PF_3, producing ReF_5. Reaction of SeF_4 with OsF_6 and IrF_6 produces complexes where the metal is in its +5 oxidation state. Reaction of PtF_6 and SeF_4 leads to the formation of an adduct Pt(IV) fluoride and SeF_4.[31]

$$PtF_6 + SeF_4 \longrightarrow (SeF_4)_2\,PtF_4 + SeF_6 \qquad (19)$$

The general conclusion we can draw from this work is that there is a marked difference in the reactivity of first, second and third row transition elements of a given group.

Halogen exchange reactions

A halogen exchange process occurs when MoF_6 and UF_6 are reacted with the following halides: $PC\ell_3$, $AsC\ell_3$, $SbC\ell_3$, $TiC\ell_3$, $CC\ell_4$, $BC\ell_3$ and PBr_3. Only $BC\ell_3$, $TiC\ell_3$ and PBr_3 proved able to react with WF_6. MoF_6 reacts with all the ionic chlorides of group 1A elements, but UF_6 does not react with $KC\ell$, $RbC\ell$ and $CsC\ell$. On this basis, MoF_6 is seen as the stronger fluorinating agent.[32] Halogen exchange reactions confirm that UF_6 and MoF_6 have comparable properties while WF_6 is a less reactive reagent.

Reactions of UF_6, MoF_6 and WF_6 with nitryl fluoride, nitrosyl fluoride and nitrosyl chloride[24,29]

The behaviour of UF_6, MoF_6 and WF_6 towards nitryl fluoride, nitrosyl fluoride and nitrosyl chloride was investigated, and reactions of the three metal hexafluorides with NOF and NO_2F produced solid compounds of general composition $NO_x.F.MF_6$ (x=1,2 - M=U,Mo,W). Analysis of the vapour pressure released from each of these reactions showed that nitrosyl and nitryl fluorides combine with each of the hexafluorides in a 1:1 molecular ratio producing solids of varying volatility. Analysis of the infrared spectra of the products showed the presence of bands assigned to NO_x^+ (x=1,2) and MF_7^- and also bands similar to those of gaseous NO_xF and MF_6.[44] Data obtained for the compounds NO_xMF_7 indicate the existence of the following equilibria:

$$NO_xF + MF_6(g) \rightleftharpoons NO_xF.MF_6(s) \rightleftharpoons NO_xMF_7^-(s) \quad (20)$$

M=U,Mo,W; x=1,2

The complex formed is stabilised by partial acceptance of a fluoride ion by the metal hexafluoride.

The oxidation of nitrosyl chloride probably occurs by ionic dissociation of the nitrosyl chloride. An unstable complex ion ($MF_6C\ell^-$) is formed by transfer of a chloride ion to the metal hexafluoride. $MF_6C\ell^-$ then dissociates giving MF_6^- ion.

Nitric oxide does not react with tungsten hexafluoride. All three hexafluorides (UF_6, MoF_6 and WF_6) were inert towards nitrous oxide. The lack of reaction of WF_6 is consistent with its being classified as the least reactive hexafluoride.

1.8b Reactivity of UF_6, MoF_6 and WF_6 in solution

Reactions in anhydrous hydrogen fluoride[59]

The redox couples MF_6/MF_6^-, M=Mo,W, have been identified in neutral and basic solutions of anhydrous hydrogen fluoride, as shown in eqn. 21

$$MF_6 \underset{e^-}{\overset{e^-}{\rightleftharpoons}} MF_6^- \qquad M=Mo,W \qquad (21)$$

The redox process is a simple one electron transfer reaction. The electrochemical potential values of the couple MF_6/MF_6^- were determined for both WF_6 and MoF_6. $E_{1/2}(WF_6/WF_6^-)$ =-0.10V vs. Cu/CuF_2 and $E_{1/2}(MoF_6/MoF_6^-)$ = 0.91V vs. Cu/CuF_2. Comparison of the two couples shows WF_6 as a very mild oxidant since it is reduced at a negative potential with respect to Cu/CuF_2 reference electrode. MoF_6

is a stronger oxidant and is reduced at more positive potential. The difference between the two couples is 1.01V. This is significant in relation to electrochemical work carried out in CH_3CN, which is described below.

Uranium hexafluoride can be reduced by hydrazinium(+2) at 0° in hydrogen fluoride or carbon tetrachloride. If excess UF_6 is used the product of the reaction is hydrazinium-bis-hexafluorouranate ($N_2H_6(UF_6)_2$). With excess hydrazinium(+2)fluoride, the product is hydrazinium(+2)heptafluorouranate(V) ($N_2H_5UF_7$).[33]

Reactions of MoF_6 and WF_6 in sulphur dioxide

Molybdenum and tungsten hexafluorides were reacted with the alkali metal iodides in sulphur dioxide medium. Both hexafluorides were reduced to their respective hexafluorometallates(V),[34] (eqns. 22,23)

$$2\ MoF_6 + 2MI \xrightarrow{SO_2} I_2 + 2M\ MoF_6 \qquad (22)$$

$$2\ WF_6 + 2MI \xrightarrow{SO_2} I_2 + MWF_6 \qquad (23)$$

(M=alkali metal, but not Li).

Reactions of UF_6, MoF_6 and WF_6 in iodine pentafluoride

The oxidising abilities of some hexafluorides towards iodine in iodine pentafluoride, have been investigated. The work was performed in this department by Berry et al. Molybdenum and tungsten hexafluorides were both inert towards iodine in iodine penta-

fluoride medium.[35] However, UF_6, as well as ReF_6, oxidised iodine to I_2^+ in iodine pentafluoride. The behaviour of UF_6 towards I_2 in IF_5 depended on the stoichiometry of the reaction. If the mole ratio of UF_6 to I_2 is 1:1, the I_2^+ cation formed immediately, but when the mole ratio UF_6:I_2 is 10:1 greater, the concentration of the I_2^+ formed initially diminishes gradually and uranium pentafluoride is precipitated, as in equation 24.

$$10\ UF_6 + I_2 \longrightarrow 10\ UF_5 + 2\ IF_5 \qquad (24)$$

The reaction is believed to occur with the formation of $I_2^+UF_6^-$ initially, then formation of U_2F_9 and disproportionation, giving IF_5.

ReF_6 oxidised I_2 in IF_5, also giving I_2^+ with a large excess of oxidant used

$$ReF_6 + I_2 \longrightarrow I_2^+ + ReF_6^- \qquad (25)$$

From this work and previous results, the oxidising ability in iodine pentafluoride of metal hexafluorides are in the order $UF_6 > ReF_6 > MoF_6, WF_6$.

Reaction of the hexafluorides in acetonitrile solution

Acetonitrile has proved to be a suitable medium for carrying out redox reactions between some metal hexafluorides and 3d and post-transition metals.[3,28]

Molybdenum hexafluoride oxidises Tℓ metal in CH_3CN[60] at room temperature, yielding a pure $Tℓ^{III}$ salt, colourless

$Tl^{III}(MoF_6)_3.5MeCN$, when a high concentration of MoF_6 is used. If the mole ratio Tl:Mo = ca. 1:2, yellow solids of $Tl(MoF_6)_2$ are isolated. These are spectroscopically identical to Tl^{III} salt.

Tl^{III} salt is produced when the yellow solids are oxidised by MoF_6 in MeCN. The yellow solids react slowly with thallium metal. These solids have been formulated as a mixture of $Tl^{I}.Tl^{III}$ with an atomic ratio Tl:Mo always approximating 1:2.

Same behaviour is recorded between thallium metal and UF_6, but a concentration of at least 1 mol dm^3 of UF_6 is required to produce Tl^{III} hexafluorouranate(V).

$Tl^{III}(MoF_6)_3.5MeCN$ oxidises Cu^{I} to Cu^{II} in CH_3CN at room temperature, but the reaction is incomplete. Cu^{I} is also oxidised by the yellow solid of $Tl^{I}.Tl^{III}$ in CH_3CN. All this implies that the Tl^{III}/Tl^{I} couple is more strongly oxidising than the couple Cu^{II}/Cu^{I}.

Tl(I) with PF_6^- as counter anion is not oxidised by WF_6, Cu^{II} or NO^+ in CH_3CN at room temperature.

The reactions of Tl^{III} and Tl^{I} in CH_3CN suggest that the Tl^{III}/Tl^{I} couple is less oxidising than is MoF_6/MoF_6^- but more than Cu^{II}/Cu^{I}.

Molybdenum and uranium hexafluorides show an appreciable similarity in their behaviour towards some transition metals. Previous work showed that both hexafluorides oxidise copper metal to Cu^{II}.[28] The Cu^{II} hexafluoromolybdate(V) and hexafluorouranates(V) can be reduced to Cu^{I} by reaction with Cu metal. Tungsten hexafluoride reacted differently, probably because of the similarity in the potential values of the couples Cu^{II}/Cu^{I} and WF_6/WF_6^-, and also because of a fluoride ion transfer reaction.[36]

$$WF_6^- + WF_6 \overset{MeCN}{\rightleftharpoons} WF_7^- + WF_5 \qquad (26)$$

Cyclic voltammetry was used to identify the redox couples MF_6/MF_6^- (M=U,Mo,W). A distorted wave at 2.33V was assigned to the UF_6/UF_6^- couple. Waves assigned to $E_{1/2}(MoF_6/MoF_6^-)$ = 1.60V and $E_{1/2}(WF_6/WF_6^-)$ = 0.51V vs. Ag^+/Ag, respectively. The difference between the MoF_6/MoF_6^- couple and WF_6/WF_6^- couple is 1.09V. Comparison of these results with the electron affinities measurements for the MF_6 (M=U,Mo, and W) confirms that the trend of oxidising abilities is as suggested previously and is $UF_6 > MoF_6 > WF_6$. Although keeping the same order of oxidising abilities, the behaviour of UF_6, MoF_6 and WF_6 is to some extent different and dependent on the nature and type of ligands in use.

It is apparent from the material presented in this chapter that considerable progress has been made in determining the chemistry of UF_6, MoF_6 and WF_6, and that the main features of the chemistry of these hexafluorides are now clear. One of the objectives of the work carried out in this department is to determine how far these compounds can be used in anhydrous acetonitrile to oxidise metals and non-metals. As already illustrated, the products from such reactions are solvated metal cations, fluoroanion salts and these compounds are very useful starting materials to develop the non-aqueous coordination chemistry of the element in question.

The initial study demonstrated the feasibility of the approach for a range of first row transition and non-transition metals. Subsequently, attention has been directed to those elements where oxidation is rapid,

for example, thallium,[60] iron, copper,[21] and iodine. Not all metals are oxidised rapidly, for example, in the initial study[3] the oxidation of nickel metal by MoF_6 was not observed, even though a reasonably rapid reaction did occur between nickel and WF_6. The aim of the present work was to re-examine the problem of "difficult" metals with particular emphasis on nickel. For comparison, oxidation of cobalt and zinc has also been re-examined as the initial study suggested that these metals would present little difficulty. Results obtained for these metals are presented and their behaviour compared with work which has been carried out in the department by others on iron and copper. This has enabled the factors which are important in the latter part of the 3d series, i.e., Fe, Co, Ni, Cu, and Zn to be assessed.

CHAPTER II

EXPERIMENTAL TECHNIQUES

As this work was concerned with anhydrous reagents and the complexes prepared are moisture-sensitive, all work was carried out in a dry atmosphere. For this purpose the use of a vacuum line and a dry atmosphere box was required.

2.1 Vacuum Line and Dry Box Techniques

All manipulations were performed in a conventional Pyrex glass vacuum system. This was fitted with a "Jencons" mercury diffusion pump connected to an "Edwards high vacuum" rotary oil pump. The vacuum provided was better than 0.001 torr. Standard glass joints were greased with Apiezon black wax, Voltalef Kel-F or high vacuum Apiezon N. All reactions were performed in Pyrex double-limb reaction vessels (Fig. 1) which were dried and carefully flamed out before use. Some of the work was performed in a Lintott inert atmosphere glove box in which the concentration of water was kept at less than 10 p.p.m. and usually below 5 p.p.m. The drying of the glove box was possible by using molecular sieves. Manganese oxide was used to remove oxygen. The glove box was fitted at one end with an evacuable air-lock, to permit introduction of apparatus and material under dry conditions.

2.2 Electronic Spectroscopy

After synthesis and isolation of a complex, we usually proceed to the study of its physical and chemical properties. Electronic and vibrational spectroscopy were two of the principal methods used in this

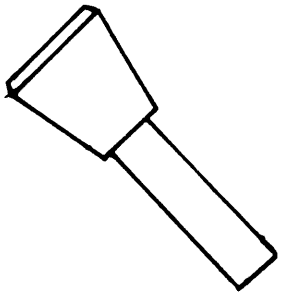

ROTAFLO STOPCOCK

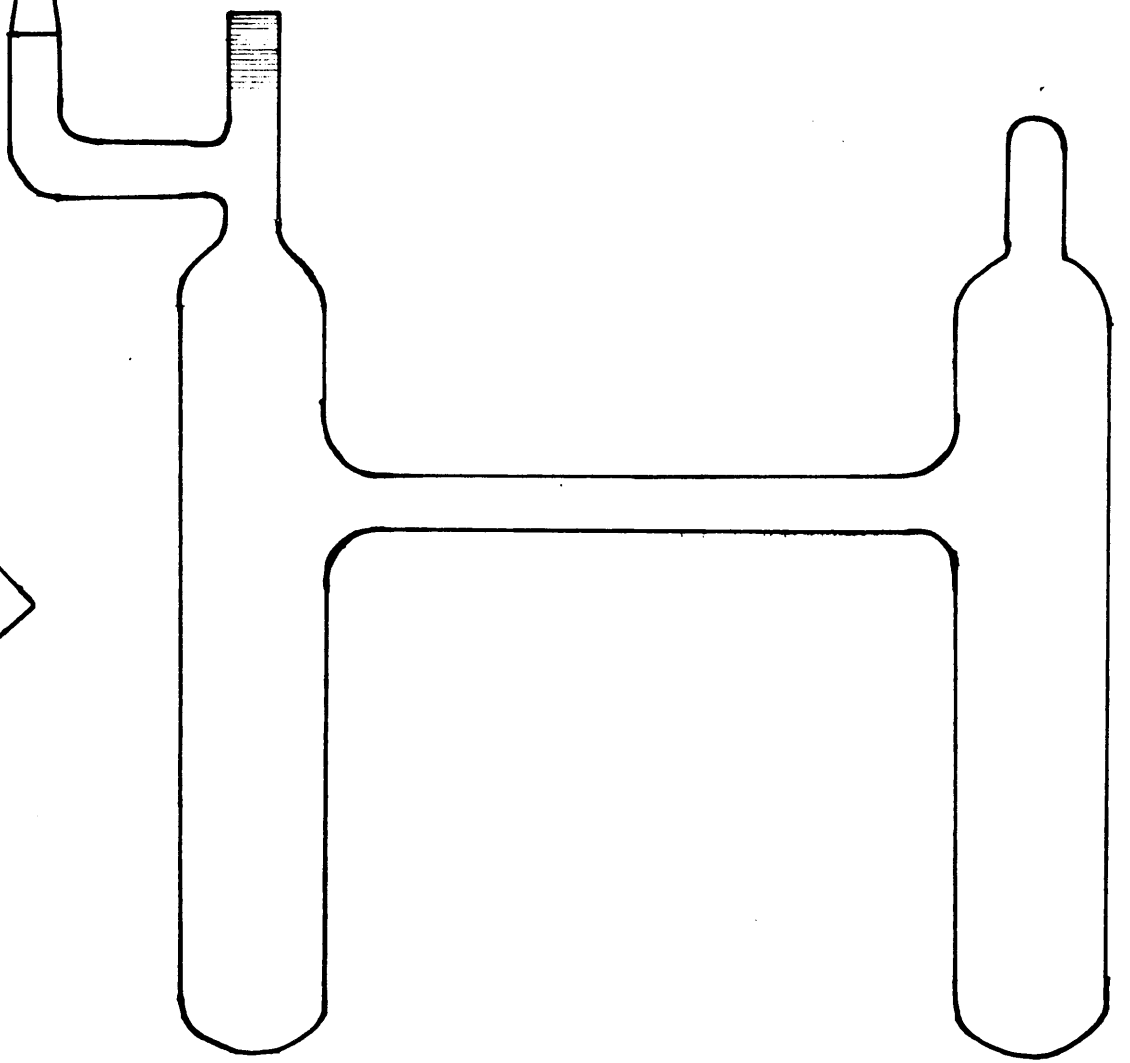

fig1 - DOUBLE-LIMBED REACTION VESSEL

work. In short, study of the band widths and positions in the electromagnetic spectrum gives valuable information on the electronic structure of the central atom and the magnitude of the ligand field splitting (Δ). Also, bonding characteristics and distortion of the symmetry of the environment can be deduced with appreciable accuracy from the study of these spectra. In brief, in the free transition ion, the five orbitals of the d-electrons possess equal energies. When a complex is formed the d-orbitals are split as a result of the electrostatic repulsion of the ligand.[14] In octahedral complexes, such as those used in this work, the ligands are along the x, y and z axes. The orbitals dx^2-y^2 and dz^2 are those with higher energies because they point in the direction of the ligands. dxy, dxz, and dyz point between the ligands and their energies will be lower. The eg levels, that is, dx^2-y^2 and dz^2 orbitals, are higher by 3/5 Δ and the t_{2g} levels, that is, dxy, dxz, and dyz, are lower by 2/5 Δ. Δ is the crystal field splitting and it can be deduced from the energy of the low intensity d-d bands that appear in the visible or near u.v. regions of the spectra of transition metal complexes. If the electron pairing energy is known, the electronic structure of the central atom can also be predicted.

2.2.a - Electronic absorption spectroscopy[37,38]

Information on the splitting of the d-orbitals of a transition metal as a result of complex formation, and the electronic structure of the complex formed is usually available from the study of its electronic spectrum, and will be illustrated more extensively in Chapter 3.

Changes in the electronic distribution of a molecule usually occur in the region which extends from 1×10^4 cm^{-1} to 5×10^4 cm^{-1} in the electromagnetic spectrum. Electronic transitions result from the excitation of an electron from the ground state to a higher energy level. Not all transitions between the different energy levels are possible. However they do obey selection rules which depend on the symmetry of the molecule.

2.2.b - Selection rules

Selection rules determine whether a particular transition is permitted or not. These rules can be described as follows:

(1) Transitions that involve a change in the number of unpaired electron spins ($\Delta S \neq 0$) are called spin-forbidden.

(2) Transitions during which there is redistribution of electrons in a single quantum shell are forbidden. Therefore d → d and p → p transitions are forbidden and only s → p and p → d transitions are allowed. This is the Laporte selection rule and d → d and p → p transitions are said to be orbitally forbidden. g → g (centrosymmetric orbitals) and u → u (anticentrosymmetric orbitals) transitions are said to be partly forbidden. Finally, for a transition to occur, it should involve only one electron. However, these rules are not strictly obeyed. d - d transitions may occur but their intensities may be relatively weak. The presence of d - d bands in an octahedral complex is assumed to be due to the interaction of the wave function of the d-orbitals and the vibrational wave functions of the complex. It is also believed that a

d - d transition is possible, because of the overlap of the d-orbitals of the metal and the p-orbitals of the ligand. Hence this is no longer a pure d - d transition. It is in fact an allowed dp → dp transition. The greater the mixing of the d and p orbitals, the higher the intensity of the corresponding band. The d and p mixing of orbitals is more likely to occur in molecules with slightly distorted Oh symmetry, such as MoF_6^- ($4d^1$), WF_6^- ($5d^1$) and UF_6^- ($5f^1$) which also have unfilled d and f shells.

2.2.c - Charge transfer spectra

Charge transfer spectra occur at high energies and are due to transition of electrons either from a metal orbital to a ligand orbital or vice versa. Ligand to metal charge transfer corresponds to a metal reduction. The more easily the metal is reduced and the ligand oxidised the lower the energy of the transition. Metal to ligand charge transfer is a type of transition requiring a readily-oxidisable ligand.

2.2.d - Electron transfer within the ligand

All organic ligands absorb in the ultra-violet region of the spectrum and a number of them absorb in the visible region also. The absorption of light by these ligands is due to transitions of the type:

a) $n \rightarrow \sigma^*$ transitions; they correspond to transitions of low energy of the internal non-bonding lone pairs. This type of transition limits the use of some solvents in the ultra-violet spectrum, such as water, alcohols and amines.

b) $\pi \rightarrow \pi^*$ transitions; they occur when the π-bonding orbital is the highest occupied level (HOMO) and the π^* orbital is the lowest unoccupied level (LUMO).

c) $n \rightarrow \pi^*$ transitions; they involve the transition of electron pairs from the π-bonding orbitals of lower energies to π-anti-bonding orbitals of higher energies. This type of transition occurs in molecules that have atoms involved in π-bonding and also contain non-bonding electron pairs, e.g. aldehydes and ketones. Pyridine has both $n \rightarrow \pi^*$ and $\pi \rightarrow \pi^*$ transitions.

2.2.e - Sample preparation for u.v. spectroscopy

Two cells are needed when recording a u.v./visible spectrum. One is used as a reference cell and contains the solvent. The second is the sample cell containing the solution to be studied (Fig. 2). The sample cell was specially designed for handling moisture-sensitive samples. It consists of a 1 cm Spectrosil cell connected to a side reaction vessel. Because the samples are air-sensitive, the reactions were performed in the side reaction vessel, then the solution was tipped into the sample cell. The reference cell was used to compensate for any loss of radiation by scattering and reflection due to the solvent. All spectra were recorded on a Beckman UV5270, u.v. visible-2 spectrophotometer.

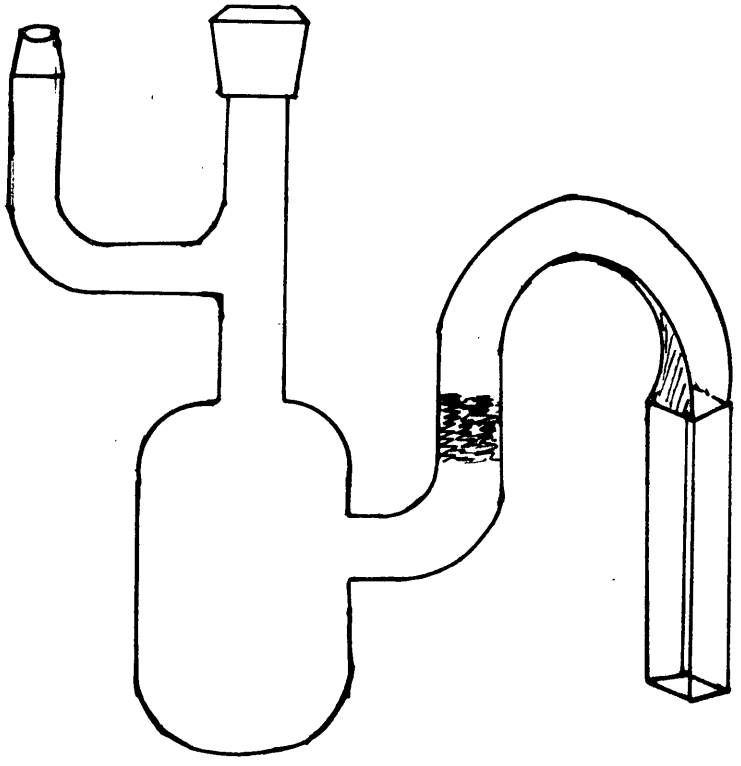

FIG 2- EVACUABLE CELL FOR ELECTRONIC SPECTROSCOPY

2.3 Vibrational Spectroscopy[39,40]

Infrared and Raman spectroscopy were used to identify organic ligands and inorganic anions in the complexes prepared. Raman and infrared spectroscopy are based on different concepts, but both methods yield the same type of information. An infrared band is observed as a result of an overall change of the electric dipole moment during a normal mode of vibration, whereas observation of a Raman band depends exclusively on a change in the polarizability during the vibration. Following the rule of Mutual Exclusion, for molecules with a centre of symmetry, fundamental transitions which are active in the infrared are forbidden in the Raman and vice versa. Hence the two methods complement each other.

Vibrational and rotational spectra are determined by the position of atoms in space, their mass, bond lengths and angles. When a free ligand is coordinated to an atom or ion, these criteria are expected to vary slightly and changes in the spectra occur, e.g. changes in band positions or band intensities, appearance of new bands and, finally, splitting of single peaks in the free ligand into numerous closely spaced bands. in the complex So infrared spectra of free ligands are different from those of coordinated ligands and it should be possible to correlate the changes in spectra with changes in geometry. As a result of coordination the stretching frequencies of the C≡N bond in acetonitrile are higher than in the free molecule. The acetonitrile molecule belongs to the point group C_{3v} and has 18 degrees of internal freedom. The eighteen Cartesian displacement vectors for the entire molecule generate the following reducible representation.

C_{3v}	E	$2C_3$	$3\delta_v$
Γ	18	0	4

The representation Γ can be reduced as follows:

$$\Gamma = 5A_1 + A_2 + 6E$$

where $A_1 + E$ are translations

$A_2 + E$ are vibrations

and $4A_1 + 4E$ are genuine internal vibrations

Acetonitrile coordinates via its nitrogen lone pair. Coordination of CH_3CN to a metal is evidenced by its vibrational spectra. The process is usually followed by an increase in the C≡N stretching frequency (ν_2) which is produced by an increase in the C≡N force constant. The increase of the force constant is due to a strengthening of the binding between carbon and nitrogen atoms. This gives more "s" character to the triple bond and, therefore, an increase in the force constant. The observed increase in the C-C stretching frequency (ν_4) agrees with the change in hybridization of the carbon.

In the case of octahedral molecules (MX_6) with the O_h point group, the twenty one Cartesian displacement vectors (three per atom) form a basis for the following representation.

O_h	E	$8C_3$	$6C_2$	$6C_4$	$3C_2(=C_4^2)$	i	$6S_4$	$8S_6$	$3\delta_n$	$6\delta_d$
Γ	21	0	-1	3	-3	-3	-1	0	5	3

Γ reduces to the following

$$\Gamma = A_{1g} + E_g + \ldots + 3T_{1u} + T_{2g} + T_{2u}$$

From the O_h character table it can be determined that T_{1u} are translations and T_{1g} are rotations, and as genuine internal vibrations the following:

$2T_{1u}$: infrared active

A_{1g}, E_g, T_{2g} : Raman active

T_{2u} : inactive

The vibrational spectra of some MF_6 molecules and MF_6^- anions were recently studied by Laser Raman spectroscopy.[45] Salts of the general formula $NO^+ MF_6^-$ (M = Mo, Tc, Re, Os, Ir, U and Np) were prepared by reaction of nitric oxide with molecular hexafluorides. As WF_6 does not oxidise NO, KWF_6 was used instead. In addition to the NO^+ vibration, all spectra showed two vibrations that were assigned to $\nu_1(a_{1g})$ and $\nu_5(t_{2g})$ of the octahedral MF_6^-, according to the O_h character table. ν_1 was the vibration of highest symmetry. ν_5 was lower in frequency. $\nu_2(E_g)$ vibration was the weakest vibration observed. In the solid phase splitting of degenerate vibrations was also observed. Indeed, the ν_5 and ν_2 vibrations are split in the spectrum of UF_6^-.

Another feature of importance is the general trend of decreasing frequencies of ν_1 and ν_2 vibrations as a result of reduction in the oxidation state of the central metal atom. The ratio of ν_1^{V}/ν_1^{VI} for the same central atom is almost constant for all the elements cited above and is equal to 0.93-0.94. For Tc it is lower and it equals 0.86.

The decrease in the stretching frequencies of ν_1 and ν_2 results from the fact that, in the higher oxidation state, the ligands are probably closer to the central atom, causing a large polarization and increasing covalent character of the bond. The increase in the ν_1 frequencies is observed going from the second to the third transition series, and is demonstrated by the pairs Mo-W and Tc-Re. Also, ν_1 decreases along the same series with increase in mass of the elements. In the second series this is observed in Mo and Tc and in the third series it is observed in W, Re, Os and Ir. It is also observed in U and Np. These observations were made for both the molecular hexafluorides and their respective anions. The first trend shows an increase in mass of the central atom and a constant electronic structure. The second trend shows a decrease in ν_1 and implies a decrease in average bond energy.

2.3.a - Sample preparation for Raman spectroscopy

No special plates or cells are required when preparing a sample for Raman spectroscopy. The solid or solution samples are simply loaded in a Pyrex glass capillary in vacuo (Fig. 3). The spectra were recorded on a Spex Ramolog instrument employing either an argon ion (488.0, 514.5 nm) or a krypton ion (647.1, 520.8, 568.2 nm) laser source.

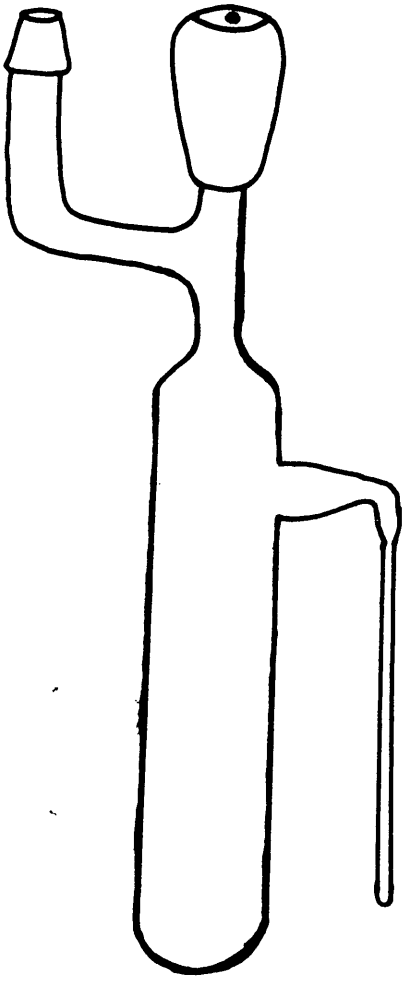

Fig3: Reaction vessel with Raman capillary

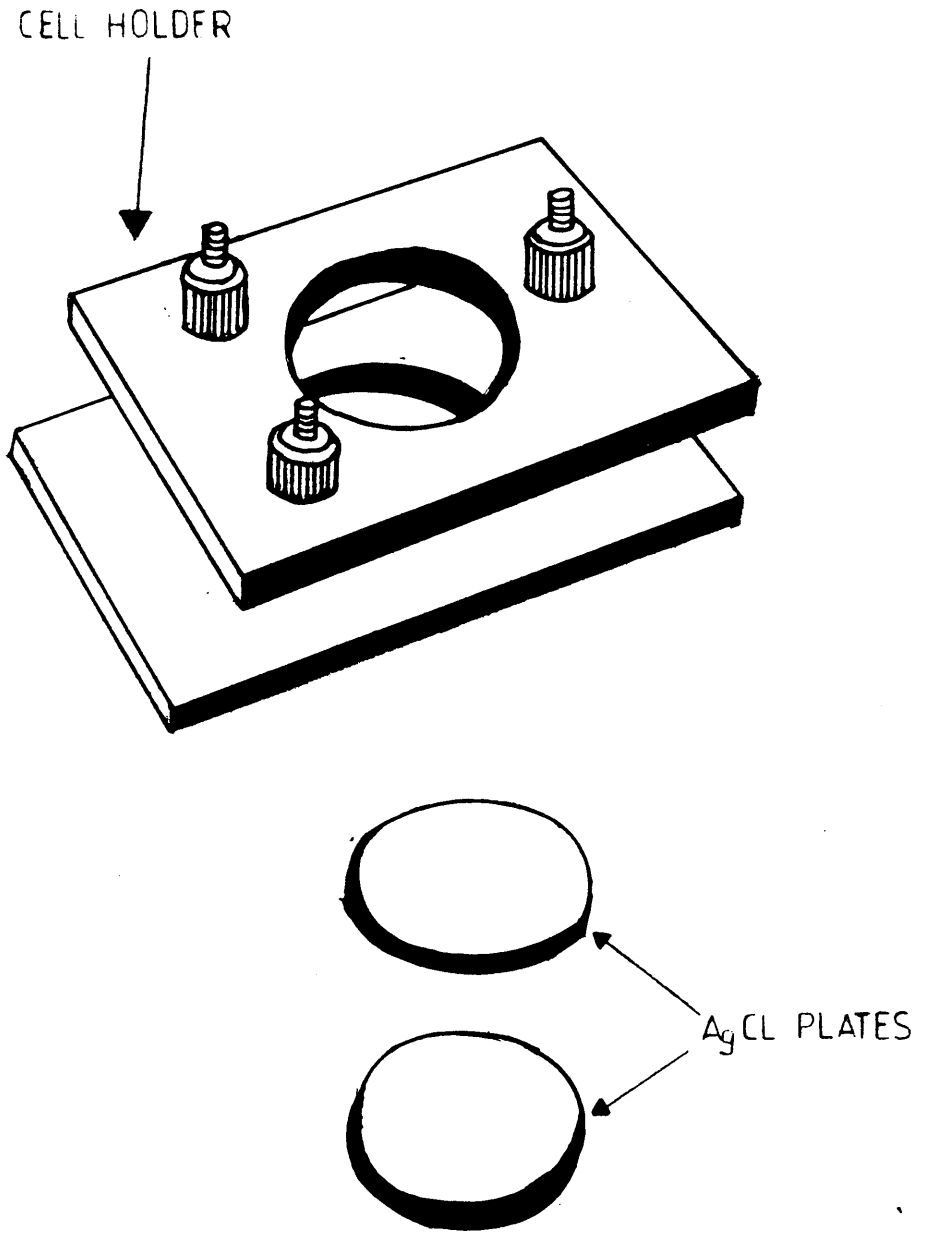

FIG 4 - DEMOUNTABLE CELL FOR INFRARED SPECTROSCOPY

2.3.b - Sample preparation for infrared spectroscopy

A small amount (~2-5 mg) of the salt to be studied was finely ground using an agate mortar and a pestle. The finely ground solid was then wetted with one or two drops of Nujol or Fluorube, and the paste obtained mixed thoroughly. A few drops of the paste were then placed between two AgCℓ plates which were placed on a cell holder (Fig. 4). An infrared spectrum was recorded over the region 4000-350 cm^{-1} on a Perkin-Elmer 983 spectrometer with data station.

Nujol is a suitable mulling agent for infrared spectroscopy because it absorbs only at 2900, 1460, 1380 and 725 cm^{-1}. Fluorube was alternately used to examine those regions where Nujol absorbs. Silicon plates were used for scanning at lower frequencies (down to 200 cm^{-1}).

2.4 Cyclic Voltammetry[41,42]

Except for purely analytical problems, cyclic voltammetry has been more widely used than classical polarography for the last few years. Cyclic voltammetry (C.V.) is used to study simple redox processes in organic and inorganic chemistry and to establish if a newly prepared compound can be readily oxidised or reduced to a known compound.

2.4.a - Description and characterisation of voltammograms

Voltammograms are best described as current-voltage curves. A typical voltammogram is shown in Fig. 5. The dotted line is that which would be obtained in absence of reducible metal ions, when only the supporting electrolyte is present.

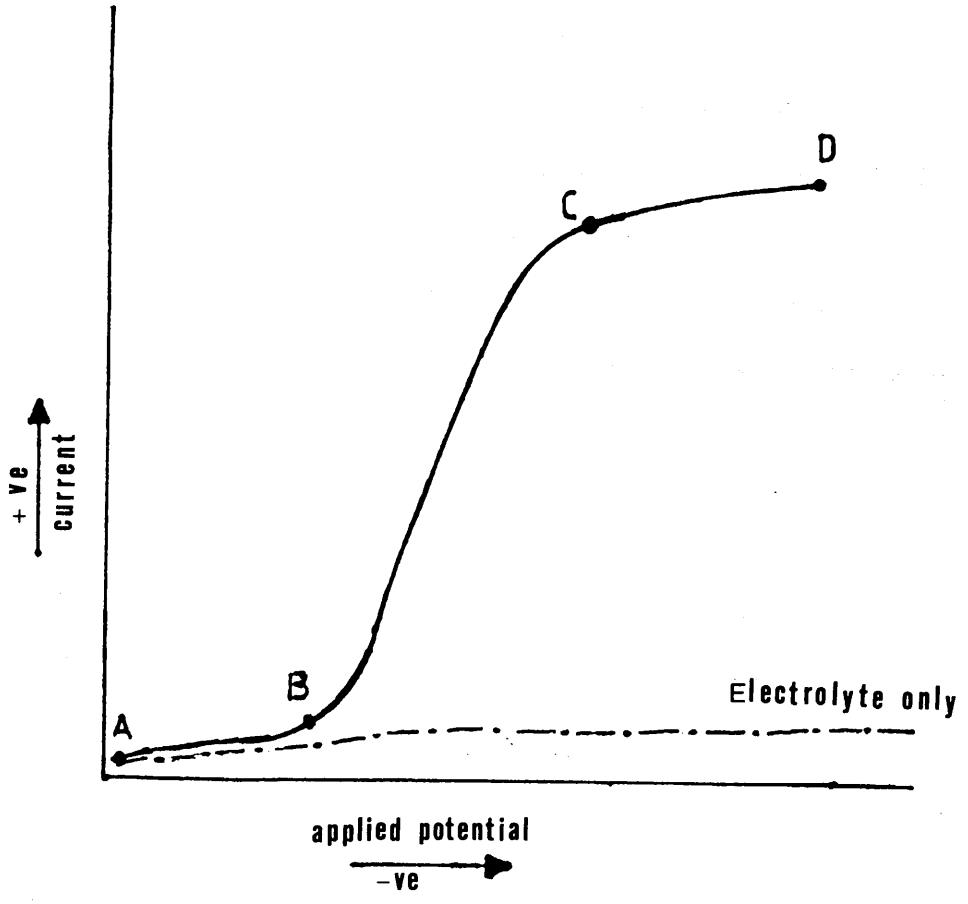

Fig 5 - A TYPICAL VOLTAMMOGRAM

The same interpretation holds for either a one-electron reduction or oxidation, but for brevity only the reduction process will be discussed.

If we suppose that A is the starting point for the reduction process, then as the applied potential increases in a negative direction, the current also increases slowly until point B. This is called the residual current. The residual current is essentially due to a charging near the electrode surface as an electrical double layer is formed, and a diffusion current due to the presence of oxidisable and reducible trace species in solution. The residual current can be described as a non-Faradaic current, because its variation with potential does not obey Ohm's law. When the reduction of the species present begins, the current rises sharply until point C. At this point the reduction process is at its maximum. Species approach the electrode by a diffusion process. Because of the presence of the residual current, the current rises again slowly at a more negative potential.

There are two types of voltammetric waves, reversible and non-reversible. In the reversible case, the half wave potential equals the formal electrode potential $E_{\frac{1}{2}} = E_o$; $E_{\frac{1}{2}}$ is the potential corresponding to a position half way up the curve. In the non-reversible case, E_o is no longer equal to $E_{\frac{1}{2}}$.

Systems must always be tested for reversibility. Non-reversibility is sometimes caused by a further reaction of one of the species present in the system. This is represented by the following scheme.

$$A \xrightarrow{-1e^-} A^+ \longrightarrow C^+$$

A is oxidised electrochemically to produce B^+. B^+ reacts further and possibly decomposes, producing C^+. The reduction potential of the two species, B^+ and C^+ being different, the wave is non-reversible. One way of checking the reversibility of a system is by cyclic voltammetry. In this method the potential of the working electrode is varied between fixed limits, at a constant rate, within the voltammetric range of the solution. A typical reversible cyclic voltammogram is represented in Fig. 6, for a one-electron transfer process for the Cp_2Fe/Cp_2Fe^+ couple in acetonitrile. The decrease of the surface concentration of the reactant A and the increase of the surface concentration of the reactant B, are potential dependent. When the concentration of reactant A becomes negligible, current and potential are at a maximum. The current curve starts to decay. The same process occurs in the opposite direction with increase of the concentration of A and decrease of the concentration of B.

$$E_R = E_{\frac{1}{2}} - \frac{0.0285}{n} V$$

and

$$E_{ox} = E_{\frac{1}{2}} + \frac{0.0285}{n} V$$

E_R and E_{ox} are respectively the reduction and the oxidation potentials. n is the number of electrons transferred during the electrochemical reaction. $E_{\frac{1}{2}}$ is the half wave potential. The peak potential of an oxidation wave is more positive than the corresponding half-wave potential with a value of (0.0285/n)V. The peak potential of a reduction wave is more negative than the corresponding wave potential with the

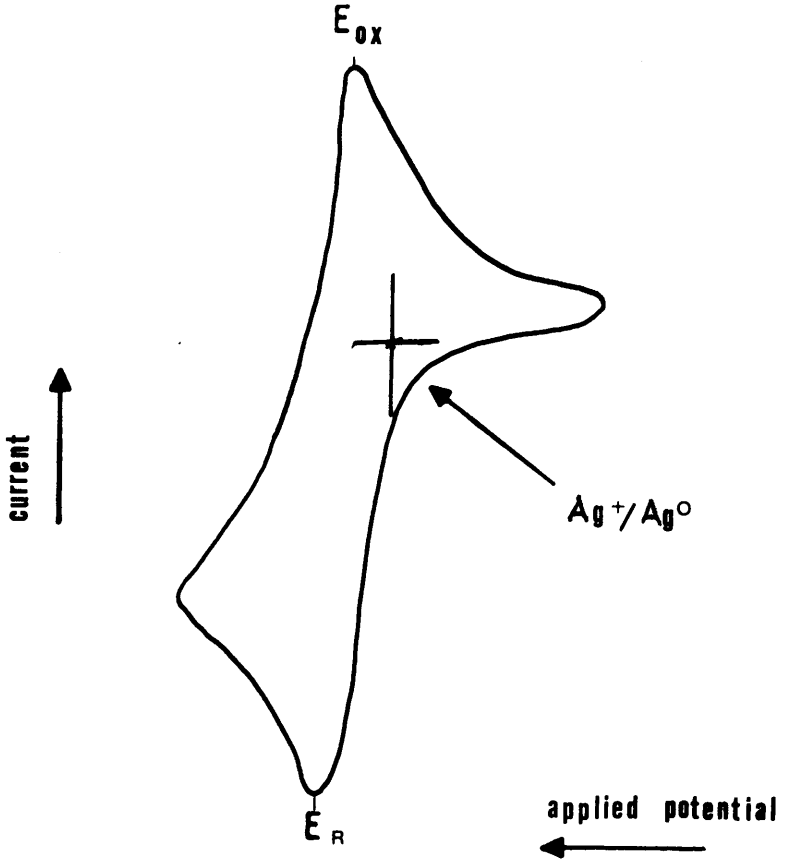

$$\frac{E_{ox} + E_R}{2} = E_{1/2}$$

Fig 6- CYCLIC VOLTAMMOGRAM OF $(\eta^5\text{-}C_5H_5)_2Fe$

same value. The average separation between the two peak potentials is then (0.057n) V. The peak to peak separation is increased when the electrode transfer reaction is not reversible. In this case, the charge transfer at the electrode is extremely slow, and the current is to a great extent controlled by the rate of the charge transfer process. The Nernst equation can not be applied in this case. Quasi-reversible waves are obtained when a rapid electron transfer process is followed by a slow chemical reaction. The current depends on both charge transfer and mass transport. The Nernst equation is in this case not fully satisfied and the height of the anodic peak is smaller than the height of the cathodic peak, when the starting material is the oxidised form of the couple. It is the reverse when the starting material is the reduced form of the couple.

Usually cyclic voltammetry measurements are performed using a stationary electrode, and transport of reducible or oxidisable species is by diffusion process. To ensure this, 0.1M of tetraethylammonium tetrafluoroborate (Et_4NBF_4) was used as a supporting electrolyte. Careful purification of the solvent used is necessary for the obtention of good results. Trace impurities and presence of water can give misleading results.

2.4.b - Role of the supporting electrolyte

Electrolytes are species which dissociate into ions when dissolved in a solvent. There are two types of electrolytes, strong and weak. Strong electrolytes ionise completely while weak electrolytes ionise to a lesser extent, with ionization increasing with dilution,

according to Ostwald's law.

Electrolytes are used to regulate the cell resistance and ensure transport of species by electrical migration. They are usually chosen to give as small as possible resistance values when dissolved in the solvent, so that the uncompensated I.R. drop is minimised.

For the present work Et_4NBF_4 was chosen amongst others as previous work performed in this department showed it to be the most suitable to use for cyclic voltammetry in the solvent acetonitrile. The potential range of the electrolyte and the solvent combination was found to be +3.0 to -2.8V vs. Ag^+/Ag.

2.4.c - Preparation of the electrolyte Et_4NBF_4

Et_4NBF_4 was prepared by neutralising fluoroboric acid with tetraethylammonium hydroxide, . The product obtained was recrystallised with ethanol twice and then dissolved in acetonitrile. CH_3CN was removed by rotary evaporation (40-45°C) and the white compound obtained was pumped under vacuum overnight and stored in the dry box.

2.4.d - Purification of acetonitrile[5]

Acetonitrile must be carefully purified before use, and should be free from oxidisable and reducible impurities. The method of purification used was developed in this department and is an extension of the method of Walter and Ramaley. It consists of a series of refluxes of HPLC Grade S acetonitrile (Rathburn Chemicals Ltd.) in a

Pyrex still equipped with 0.75m vacuum jacketed separating column and protected from atmospheric moisture. The first step of the purification consisted of a reflux of the solvent over $A\ell C\ell_3$ (15g ℓ^{-1}) for 1h. The solvent was then distilled off. $A\ell C\ell_3$ was used to remove acrylonitrile present in the solvent.

The second step consisted of a reflux of the solvent over $KMnO_4$ (10g ℓ^{-1}) and Li_2CO_3 (10g ℓ^{-1}) for 15 min. $KMnO_4$ and Li_2CO_3 are used to remove trace amounts of aromatic impurities and also to neutralise any $HC\ell$ possibly formed during step 1. During step 3 acetonitrile was refluxed over $KHSO_4$ (15g ℓ^{-1}) for 1h. $KHSO_4$ is a strong enough acid to decrease the amine content, probably generated from step 2, below the level detectable by gas chromatography. This is followed by a reflux of acetonitrile (1h) over CaH_2 (20g ℓ^{-1}). To ensure further dryness acetonitrile is refluxed for ½h over P_2O_5 (1g ℓ^{-1}). The same operation is repeated a second time.

After each reflux acetonitrile is rapidly distilled off. At each step it is topped and tailed by approximately 3%. After each purification acetonitrile is transferred to a glove box and stored over previously activated 3A molecular sieves. Acetonitrile is degassed in vacuo three times before use. If traces of impurities persist the solvent is treated with activated alumina (neutral 60 mesh) in vacuo. Purified acetonitrile has an absorbance of <0.05 at 200 nm and an apparent U.V. cut-off point at ca. 175 nm. The U.V. spectrum was recorded with reference to distilled water.

2.4.e - Electrochemical cells

Room temperature and low temperature electrochemical cells (Figs. 7,8) were used for the present work. The room temperature cell was used more often. It was designed to be used when studying air-sensitive material. It is a three-compartment evacuable cell. These compartments are respectively, the reference, the bridging, and the working compartments. The three compartments were joined by B14 and B19 greaseless "O" rings and were made from 10, 15 and 24 mm diameter glass tubing. Connection between the different parts of the cell was by Unfired Vycor tips joined to glass (4 mm ϕ) by heat shrunk P.T.F.E. tubing. The working compartment was fitted with three electrodes. They were, a working electrode, a reference, and an auxiliary electrode. The reference electrode was made by Ag dipping into 0.1 mol dm^{-3} $AgNO_3$ solution. The working and the auxiliary electrodes were both platinum wires (1.0 mm ϕ) which were sealed through glass by spot welding to tungsten wire; the whole assembly was sheathed in uranium glass.

The low temperature cell (Fig. 8) was designed to study species between -30 and -35°C. It was a less complicated cell and consisted only of a working and an auxiliary electrode. For the present work, WF_6/WF_6^- was used as internal reference couple.

2.4.f - Preparation of solutions for cyclic voltammetry

Solutions for electrochemical studies were prepared in a dry atmosphere glove box. The sample for analysis was first sealed in a frangible ampoule and the cyclic voltammetry cell was evacuated

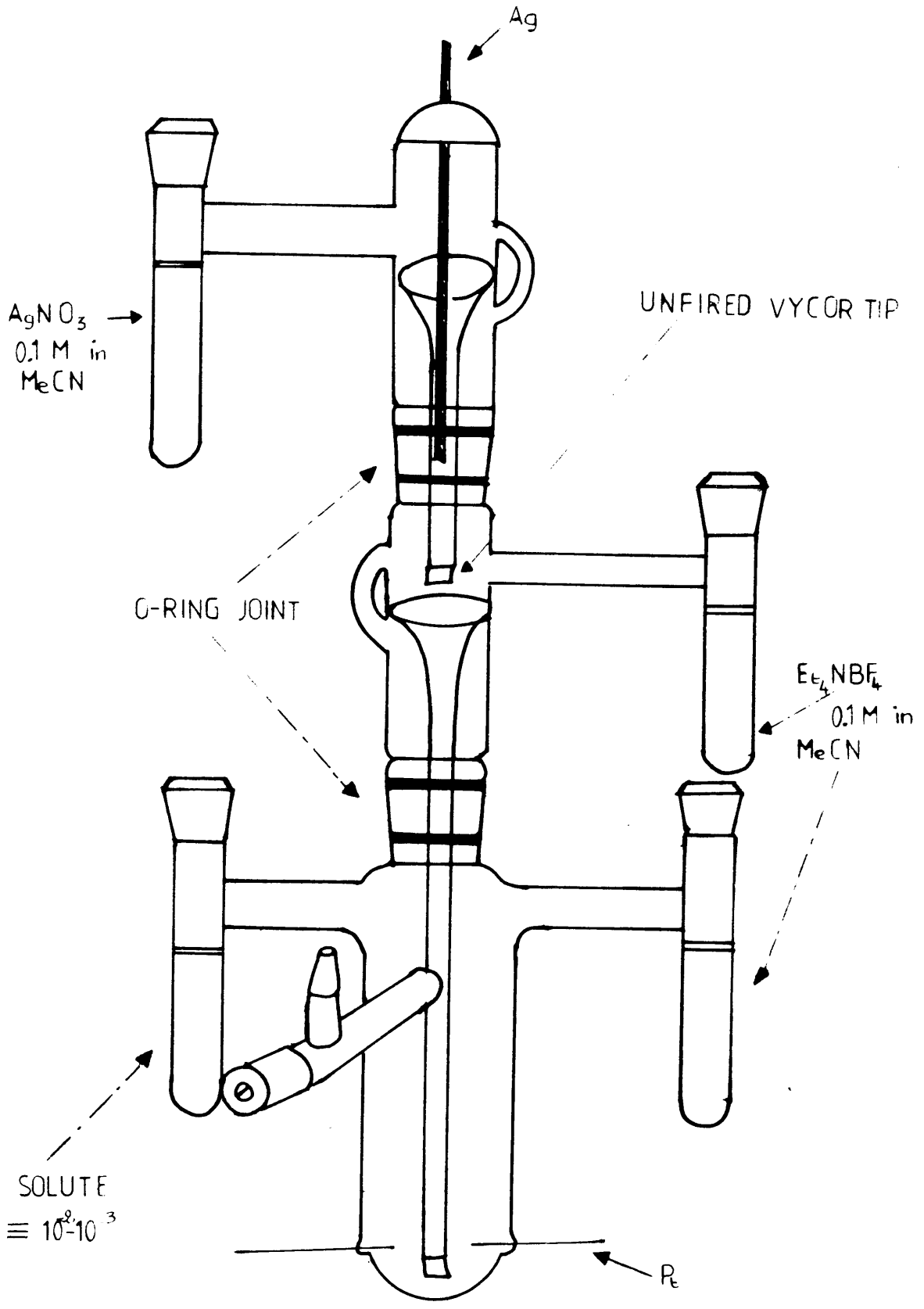

Fig 7 - EVACUABLE CELL FOR CYCLIC VOLTAMMETRY

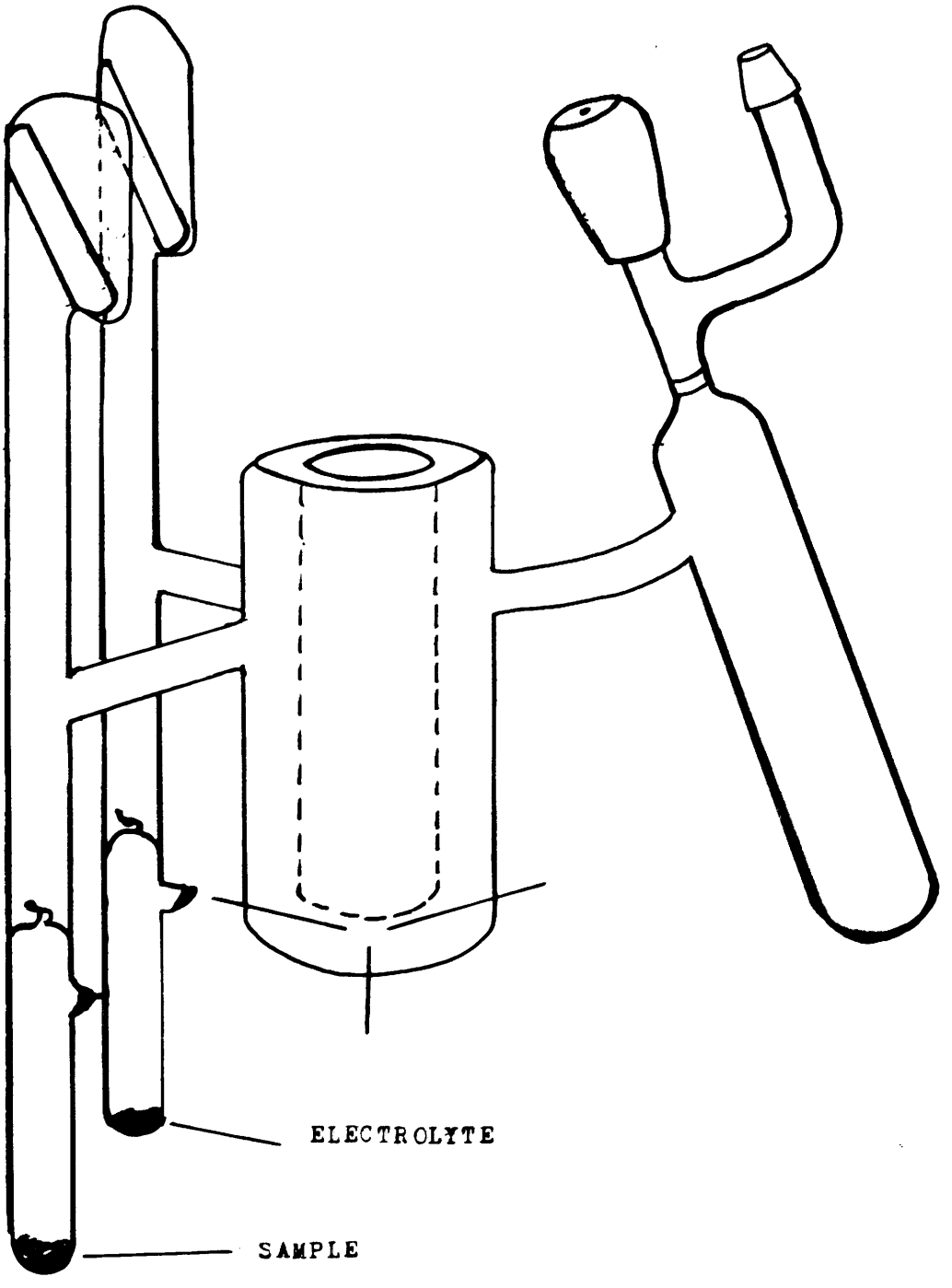

FIG 8 - LOW TEMPERATURE C.V. CELL

and degassed on the vacuum line. The sample as well as the c.v. cell were then transferred to the glove box. The electrolyte solution was made up from 15 ml of solvent acetonitrile and 0.1M of electrolyte. The solution was loaded in the working and bridging compartments (8 cm^3 and 2 cm^3, respectively). The reference compartment was loaded with silver nitrate solution (2 cm^3, 0.1 mol dm^{-3} in CH_3CN). The ampoule with the sample was loaded into one of the working compartment's ampoules. The cell was then reconnected to a vacuum line, where it was re-evacuated and the solutions degassed. It was then connected to a potentiostat (Princeton Applied research model 173 Potentiostat/Galvanostat, linked to a JJ 'XY' plotter, type PL51). When the potential range of the electrolyte was determined, the sample ampoule was broken and the solute dissolved into the electrolyte solution. A voltammogram was recorded at a variety of scan rates, current amplification and voltage scale factors. Fast scan rates ($\geqslant$ 500 mV) were used to study electrochemical processes, which would undergo irreversible reactions in the time scale of a slow scan rate.

A different process was used to prepare the low temperature cell. Approximately 0.005 mmol of the compound and $\simeq$1 mmol of the electrolyte were each loaded in previously evacuated and degassed break-seal tubes. The tubes were connected back to the vacuum line and left to degass overnight, then sealed to the low temperature cell. Acetonitrile was vacuum distilled into the side-arm vessel of the cell. The seal of the tube containing the electrolyte was broken using a bar magnet. The electrolyte was dissolved in CH_3CN and tipped into the working compartment.

When the potential range of the electrolyte was determined the seal of the tube containing the compound was broken, also using a bar magnet. The compound was dissolved in acetonitrile and a voltammogram was recorded both at room temperature and at low temperature. The solution was cooled down by means of a cold finger which dipped into the solution. All voltammograms were recorded on a "Princeton Applied research model 173 Potentiostat/Galvanostat", linked to a JJ 'XY' plotter, type PL51.

2.5 Preparation of Thin Films of Nickel[46,47]

A variety of methods are available for the preparation of metallic films. They are widely used in crystallography and surface chemistry studies.

Evaporated metal films are made up of small crystallites which adhere together, producing a large specific surface and a porous structure. The large specific surface results from the aggregation of primary particles and the removal of part of a parent solid results in the formation of pores.

Evaporated nickel films were the subject of study of Anderson and Baker, and other workers. In the present work nickel films were prepared by vacuum evaporation. The making of the film was performed under vacuum at a pressure below 10^{-3} torr, in a double limb reaction vessel (Fig. 9). A pair of tungsten electrodes, sealed in glass, were connected to one side of the double limb reaction vessel. A nickel wire of approximately 0.5 mm diameter was spot welded to the tungsten electrodes. Before making the film, the reaction vessel was carefully

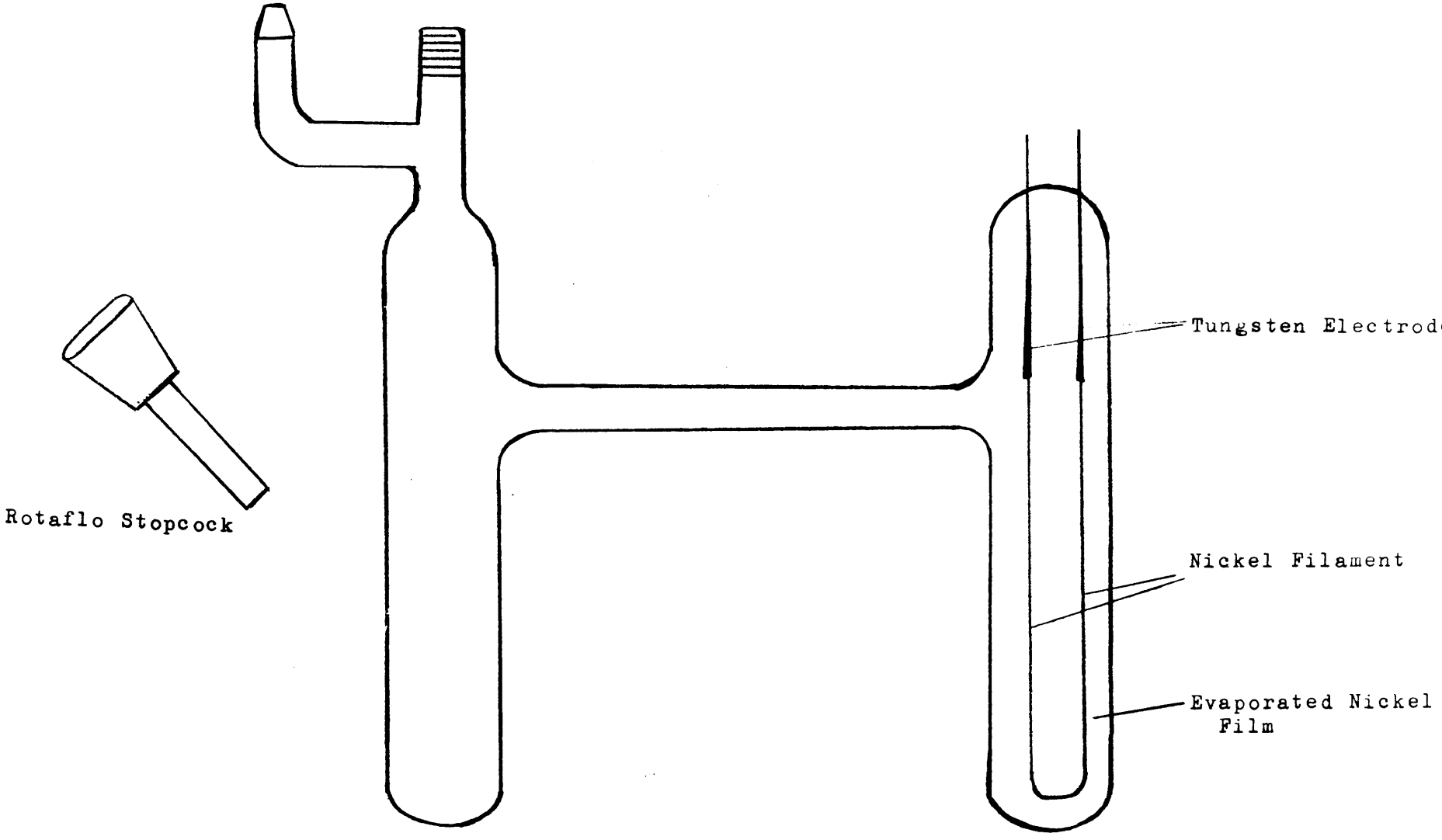

Fig9- Double-Limbed reaction vessel for prepration of nickel film.

flamed out. A current of magnitude 5 amps was then applied for a duration of approximately two days, and the temperature of the nickel wire was kept below that of the evaporation of nickel (< 1450°C). The reaction vessel was evacuated at regular intervals to ensure the removal of the nickel oxide layer that had detached from the wire. When the deoxidation process was finished the magnitude of the current was increased and with it the temperature of the nickel wire. At this stage molecules from the nickel wire were converted to the gaseous phase by heating. The gaseous material was then deposited on the glass walls of the reaction vessel as a film. This operation was continued until the required thickness of film was attained. The specific surface of the nickel film can easily be calculated from the formula:

$$S = \frac{6}{\rho \ell}$$

where S = specific surface

ℓ = edge of a particle supposed to be perfectly cubic

ρ = density of the solid.

2-6 Quantitative analysis

Quantitative analysis of the compounds prepared was by Malissa and Reuter, Elbach, West Germany and also be atomic absorption spectroscopy in Glasgow University, where the analysis was carried out by Mr. J. McCaig.

A brief account on the method used for the analysis and quantitative determination of nickel and molybdenum is given below, as

well as an introduction to the method of atomic absorption spectroscopy.

Principle of the method

Atomic absorption spectroscopy is one of the most important techniques for the analysis of the elements. The method is based on the absorption of radiation in the UV-visible region of the spectrum.

Atomic absorption involves the excitation of valence electrons; this necessitates the conversion of the element to the atomic state. The common way to produce atoms is to use a reducing flame such as the C_2H_2-N_2O flame. Each element can undergo many electronic transitions, which result in a series of sharp lines forming a spectrum, but each element has its uniquely characteristic spectrum.

The change in energy within an atom, when an electronic transition is involved, is related to the frequency of the radiation emitted by Planck's law

$$\Delta E = h \nu$$

where h is Planck's constant, ν is the frequency in hertz.

When a parallel beam of continuous radiation of intensity I_o passes through a flame containing the sample in the form of atomic vapour, only part of the radiation is transmitted. This can be expressed by the Lambert-Beer law as

$$A = \log \frac{I_o}{I} = \varepsilon \ell c$$

A: absorbance

C: concentration of the analyte atoms in the flame (number of atoms per cm^3)

ℓ: length of absorption cell (cm)

ε: is a constant for a given system.

This expression predicts a linear relationship between absorbance and concentration as long as ε and ℓ remain constant.

Sample preparation

To perform atomic absorption analysis, samples of the complexes (~ 30 mg) were prepared in frangible ampoules to prevent air attack and loss of volatile components. The external surface of the ampoule was washed with acetone and dried thoroughly before accurately weighing it. The ampoule was then broken over a large filter funnel leading to a 100 cm^3 conical flask where the contents of the ampoule were quantitatively transferred. Using a Pasteur pipette; both the ampoule and the funnel were washed with 5 cm^3 of "Analar" HNO_3 to remove any residues. The ampoule was finally rinsed with 10 cm^3 of distilled water, the washings being added to the conical flask via the funnel. The resulting solution was "digested" just below its boiling point for approximately 30 minutes and then cooled. It was transferred quantitatively to a 100 cm^3 volumetric flask and H_2O was added to bring the total volume of the solution to 100 ml. If there was any evidence for pieces of glass from the frangible ampoule, they were removed from the solution by filtering it through a tared sinter/glass

crucible. The weight thus obtained was used to correct the original sample weight.

10.00 cm^3 of this solution was taken and diluted to 100 cm^3 in a volumetric flask and this was used for all subsequent spectrophotometric measurements. Samples for molybdenum analysis were prepared in an identical manner with addition of 0.1% w/v Na_2SO_4 at the final dilution stage to minimise interference effects in the N_2O-C_2H_2 flame.

Standard solutions in the range 0-5 $\mu g/cm^3$ for Ni and 0-50 $\mu g/cm^3$ for Mo were prepared by serial dilution of the appropriate "Spectrosol" standard nickel(II) nitrate solution or molybdenum dissolved in HCℓ solution. In each case the sample and standard solutions were matrix matched with respect to HNO_3 and Na_2SO_4 concentrations.

The absorbances of the nickel and molybdenum solutions were obtained using a Perkin Elmer 306 Atomic Absorption Spectrophotometer, with an air-acetylene flame for nickel and a nitrous oxide-acetylene flame for molybdenum. In each case the manufacturer's standard operating conditions were used, as outlined in Table(1.2).

The average absorbance for the calibration standards were used to construct calibration graphs for each element and the solution concentration of the unknown samples was obtained by reading off the Absorbance-Concentration plot. The values in $\mu g/cm^3$, thus obtained were then converted to unit/percentage using the following formula:

$$\text{Wt \%} = \frac{\text{Concentration } (\mu g/cm^3) \times \text{sample volume} \times \text{dilution factor} \times 10^{-4}}{\text{Wt}}$$

Concentration : value in $\mu g/cm^3$ read from graph

Sample volume : 100 cm^3

Dilution factor : 10

Table 1.2 : Operating conditions.

	Ni	Mo
Wavelength	232.0 mm	313.3 mm
Slit	0.2 mm	0.7 mm
Flame	Air-acetylene (oxidizing	Nitrous oxide-acetylene (reducing)
Burner length	10 cm	5 cm
Linear range	0-5 g/cm^3	0-50 g/cm^3
Source	Hollow cathode "Intensitron" lamp	Hollow cathode "Cathodeom" lamp
Matrix	5% HNO_3 soln	5% HNO_3+0.1% W/v Na_2SO_4
Signal mode	10 s integration	10 s integration.

CHAPTER III

Oxidation of cobalt by WoF_6, MoF_6, UF_6 and NO^+ in CH_3CN

INTRODUCTION

Cobalt was first discovered by Brandt in about 1735. It mainly occurs associated with nickel, silver, lead and iron in several ores, for example, Cobaltite, Smaltite and Erythrite.[50] Cobalt metal is ferromagnetic and like, iron and nickel, it is hard with a white silvery appearance.

The element is known to exist in two forms, hexagonal close packed below 661 K and cubic close packed above the same temperature. In the cubic form each atom has 12 nearest neighbours situated at 2.506 Å, and in the hexagonal form there are six at 2.507 Å and six at 2.497 Å. This makes an average distance of 2.502 Å. The stable structure of cobalt at room temperature depends on the grain size, hence it is cubic close packed for small grain size and for larger grain size the stable structure is the hexagonal close packed form. Table 3-1 summarises some of the physical properties of cobalt metal.[48]

Cobalt(II) is the only d^7 ion of common occurrence in aqueous chemistry. The divalent and trivalent oxidation states are those most often encountered in its aqueous chemistry. Co(II) is more stable, with respect to oxidation, in acid solution than it is in basic solution. Addition of complexing agents such as NH_3 facilitate the oxidation of cobalt(II) to Co(III). Similar to iron(II), cobalt(II) forms a wide range of hydrated salts.

When heated in air at a temperature above 573 K, massive cobalt is oxidised producing Co_3O_4 and CoO. The metal also reacts with the halogens producing CoX_2 ($X = C\ell^-, Br^-, I^-$) and CoF_3 with fluorine.[14,37]

Table 3_1 Some physical properties of cobalt metal

Atomic weight (Mg/g mol^{-1})	58.93
Crystal structure	Hexagonal close packed,or, Cubic close packed.
Atomic radius (A)	1.25
Principal oxidation number	+2, +3
Ionic radii (A)	0.72, (for Co^{II}) 0.63, (for Co^{III})
Ionization energies (Ei/ev)	7.86, 17.06
Electron affinity (Ee/ev)	0.9
Electronegativity	1.8
Density (ρ/kgm^{-3})	8900
Melting point (Tm/k)	1765
Boiling point (Tb /k)	3170
Specific latent heat of fusion (L /Jkg^{-1})	25 X 10^4
Specific heat capacity (Cp /Jkg^{-1} K)	420

A number of complexes of Co(II) are known to exist with different stereochemical structures; among them the octahedral and tetrahedral geometries being the most common. Often, octahedral complexes of Co are pink, while tetrahedral complexes are blue, or sometimes green. This, however, does not constitute a rule, as orthosilicate and anhydrous cobalt chloride are blue, while anhydrous cobalt bromide is green, but all contain octahedral Co(II). Some tetrahedral derivatives, for example, $Co(DPM)_2$ are pink (DPM = dipivaloymethanoate).

Octahedral Co(II) complexes can be either high spin having the electronic configuration $t_{2g}^{5} e_g^{2}$, or low spin with the electronic configuration $t_{2g}^{6} e_g^{1}$, the latter being subject to Jahn-Teller distortion. A strong field is required to cause spin-pairing, thus low spin complexes are fewer than high spin complexes. Almost all known tetrahedral complexes are high spin with the electronic configuration $e^4 t_2^3$. The theory for the interpretation of the spectral properties of cobalt(II) is essentially known,[61,62] but assignments are somewhat tentative because its electronic spectra are often poorly resolved.[37]

Cobalt(II) forms many stable octahedral ($t_{2g}^{5} e_g^{2}$) and tetrahedral ($e^4 t_2^3$) complexes, for example, $[Co(MeCN)_6][BF_4]_2$ and $[Bu^n_4N][CoI_4]$.[63] Anhydrous cobalt(II) salts react with ammonia, producing ammines, for example $[Co(NH_3)_6]X_2$ (X = Cl, Br, I, ClO_4 and BF_4). These complexes contain the octahedral $[Co(NH_3)_6]^{2+}$ ion.

Methyl cyanide forms complexes with cobalt either by recrystallisation of anhydrous halides from methyl cyanide or by reaction of the metal with halogens in acetonitrile medium. The tetrahedral $CoX_2.3MeCN$

which is formed contains one uncoordinated acetonitrile that is removed by pumping under vacuum, giving $CoX_2.2MeCN$. Reaction of cobalt with bromine in acetonitrile produces unstable $[Co(MeCN)_6^{2+}][Br_3^-]_2$.

The preparations of the hexafluoromolybdate(V) and hexafluorotungstate(V) of cobalt(II) in acetonitrile have already been performed in this department and infrared and Raman spectra of the solid complexes were recorded.[3,36] The coordinating ability of acetonitrile towards 3d and post-transition elements in presence of the anions WF_6^-, MoF_6^- was demonstrated. In the present work the spectral properties of cobalt(II) in acetonitrile have been investigated in order to determine the environment about cobalt(II) and the strength of the ligand field. It is hoped that this could be useful to others in the characterisation of new cobalt(II) complexes or in the use of cobalt(II) as a spectroscopic probe. The electronic spectra presented were interpreted using ligand field theory. The electrochemical properties of cobalt(II) in acetonitrile have also been investigated using cyclic voltammetry.

3.1 Experimental

Cobalt powder, purity 99.99%, was used as supplied (Goodfellow Metals Limited).

Acetonitrile (Rathburn Chemicals Ltd.) was purified according to the method described in Chapter II and was stored in an argon atmosphere glove box (Lintott Engineering).

MoF_6 (Ozark Mahoning), WF_6 (Ozark Mahoning) and UF_6 (British Nuclear Fuels Ltd.) were purified by low temperature trap-to-trap distillation over activated sodium fluoride. They were stored at

77K over activated sodium fluoride, in specially designed breakseal flasks to prevent their hydrolysis.

$NOPF_6$ (Fluorochem Ltd.) was used, as supplied, and stored in an argon atmosphere glove box.

Weighing of the chemicals inside the glove box was by means of an electronic balance (Type Sartorius Model 1205 MP) with an estimated error of ± 0.004g.

Special care was taken to avoid contamination of reagents and material by moisture and oxygen, so all glassware was flamed out under vacuum before use, using a gas/oxygen torch. Reactions and preparation of samples for analysis were performed either in the dry glove box or on a conventional high-vacuum system.

3.2 Oxidation of Cobalt Metal by WF_6 in CH_3CN

A flamed-out reaction vessel was loaded with cobalt metal in the dry box. When the reaction vessel was re-evacuated, acetonitrile and tungsten hexafluoride were added by vacuum distillation at 77K. The solution mixture was shaken for a few hours before completion of the reaction. When using a large excess of WF_6 the reaction was almost instantaneous. After removal of the volatile material a pink solid was isolated. This was redissolved in acetonitrile and its electronic spectrum recorded.

In order to analyse the spectrum, the assumption that Co(II) was present as $[Co(NCMe)_6]^{2+}$ in MeCN was made. Reference to Tanabe-Sugano and Orgel diagrams for octahedral d^7 species shows that

the ground state (^4F) of the free ion splits into $^4A_{2g}$, $^4T_{2g}$ and $^4T_{1g}$ components. A high spin d^7 ion has two spin quartet free ion terms, ^4F and ^4P, and a number of doublet states.[38] The electronic spectrum of a solution of solvated Co(II) hexafluorotungstate(V) presents a multistructured band in the visible region ν_{max} 20,600 cm^{-1} and a very weak band in the near infrared at ν_{max} 9,600 cm^{-1} (Fig. 10).

The multistructured band shows three maxima. By reference to the energy level diagram (Fig. 11) we can straightforwardly assign the weak band to the $^4T_{1g} \longrightarrow {}^4T_{2g}$ transition. We may also, tentatively, assign two of the maxima in the multistructured band to $^4T_{1g} \longrightarrow {}^4A_{2g}$ ν_{max} 19,800 cm^{-1} and $^4T_{1g} \longrightarrow {}^4T_{1g}$ (P) ν_{max} 20,600 cm^{-1}. The third maximum probably originates from a spin-orbit coupling effect where states of different spin multiplicity mix. This results in the borrowing of intensity by spin forbidden bands from spin allowed bands.[37] On this basis it is possible to interpret the spectrum of the solution of solvated $[Co(NCMe)_6]^{2+}$ in acetonitrile. The expressions of the crystal field of the d^7 configuration relative to the ^4F free ion term as zero are given below:

Term	Energy
$^4T_{1g}$ (F)	$\frac{1}{2}[15B - \frac{3}{5}\Delta - (225B^2 + 18B\Delta + \Delta^2)^{\frac{1}{2}}]$
$^4T_{2g}$ (F)	$^1/_5\ \Delta$
$^4T_{1g}$ (P)	$\frac{1}{2}[15B - \frac{3}{5}\Delta + (225B^2 + 18B\Delta + \Delta^2)^{\frac{1}{2}}]$
$^4A_{2g}$ (F)	$^6/_5\ \Delta$

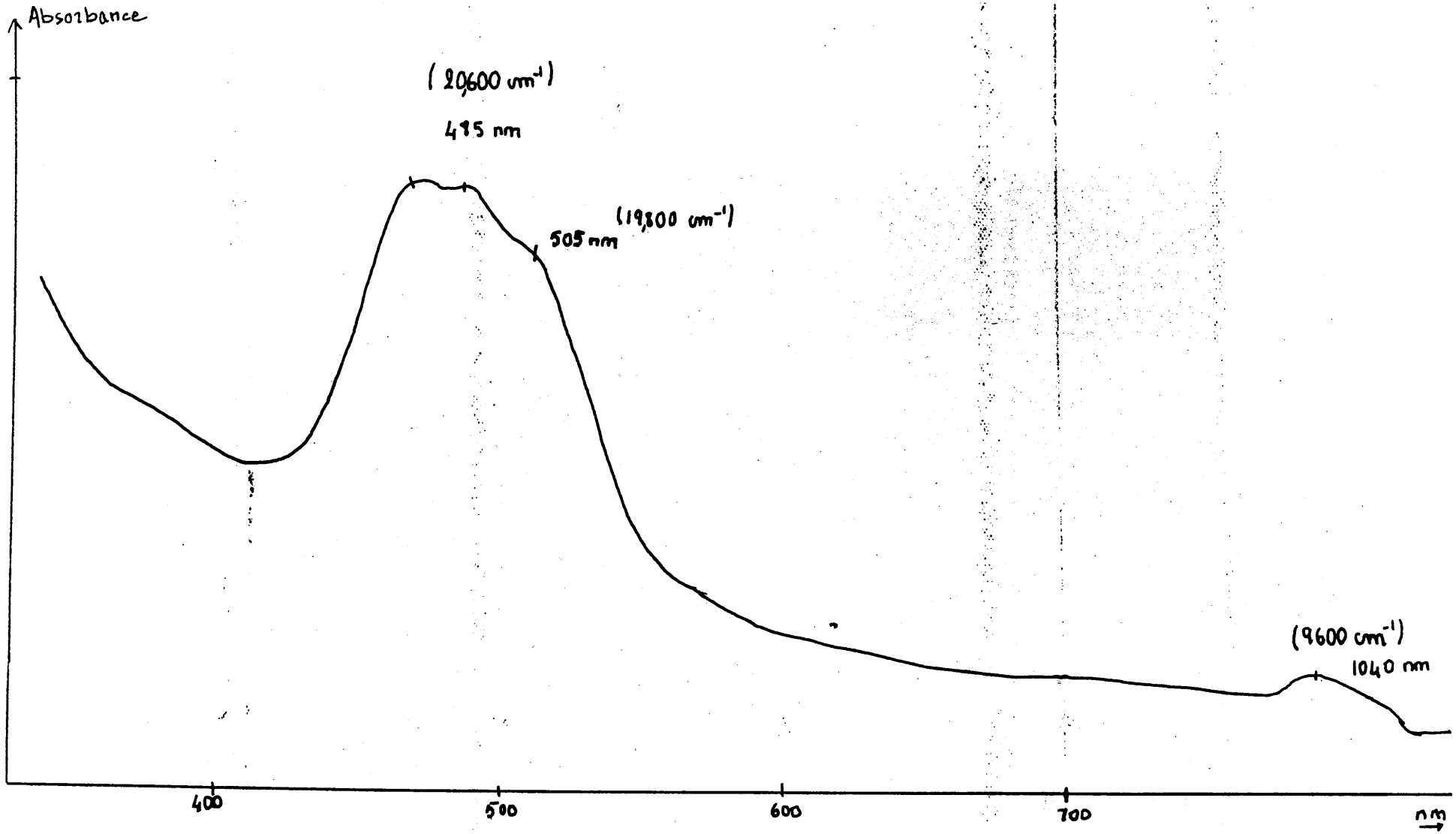

fig 10 - U.V spectrum of $(Co(NCMe)_2)(WF_6)_2$

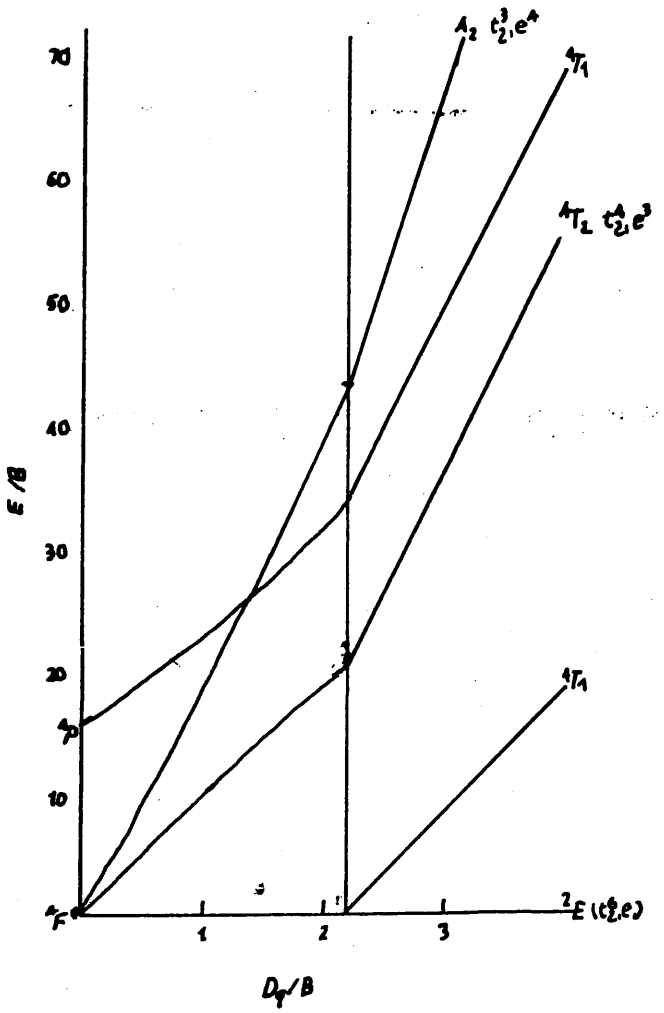

fig 11 – Partial energie level diagram (Tanabe–Sugano) for d^7 ions in an octahedral field

The observed bands assigned to $^4T_{1g}(F) \longrightarrow {}^4T_{2g}(F)$, $^4T_{1g}(F) \longrightarrow {}^4T_{1g}(P)$ and $^4T_{1g}(F) \longrightarrow {}^4A_{2g}(F)$ transitions have energies

Transition	Energy
$^4T_{1g}(F) \longrightarrow {}^4T_{2g}(F)$;	$\frac{1}{5}\Delta - \frac{1}{2}[15B - \frac{3}{5}\Delta - (225B^2 + 18B\Delta + \Delta^2)^{\frac{1}{2}}]$ (1)
$^4T_{1g}(F) \longrightarrow {}^4T_{1g}(P)$;	$\frac{1}{2}[-\frac{3}{5}\Delta + (225B^2 + 18B\Delta + \Delta^2)^{\frac{1}{2}}]$ $-\frac{1}{2}[15B - \frac{3}{5}\Delta - (225B^2 + 18B\Delta + \Delta^2)^{\frac{1}{2}}]$ (2)
$^4T_{1g}(F) \longrightarrow {}^4A_{2g}(F)$;	$\frac{6}{5}\Delta - \frac{1}{2}[15B - \frac{3}{5}\Delta - (225B^2 + 18B\Delta + \Delta^2)^{\frac{1}{2}}]$ (3)

Δ is the ligand field splitting parameter, it expresses the magnitude of the interaction between the two $^4T_{1g}$ states - and it also gives an idea on the size of the interaction between the transition metal atom and the ligand. B is the Racah parameter; it is introduced to measure the different types of electron-electron interactions which occur. For a given ion, the Racah parameter B varies as a function of the ligand bound to that ion. Its value decreases upon coordination of the free ion. The reduction of the value B in a complex ion is expressive of the degree of covalency in the metal-ligand bond, and generally, the greater the covalency in the metal-ligand bond, the greater the reduction in B. During complex formation, the lone pair of the ligand tends to penetrate the d-shell of the metal ion. This decreases the effect of the nucleus on the d-electrons and tends to expand the d-shell.

When Δ and B values are known it is possible to determine the region of spectrum where transitions are expected by using a Tanabe-Sugano diagram. In the present case the energies of the transitions involved are known; this enables the determination of Δ and B. The Tanabe-Sugano diagram is presented as a function of E/B (E is the energy of a state), versus d_q/B ($d_q = 0.1\ \Delta$). The horizontal baseline represents the ground state. A vertical from the ground state to an excited state gives a direct measure of the transition energy as a function of d_q and B. The expressions (1), (2) and (3) are then divided by B and similarly the energies of the terms themselves are also divided by B and expressed as functions of Δ/B (equations 4, 5 and 6).

$$\frac{E(^4T_{1g}(F) \longrightarrow {}^4T_{2g}(F))}{B} = \frac{1}{2}\left[\frac{\Delta}{B} - 15 + \left(225 + 18\frac{\Delta}{B} + \frac{\Delta^2}{B^2}\right)^{\frac{1}{2}}\right] \qquad (4)$$

$$\frac{E(^4T_{1g}(F) \longrightarrow {}^4T_{1g}(P))}{B} = \left(225 + 18\frac{\Delta}{B} + \frac{\Delta^2}{B^2}\right)^{\frac{1}{2}} \qquad (5)$$

$$\frac{E(^4T_{1g}(F) \longrightarrow {}^4A_{2g}(F))}{B} = \frac{1}{2}\left[\frac{3\Delta}{B} - 15 + \left(225 + 18\frac{\Delta}{B} + \frac{\Delta^2}{B^2}\right)^{\frac{1}{2}}\right] \qquad (6)$$

Now we can either use the free ion value of B and determine the ratios E_1/B, E_2/B and E_3/B and by plotting them in a Tanabe-Sugano diagram determine the value of Δ and B', or, we can also determine the value of Δ from equations 4, 5 and 6, provided that we eliminate the B's appearing in each equation. This is feasible if we divide equation 6 by equation 4 and substitute the expression $\left(225 + 18\frac{\Delta}{B} + \frac{\Delta^2}{B^2}\right)^{\frac{1}{2}}$ by the numerical value of $\frac{E(^4T_{1g}(F) \longrightarrow {}^4T_{1g}(P))}{B}$ which equals 20600/B. The

value of Δ determined by this method is equal to 10,200 cm^{-1} and $B' = 775\ cm^{-1}$.

The magnitude of the ligand field splitting parameter (Δ) and the value of B for some relevant CoL_6^{2+} complexes as well as the energies of the electronic transitions of the same ligands are summarised in Table (3.2). Comparison of these parameters show that acetonitrile has a stronger ligand field than ammonia and water, hence it is most probably a better σ-donor.

The reduction of 70% in the value of B for solvated $[Co(CH_3CN)_6]^{2+}$ fits perfectly the literature expectations,[37] and, as expected, the energy difference $\nu_2-\nu_1$ equals the above determined value of 10 d_q.

The transition $^4T_{1g}(F) \longrightarrow {}^4T_{1g}(P)$ and $^4T_{1g}(F) \longrightarrow {}^4T_{2g}(F)$ are far more intense than the $^4T_{1g}(F) \longrightarrow {}^4A_{2g}(F)$ transition, probably because the latter is attributed to a two-electron jump from the $t_{2g}^5 e_g^2$ ground state to the $t_{2g}^3 e_g^4$ excited state.

Previous work[3] reports that the solid isolated is $[Co(NCMe)_5][WF_6]_2$. A possible explanation is that a loss of acetonitrile may have occurred during the isolation of the compound under vacuum. Unpublished work performed in this department indicates that coordinated acetonitrile is easily lost from $[Fe(NCMe)_6][PF_6]_2$ on thermal decomposition.[49] D.T.A. analysis has shown that the first acetonitrile was lost at 38°C. The overall process is considered to be:

$$Co(s) + 2WF_{6\ solv} \longrightarrow [Co(NCMe)_6]^{2+} + 2WF_6^-$$

$$\longrightarrow [Co(NCMe)_5][WF_6]_2\ (s)$$

Table 3-2 : Spectral parameters for octahedral Co (II) complex

CoL_6^{2+}	ν_1 cm^{-1}	ν_2 cm^{-1}	ν_{33} cm^{-1}	10 dq cm^{-1}	B cm^{-1}	Ref.
$CoCl_2$	6600	13300	17150	6900	780	66
$(Co(H_2O)_6)^{2+}$	8100	16600	19400	9200	825	67
$(Co(NH_3)_6)^{2+}$	9000		21100	10200	885	67
$(Co(bipy)_3)^{2+}$	11300		22000	12670	791	68
$(Co(MeCN)_6)^{2+}$	9600	19800	20600	10200	775	this work
$(Co(py)_6)^{2+}$	9800		20400			65

bipy > MeCN ~ NH_3 > H_2O > Cl

3.2a - Infrared spectrum of cobalt(II) hexafluorotungstate

Raman spectra could not be recorded, possibly because fluorine is a weak Raman scatterer. Evidence for WF_6^- anion as well as the coordination of acetonitrile has however been obtained from the infrared spectrum recorded for the solid $[Co(NCMe)_5][WF_6]_2$, over the region 200-4000 cm^{-1}. A sharp intense band in the region 2295 cm^{-1} is assigned to C≡N fundamental stretch and a weaker band at 2330 cm^{-1} is assigned to a combination of the C-C stretch and the CH_3 deformation modes.[64] The intensity of the latter arises from Fermi resonance between the combination band and the C≡N stretching vibration, because both the combination band and the stretching vibration have A_1 symmetry.

The shift in the C≡N stretching vibration upon coordination of acetonitrile implies that nitrogen is the donor atom. A sharp band at ν_{max} = 600 cm^{-1} has been assigned to a WF_6^- vibration.

In the case where a large excess of WF_6 was used, the solution develops a brown colour after shaking, and a brown solid is isolated. In this case the infrared spectrum of the complex of Co(II) shows an additional band at 705 cm^{-1} assigned to the anion WF_7^-. A fluoride ion transfer presumably occurs in parallel with the oxidation of cobalt metal by tungsten hexafluoride. This has been reported earlier and the following equilibrium was proposed:[36]

$$WF_{6\ solv} + e^- \rightleftharpoons WF_{6\ solv}^-$$

$$WF_{6\ solv}^- + WF_{6\ solv} \rightleftharpoons WF_{7\ solv}^- + WF_{5\ solv}.$$

Table 3-3: Infrared spectrum of solid $(Co(NCMe)_5(WF_6)_2$

Frequency (cm^{-1})	Assignement
2330	comb. CH_3CN $(\nu_2+\nu_1)(A_1)$
2295	C≡N stretch. $(\nu_3)(A_1)$
1020	CH_3 rock. $(\nu_7)(E)$
940	C-C stretch $(\nu_4)(A_1)$
705	WF^-_7
600	$\nu_3\ WF^-6$

FIG -1.4 C.V of $(Co(CNMe)_6)(WF_6)_2$

3.2b - Cyclic voltammetry of $[Co(NCMe)_6^{2+}][WF_6]_2$

The electrochemistry of Co(II) hexafluorotungstate(V) was investigated by cyclic voltammetry at room temperature. The cell was prepared as described in Chapter II.

The cyclic voltammogram shows a wave at $E_{1/2}$ = 0.65V vs. Ag^+/Ag and a weak quasi-reversible wave at $E_{1/2}$ = 0.29V vs. Ag^+/Ag. A third wave was observed at a more negative potential, that is, $E_{1/2}$ = 1.66V vs. Ag^+/Ag. The following assignments were made by reference to previous studies of alkali metal and silver WF_6^- salts.[57,58]

$$WF_6 \xrightarrow{e^-} WF_6^- \qquad E_{\frac{1}{2}} = 0.65V \text{ vs. } Ag^+/Ag$$

$$Co^{2+} \xrightarrow{2e^-} Co(s) \qquad E_{\frac{1}{2}} = 0.29V \text{ vs. } Ag^+/Ag$$

$$WF_6^- \xrightarrow{-e^-} W(IV) \qquad E_{\frac{1}{2}} = -1.66V \text{ vs. } Ag^+/Ag$$

The potential value of the couple Co^{2+}/Co in acetonitrile solution is equivalent to the value determined in aqueous medium. In aqueous solution the cobalt-cobaltous potential could not be obtained experimentally because of lack of reversibility in the Co/Co^{2+} potential so its average value has been determined from the work of a number of investigators.

3.3 Oxidation of Cobalt by MoF_6

A flamed out reaction vessel was loaded with cobalt metal, in the dry box. Acetonitrile and molybdenum hexafluoride were added by vacuum distillation at 77K. Different ratios were used - Co:MoF_6, 1:1,

1:10, 10:1. When the solution mixture reached room temperature a pink solid was rapidly formed in each case. The complex is almost insoluble in acetonitrile and this prevented an electronic spectrum from being recorded. The solid complex was isolated and its infrared spectrum recorded (Table 3.4), which gives evidence of coordination of acetonitrile and presence of the anion MoF_6^-. A band at 625 cm^{-1} is attributed to $\nu_3(MoF_6^-)$. Coordination of acetonitrile through its nitrogen lone pair is evident from shifts in frequency of C≡N stretching vibration appearing at 2300 cm^{-1}. The band at 2330 cm^{-1} indicates a combination of the C-C stretch and the CH_3 deformation modes. An intermediate band at 945 cm^{-1} is assigned to a C-C stretch vibration.

3.4 Oxidation of Cobalt Metal by UF_6 in CH_3CN

Oxidation of cobalt metal by uranium hexafluoride in acetonitrile medium was attempted but no reaction took place. When UF_6 was added to the solution mixture Co and CH_3CN, a yellow colour quickly developed even at low temperature. UF_6 was being reduced by acetonitrile producing UF_5.[69] The yellow colour changed rapidly to green and after a few hours became brown as a result of solvent polymerisation.

The reduction of UF_6 to UF_5 was followed spectrophotometrically and spectra of UF_6 in CH_3CN were recorded every hour until polymerisation of the solvent occurred. The intensity of the bands increased with time and a band at ν_{max} = 9000 cm^{-1} has been assigned to an f-f transition. Reduction of UF_6 probably occurs in parallel with the fluorination and polymerisation of acetonitrile.

Table 3-4 : Infrared spectrum of solid

$(Co(NCMe)_6)(MoF_6)_2$

Frequency (cm^{-1})	Assignement
2330	Comb CH_3CN ($\nu_2+\nu_1$) (A_1)
2300	C≡N stretch (ν_3) (A_1)
945	C-C stretch (ν_4) (A_1)
625	$\nu_3 MoF_6^-$

3.5 Oxidation of Cobalt Metal by NO^+

The oxidation reaction of cobalt metal by NO^+ cation has apparently not been reported previously but as expected from the $E_{\frac{1}{2}}$ data obtained, it occurs readily at room temperature. The reaction procedure is basically the same as described earlier for the Co(II) hexafluoromolybdate(V) and tungstate(V).

The required amounts of Co metal and $NOPF_6$ were loaded in a flamed out reaction vessel inside the argon atmosphere box. After evacuation of the reaction vessel, solvent acetonitrile was added by vacuum distillation at 77K. The reactants were allowed to warm to room temperature and when $NOPF_6$ was dissolved in acetonitrile a non-condensible gas, presumed to be NO, was evolved. The solution mixture was shaken overnight. After completion of the reaction the pink solid formed was allowed to settle and the solution was decanted into the empty limb. Both the solid and solution were cooled to liquid nitrogen temperature and the flask was opened under vacuum to allow excess NO to be evacuated. Excess solvent was removed by slow distillation and when the compound was perfectly dry the reaction vessel was sealed off with a torch. The solid complex was stored in the dry box.

The infrared spectrum of the complex suggests the presence of coordinated acetonitrile and a strong broad band at ν_{max} 840 cm^{-1} is assigned to a $\nu_3(PF_6^-)$ vibration and a very strong band at ν_{max} 560 cm^{-1} assigned to $\nu_4(PF_6^-)$.

The electronic spectrum of the complex was recorded over the region 1,000-50,000 cm^{-1} and it indicates that the complex prepared

Table 35 : Infrared spectrum of solid $(Co(NCMe)_5)(PF_6)_2$

Frequency (cm^{-1})	Assignement
2330	comb. CH_3CN $(\nu_2+\nu_1)(A_1)$
2300	C≡N stretch $(\nu_3)(A_1)$
1050	CH_3 rock. (ν_7) (E)
945	C-C stretch $(\nu_4)(A_1)$
840	T_{1u} PF_6
560	T_{1u} PF_6
400	C-C≡bend

contains $[Co(NCMe)_6]^{2+}$ in solution.

The spectrum shows a multistructural band at ν_{max} 20,400 cm^{-1} and a weaker band at ν_{max} 9,530 cm^{-1}. A weak band was also observed at ν_{max} 29,850 cm^{-1}.

By reference to the electronic spectrum of $[Co(NCMe)_6][WF_6]_2$ solution and the Tanage-Sugano diagram for a d^7 species, the following assignments were made:

Energy	Transition
9530 cm^{-1}	$^4T_{1g}(F) \longrightarrow {}^4T_{2g}(F)$
19,230 cm^{-1}	$^4T_{1g}(F) \longrightarrow {}^4A_{2g}(F)$
20,400 cm^{-1}	$^4T_{1g}(F) \longrightarrow {}^4T_{1g}(P)$

The value of the ligand field splitting parameter (Δ) and the Racah parameter (B) were calculated using the same method as in the $[Co(NCMe)_6]^{2+}$ hexafluorotungstate(V) case.

Δ was found to be 9700 cm^{-1} and B' 735 cm^{-1}. The values are very similar to those obtained for the WF_6^- salt and are probably identical within the experimental error associated with the analytical method. The appreciable reduction in the value of B confirms the good coordinating abilities of acetonitrile towards Co(II).

The average value of B' is 755 cm^{-1} and for Δ it is 9950 cm^{-1} for $Co(NCMe)_6^{2+}$.

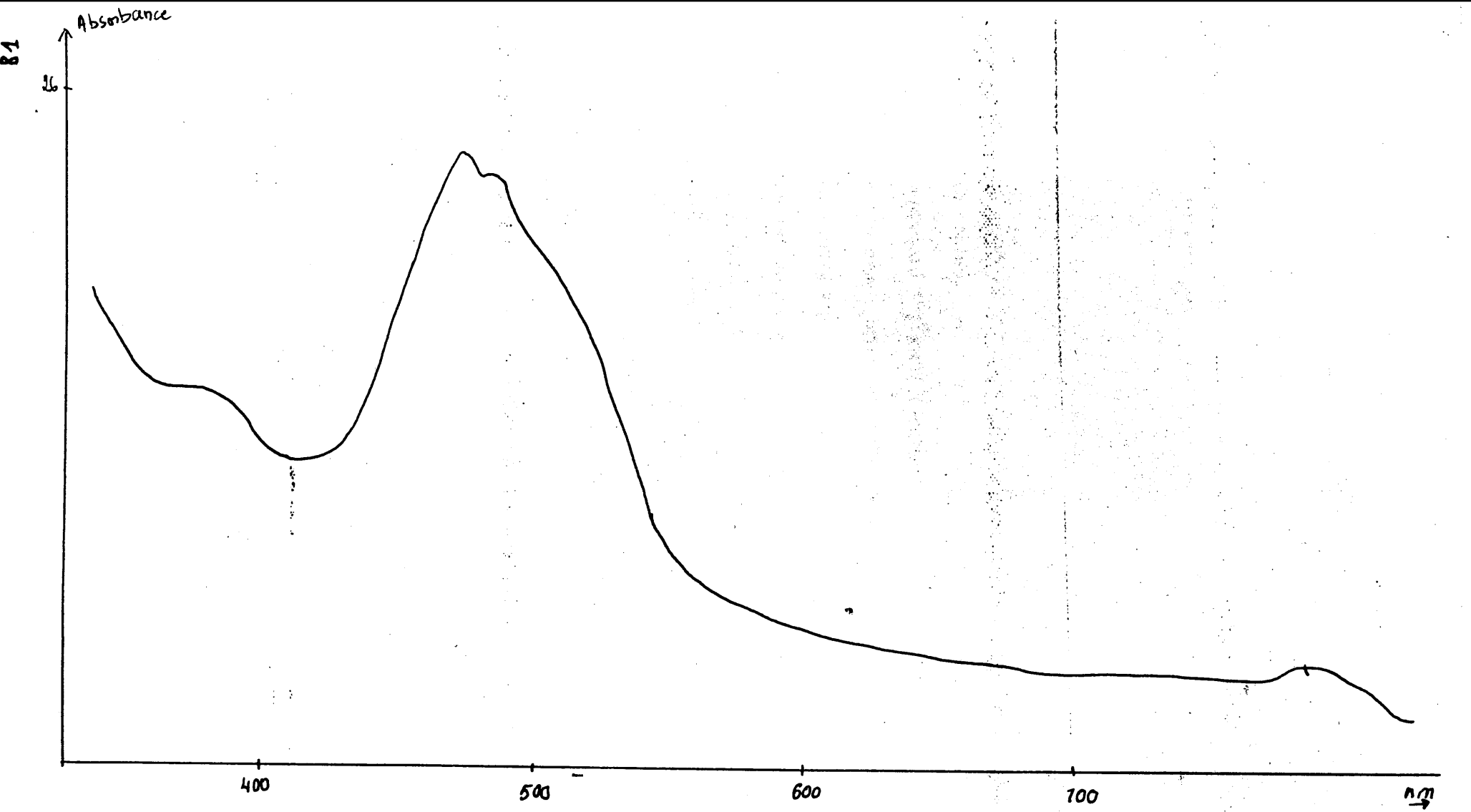

fig 13 UV – Visible spectrum of $(Co(NCMe)_6)(PF_6)_2$

3.5a - Cyclic voltammetry of $[Co(NCMe)_6][PF_6]_2$

The cyclic voltammogram recorded shows two quasi-reversible waves. The wave at $E_{\frac{1}{2}}$ =-1.33V vs. Ag^+/Ag is assigned to the oxidation of Co(II) to Co(III) and the wave at $E_{\frac{1}{2}}$ = 0.32V vs. Ag^+/Ag is assigned to the reduction of Co(II) to Co.

$$Co^{3+} + e^- \longrightarrow Co^{2+} \qquad E_{\frac{1}{2}} = -1.33V \text{ vs. } Ag^+/Ag$$

$$Co^{2+} + e^- \longrightarrow Co(s) \qquad E_{\frac{1}{2}} = 0.32V \text{ vs. } Ag^+/Ag$$

If the wave at $E_{\frac{1}{2}}$ = 1.33V corresponds to Co(III) species, MoF_6 should therefore oxidise cobalt metal to Co(III), but only a cobalt(II) species was formed when the reaction was performed. Further oxidation of the metal was not observed, probably for the kinetic reasons.

The wave assigned to the couple Co^{3+}/Co^{2+} was not observed in the voltammogram relevant to $[Co(NCMe)_6][WF_6]_2$, probably because it is masked by the wave corresponding to WF_7^-/W^V couple, or because Co(III) could not be generated due to the presence of $WF_7^- > W^V$ species in solution.

Conclusion

Cobalt metal is easily oxidized by MoF_6, NO^+ and WF_6 in presence of acetonitrile, yielding solvated $[Co(NCMe)_6]^{2+}$. The anions MF_6^- (M = P, Mo, W) were identified by the infrared spectra of these complexes which also suggests that the ligand acetonitrile is coordinated by its nitrogen lone pair. Though UF_6 is reported to be

thermodynamically the stronger oxidizing agent, no reaction occurred with cobalt metal and UF_6 was itself reduced in acetonitrile solution. Kinetic problems in oxidation of metals by the hexafluorides are encountered in a more extreme form in the reactions of nickel metal described in Chapter IV.

CHAPTER IV

Oxidation of Nickel by MoF_6, WF_6 and and NO^+ in Acetonitrile

INTRODUCTION[14,37]

Nickel metal is silver white in appearance and it shows typically metallic properties. When compact it is appreciably resistant to attack by air or water, but it becomes very reactive and pyrophoric under some conditions when the metal is finely divided.

The divalent state is an important oxidation level of the metal in its aqueous and non-aqueous chemistry. Many Ni(III) and some Ni(IV) complexes are also known. The hexafluoronickelates (III) and (IV) containing NiF_6^{3-} and NiF_6^{2-} ions are prepared by direct fluorination of melts of KCℓ-$NiC\ell_2$ mixtures at moderate temperatures and pressures of fluorine. Nickel reacts very slowly with fluorine, hence the metal and some of its alloys (e.g. Monel) are used to handle F_2 and other corrosive fluorides.

Direct reaction of nickel metal with various non-metals such as P, As, Sb, S, Sc, Te, C and B, produces binary nickel compounds. Hydrides of nickel evidently do not exist even though finely divided nickel absorbs hydrogen.

Nickel forms numerous complexes where the maximum coordination number is six. It also forms five coordinate complexes and square planar four coordinate complexes . Because of the low energy difference between these stereochemistries, equilibria between the various structural types are known to exist in solution as well as in the crystallisation of complexes containing nickel in two different stereochemistries.

Amines and some other neutral ligands can displace some or all of the water molecules in the octahedral $[Ni(H_2O)_6]^{2+}$ ion producing trans$[Ni(H_2O)_2(NH_3)_4][NO_3]_2$, $[Ni(NH_3)_6][C\ell O_4]_2$ and $[Ni(en)_3]\ SO_4$. Amine complexes of nickel are blue or purple while the hexaquonickel is green. This is specially observed when water molecules are replaced by ligands possessing a stronger ligand field.

Acetonitrile forms complexes with nickel either by recrystallisation of anhydrous halides from acetonitrile or by reaction of the metal with halogens in acetonitrile.[63] Nickel chloride and bromide form tetrahedral complexes of general formula $NiX_2.2CH_3CN$. The iodide of nickel forms the complex $NiI_2.3CH_3CN$ which is formulated as $[Ni(CH_3CN)_6^{2+}][NiI_4^{2-}]$. Reactions of nickel with bromine in acetonitrile give a stable complex formulated as $[Ni(CH_3CN)_6^{2+}][Br_3^-]_2$. The structure of these complexes has been determined from the study of their electronic spectra and magnetic properties.

Preparation of nickel hexafluorometallate salts (M=Mo,W) was previously attempted in this department.[3] Only the complex $[Ni(NCMe)_6][WF_6]_2$ was prepared, but oxidation of the metal with MoF_6 was unsuccessful, although the latter is considered to be a stronger oxidising agent, as previously described in the introduction to this thesis.

The present work was specially designed to attempt to overcome the problem of oxidation of nickel by MoF_6 and UF_6. $[Ni(NCMe)_6][PF_6]_2$ has also been prepared by the reaction of the metal with the nitrosonium ion. The complex was investigated by electronic and vibrational spectroscopy, in addition to cyclic voltammetry and atomic absorption spectroscopy.

Table4.1 Some physical properties of nickel metal

Atomic weight ($M/g\ mol^{-1}$)	58.71
Crystal structure	Face centred cubic
Atomic radius (Å)	1,25
Principal oxidation number	+2 , +3
Ionic radii (Å)	0.69
Ionization energies (Ei/ev)	7.635 , 18.168
Electronegativity	1.8
Electron affinity (Ee/ev)	1.3
Density ($\rho/Kg\ m^{-3}$)	8900
Melting point (Tm/K)	1726
Boiling point (Tb/K)	3005
Specific latent heat of fusion ($l/J\ Kg^{-1}$)	31×10^4
Specific heat capacity ($Cp/J\ Kg^{-1}K$)	460

4.1 EXPERIMENTAL

Ni powder, purity 99.99% (Goodfellow Metals Limited) was used as supplied. Nickel foil and nickel metal (purity 99%) were alternately used. Massive nickel was cleaned with sand paper inside the glove box before use.

Acetonitrile (Rathburn Chemicals Ltd.) was purified as described in Chapter II and was stored in the glove box.

MoF_6 (Ozark Mahoning), WF_6 (Ozark Mahoning), and UF_6 (British Nuclear Fuels Ltd.) were also purified, as described in Chapter II.

$NOPF_6$ (Fluorochem Ltd.) was used as supplied and stored in the dry atmosphere glove box.

Inside the glove box, the chemicals were weighed using an electronic balance (Type Sartorius Model 1205MP) with an estimated error of ± 0.004g.

The nickel film was prepared as described in Chapter II, for this purpose nickel wire of 0.5 mm thickness was used. It was spot welded to a pair of tungsten electrodes which were sealed to glass.

All glassware was flamed out before use to avoid contamination of reagents by oxygen and moisture.

4.2 RESULTS

Oxidation of nickel by WF_6 in CH_3CN

Nickel metal was loaded into a previously flamed out reaction vessel. After re-evacuation of the vessel WF_6 and acetonitrile were added by vacuum distillation at 77K. The reactants were allowed to warm up and left to shake overnight, after which a purple-blue solution was formed. A purple crystalline solid was isolated after removal of the volatile material.

The infrared spectrum of the complex was recorded (Table 2) and it shows bands assigned to coordinated acetonitrile and presence of the anion WF_6^-. A sharp intense band at ν_{max} 2300 cm^{-1} is assigned to C≡N stretching fundamental and a weaker band at 2330 cm^{-1} is assigned to a combination of the C-C stretching and the CH_3 deformation modes.[64] The intensity of the weaker band arises from Fermi resonance between the combination band and the C≡N stretching vibration as, both the combination band and the stretching vibration have A_1 symmetry. An intense band at 620 cm^{-1} is assigned to a vibration of WF_6^-.

Electronic spectrum: The purple colour of the complex under discussion is strongly suggestive of octahedral Ni(II), and by reference to previous work,[3,36] it is a reasonable assumption that Ni(II) is present as $[Ni(NCMe)_6]^{2+}$.

In an octahedral ligand field the free ion Ni^{2+} ground state ^3F splits into three electronic levels; $^3T_{1g}$, $^3T_{2g}$ and $^3A_{2g}$. The ^3P term gives rise to the $^3T_{1g}(P)$ term.[37,38] The exact way these terms

Table 4-2 – Infrared spectrum of solid $[Ni(NCMe)_6][WF_6]_2$

Frequency (cm^{-1})	Assignement
2330	Comb $CH_3CN(\nu_2+\nu_1)(A_1)$
2300	C≡N stretch $(\nu_3)(A_1)$
1030	CH_3 rock $(\nu_7)(E)$
940	C–C stretch $(\nu_4)(A_1)$
705	WF_7^-
620	$(\nu_3)WF_6$
240	Metal–N stretch

split apart is represented on a Tanabe-Sugano diagram (Fig. 4.2) which is applicable to any complex whatever the ligand, as long as the average environment about the nickel is approximately the same.[70] The $^3T_{1g}(F)$ and $^3T_{1g}(P)$ terms interact with one another and this results in curvature of lines with the same designations.[38] The expressions of the ligand field of the d^8 configuration relative to the ^3F free ion term as zero are:

Term	Energy
$^3A_{2g}$ (F)	$-\frac{6}{5}\Delta_o$
$^3T_{2g}$ (F)	$-\frac{1}{5}\Delta_o$
$^3T_{1g}$ (F)	$\frac{15B}{2} + \frac{3}{10}\Delta_o - \frac{1}{2}[225B^2+\Delta_o^2+18B\,\Delta_o]^{1/2}$
$^3T_{1g}$ (P)	$\frac{15B}{2} + \frac{3}{10}\Delta_o + \frac{1}{2}[225B^2+\Delta_o^2+18B\,\Delta_o]^{1/2}$

The three observed bands in the recorded spectrum were assigned to the following transitions:

$$\nu_1 : {}^3A_{2g}(F) \longrightarrow {}^3T_{2g}(F)$$

$$\nu_2 : {}^3A_{2g}(F) \longrightarrow {}^3T_{1g}(F)$$

$$\nu_3 : {}^3A_{2g}(F) \longrightarrow {}^3T_{1g}(P)$$

The energies of these transitions can be expressed in terms of Δ_o and B', where Δ_o represents the magnitude of the ligand field splitting parameter and B' is the Racah parameter.

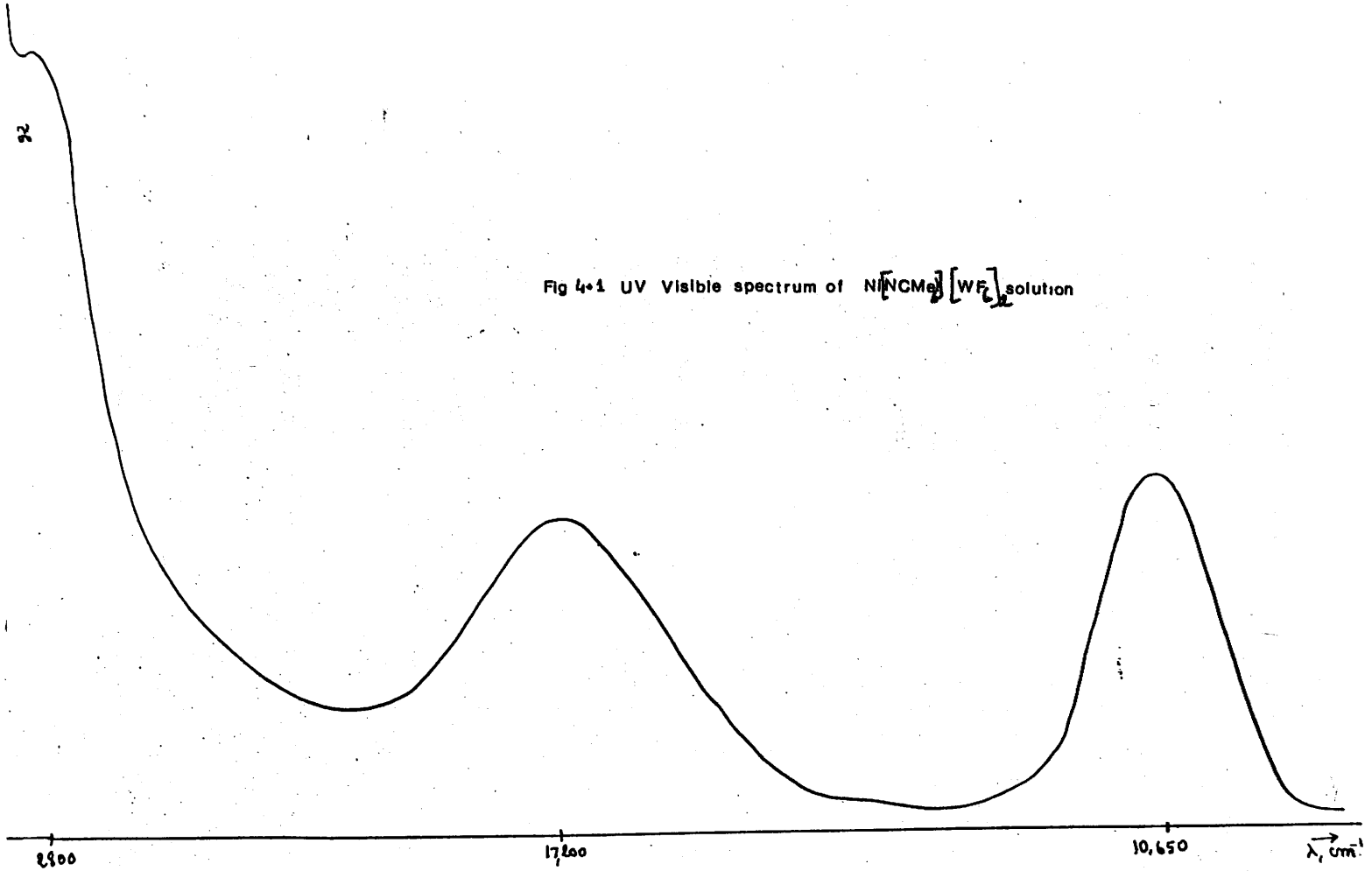

Fig 4·1 UV Visible spectrum of $Ni[NCMe]_2[WF_6]_2$ solution

Transition	Energy
$^3A_{2g}(F) \longrightarrow {}^3T_{2g}(F)$	Δ_o
$^3A_{2g}(F) \longrightarrow {}^3T_{1g}(F)$	$\frac{15B}{2} + \frac{3}{10}\Delta_o - \frac{1}{2}[225B'^2+\Delta_o^2-18B'\Delta_o]^{\frac{1}{2}}+\frac{6}{5}\Delta_o$
$^3A_{2g}(F) \longrightarrow {}^3T_{1g}(P)$	$\frac{15B}{2} + \frac{3}{10}\Delta_o + \frac{1}{2}[225B'^2+\Delta_o^2-18B'\Delta_o]^{\frac{1}{2}}+\frac{6}{5}\Delta_o$

The UV-visible spectrum recorded shows two absorption bands of intermediate intensity at ν_{max} 10650 cm^{-1} and ν_{max} 17200 cm^{-1}, and a third absorption band of high intensity in the ultraviolet region at ν_{max} = 28000 cm^{-1}.

From the frequency values experimentally obtained, Δ_o is calculated to be 10650 cm^{-1} and B' 884 cm^{-1}. The magnitude of the ligand field splitting parameter is given by the energy difference between the ground state $^3A_{2g}(F)$ and the first transition level $^3T_{2g}(F)$. The free ion value of the electron repulsion parameter B for Ni^{2+} is 1082 cm^{-1}, showing a reduction to 82% when Ni(II) is coordinated to acetonitrile.

Cyclic voltammetry: The electrochemical study of solvated $[Ni(NCMe)_6]^{2+}$ was performed using cyclic voltammetry. The voltammogram recorded features a reversible wave at $E_{\frac{1}{2}}$ = 0.65V vs. Ag^+/Ag. By reference to previous studies of alkali metal and silver WF_6^- salts,[57,58] this wave was assigned to the couple WF_6/WF_6^-. A quasi-reversible wave at $E_{\frac{1}{2}}$ = 0.29V vs. Ag^+/Ag is assigned to the couple Ni^{2+}/Ni and a wave at $E_{\frac{1}{2}}$ = -1.29V vs. Ag^+/Ag to WF_7^-/W^V couple. Assignment of the WF_7^-/W^V couple was by comparison of the $E_{\frac{1}{2}}$ value obtained in this work and the $E_{\frac{1}{2}}$ value obtained in previous work concerned with the oxidation and study of copper hexafluorotungstate salt in acetonitrile.[71]

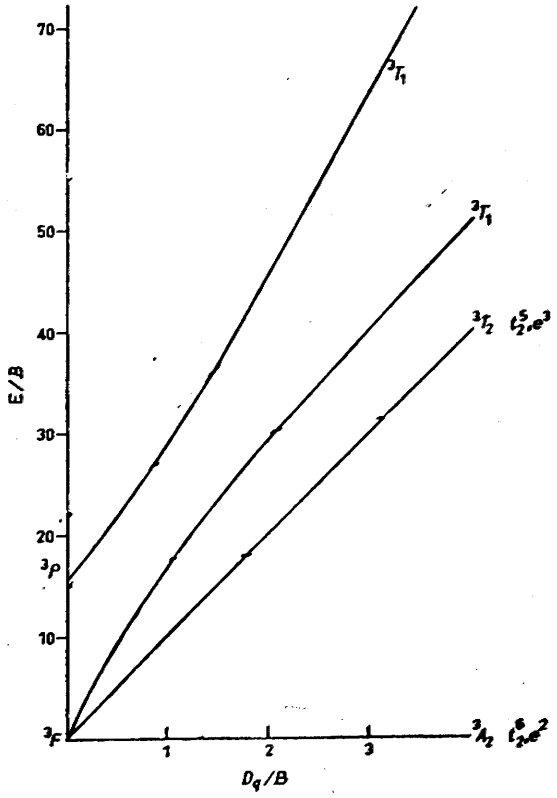

Fig **Partial** Energy level diagram (Tanabe-Sugano) for d^8 ions in an octahedral field

By reference to the same work the wave at $E_{\frac{1}{2}}$ = -1.68V vs. Ag^+/Ag is assigned to the WF_6^-/W^{IV} couple. As in the aqueous medium, nickel metal is moderately electropositive. The redox potential of the Ni^{2+}/Ni couple is -0.23V vs. NHE in aqueous medium.

Oxidation of nickel with excess WF_6

Nickel metal was oxidised in acetonitrile solution using a large excess of WF_6. The mole ratio was Ni:WF_6, 1:20; after shaking overnight a brown solid was formed in addition to the crystalline purple solid. The brown solution was decanted into the empty side of the reaction vessel and the solvent was removed by back distillation using liquid nitrogen as coolant. Slow distillation was necessary to prevent bumping. This was achieved by cooling the solution to -40°C using a bath of trichloroethylene/dry ice. When all the solvent was removed, a brown solid was isolated. The electronic spectrum of the brown solid consists only of a charge transfer band in the ultraviolet region which tails in the visible λ_{max}.

The infrared spectrum of the solid indicates the presence of a sharp intense band at 705 cm^{-1} assigned to WF_7^- and a band at 605 cm^{-1} assigned to WF_6^-[3]. The presence of coordinated acetonitrile is also evident.

In an earlier study concerned with the oxidation of iron and copper in MeCN it had been shown that a fluoride ion transfer occurs in the presence of tungsten hexafluoride involving WF_6 and WF_6^-. Oxidation of iron by WF_6 in MeCN produces iron(II) as the cation and a mixture of WF_6^- and WF_7^- as the anions. The ratio of the anions formed

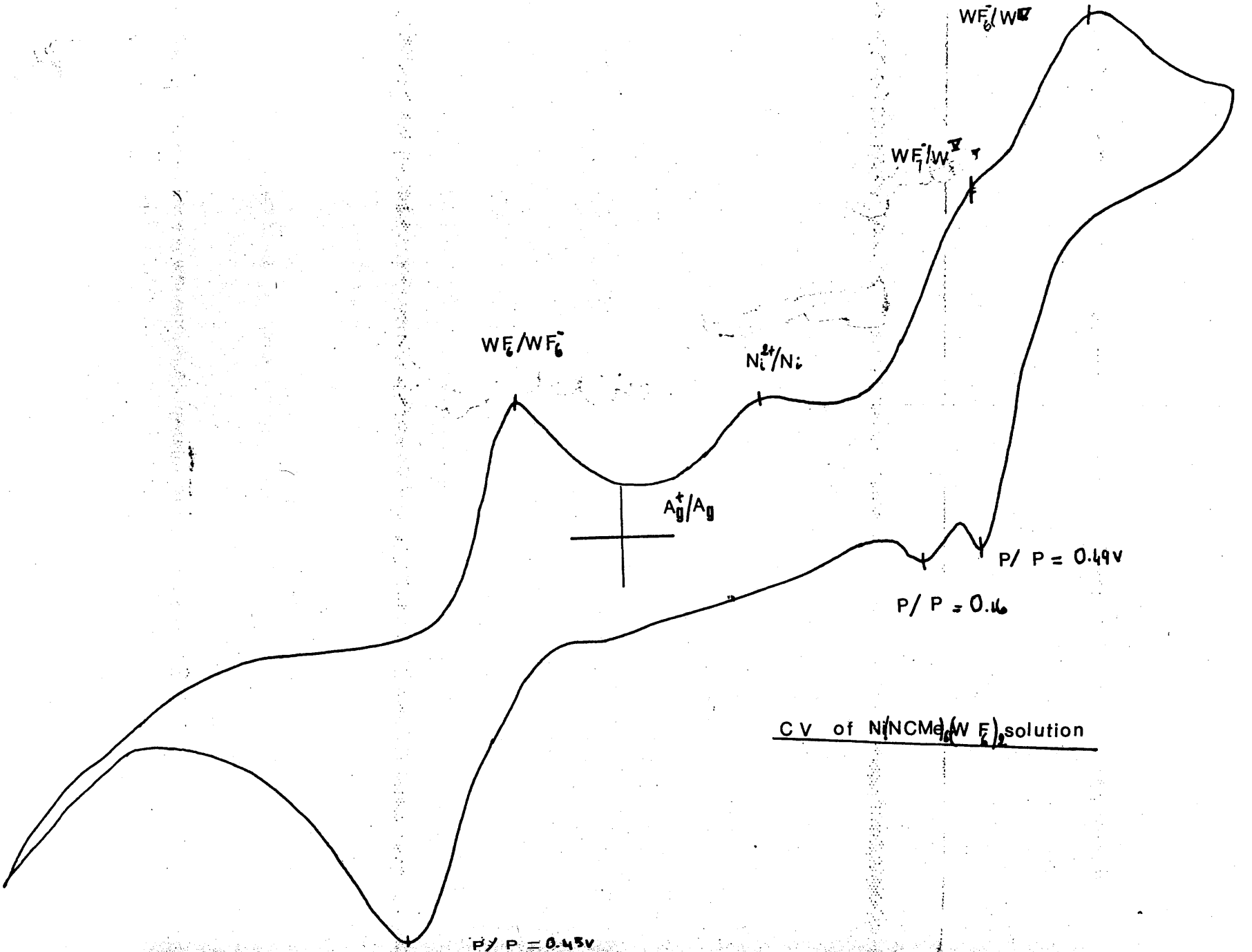

CV of Ni(NCMe)6(WF6)2 solution

is dependent upon the conditions of the reaction. The fluoride ion transfer can be expressed by the following equilibrium

$$WF_6(solv) + WF_6^-(solv) \rightleftharpoons WF_7^-(solv) + WF_5(solv).$$

Formation of the anion WF_7^- can, however, be suppressed by carrying the oxidation reaction in a 'vapour phase' in which the concentration of WF_6 on the surface of the metal is decreased.

A fluoride ion transfer has also been observed when studying the behaviour of tungsten hexafluoride towards ionic fluorides. The reactions were performed in presence of bromine and bromine trifluoride,[72] iodine pentafluoride,[73] chlorine trifluoride,[74] or, in absence of a liquid phase.[75] On the basis of their X-ray powder diffraction data analysis, the adducts obtained were formulated as $M[WF_7]$ or $M_2[WF_8]$ (M=Na, Cs, or NH_4). Similar adducts are also formed when WF_6 is reacted with nitryl or nitrosyl fluorides[44] as shown from the study of their infrared spectra.

Reaction of anhydrous thallium(I) and copper(II) fluorides with WF_6 in the presence of acetonitrile produces the adducts $TlF.WF_6$ and $CuF_2.2WF_6.5MeCN$, respectively.[36] From the analysis and vibrational spectra of these adducts, and also supported by their ^{19}F n.m.r. spectra, it is found that $Tl(WF_7)$ and $[Cu(NCMe)_5][WF_7]_2$ are formed. Both their solution and solid Raman spectra show a band at 705 cm^{-1}, attributable to a WF_7^- vibration frequency. The formation of the WF_7^- anion from WF_6 and F^- ion must be favoured by the good Lewis-acid properties of WF_6 and also by the poor solvating properties of acetonitrile towards F^- ion.

Gas phase oxidation of nickel by WF_6

A gas phase reaction was performed with the aim of preparing Ni(II) hexafluorotungstate(V) complex free from traces of WF_7^-.

The reaction of iron with WF_6/MeCN vapour had been performed in this department and the product formed is a predominantly WF_6^- salt, $[Fe(NCMe)_6][WF_6]_2$,[83] showing that formation of WF_7^- can be prevented by altering the experimental conditions and suppressing the concentration of WF_6 on the metal surface.

Nickel wire was cleaned with sand paper inside the glove box and then broken into small pieces. The metal was loaded in one side of a reaction vessel. After re-evacuation of the vessel 6 ml of acetonitrile and tungsten hexafluoride (mole ratio; $Ni:WF_6$ - 1:5) were vacuum distilled into the empty side of the reaction vessel. A white powder was formed within two hours. When dissolved in acetonitrile the white solid turned slightly purple and did not lose this colour even after drying under vacuum.

Microanalysis showed that the product was $[Ni(NCMe)_6][WF_6]_2$. Found: C, 14.8; H, 1.74; F, 23.40; N, 8.62. $C_{12}H_{18}F_{12}N_6NiW_2$ required C, 19.96; H, 1.74; F, 26.52; N, 8.15%.

The electronic spectrum of the complex was recorded and was identical to that of $Ni(NCMe)_6^{2+}$ prepared in the solution phase. It showed three regions of absorption at identical frequencies; that is ν_{max} 10,650 cm^{-1}, ν_{max} 17,200 cm^{-1} and ν_{max} 28,000 cm^{-1}, respectively.

The infrared spectrum recorded in the region 200-4000 cm^{-1} indicates the presence of coordinated acetonitrile and the anion WF_6^-.

Table 4-3 Infrared spectrum of solid $(Ni(NCMe)_6)(WF_6)_2$ gas phase reaction

Frequency (cm^{-1})	Assignement
2330	Comb $CH_3CN(\nu_2 + \nu_1)(A_1)$
2300	C≡N stretch $(\nu_3)(A_1)$
1030	CH_3 rock (ν_7)(E)
940	C-C stretch $(\nu_4)(A_1)$
620	$(\nu_3)WF_6$
340	Metal-N stretch

The band assigned to WF_7^- is, however, not observed. Coordination of acetonitrile is evident from comparison of the spectrum recorded with that of free acetonitrile. A band at ν_{max} 2300 cm^{-1} is assigned to C≡N fundamental stretch and a weaker band at 2330 cm^{-1} is assigned to a combination of the C-C stretch and the CH_3 deformation modes.[64] A band at 1035 cm^{-1} assigned to a CH_3 rock and a band at 945 cm^{-1} assigned to a C-C stretching mode.

The electrochemistry of $[Ni(NCMe)_5][WF_6]_2$ was performed and the voltammogram recorded is in all points identical to the voltammogram recorded for solvated $[Ni(NCMe)_6][WF_6]_2$ prepared in solution phase.

Oxidation of nickel by NO^+

A previously evacuated and flamed out reaction vessel was loaded with nickel foil and $NOPF_6$. After addition of acetonitrile and warming up to room temperature the solution mixture was shaken overnight, resulting in the formation of a purple solution. A purple solid was isolated after removal of the volatile material. Its structure is suggested to be $[Ni(NCMe)_6][PF_6]_2$.

Analysis by atomic absorption spectroscopy was performed and the content of nickel was 9.8%.

The infrared spectrum of $[Ni(NCMe)_6][PF_6]_2$ was recorded and indicated the presence of coordinated acetonitrile and the PF_6^- anion. The main absorption frequencies of the complex examined are tabulated (Table 4.4). The broad strong absorption at 840 cm^{-1} is assigned to the

Table 4-4 Infrared spectrum of solid $(Ni(NCMe)_6)(PF_6)_2$

Frequency (cm^{-1})	Assignement
2325	comb. CH_3CN $(\nu_2+\nu_1)(A_1)$
2300	C≡N stretch $(\nu_3)(A_1)$
1254	CH_3 def. $(\nu_3)(A_1)$
1045	CH_3 rock. $(\nu_7)(E)$
940	C-C stretch $(\nu_4)(A_1)$
840	T_1u PF_6^-
750	overtone $(2\nu_3)(A_1)$
555	T_1u PF_6^-

Fig 4-3 UV-Visible spectrum of $(NiNCMe_6)(PF_6)$

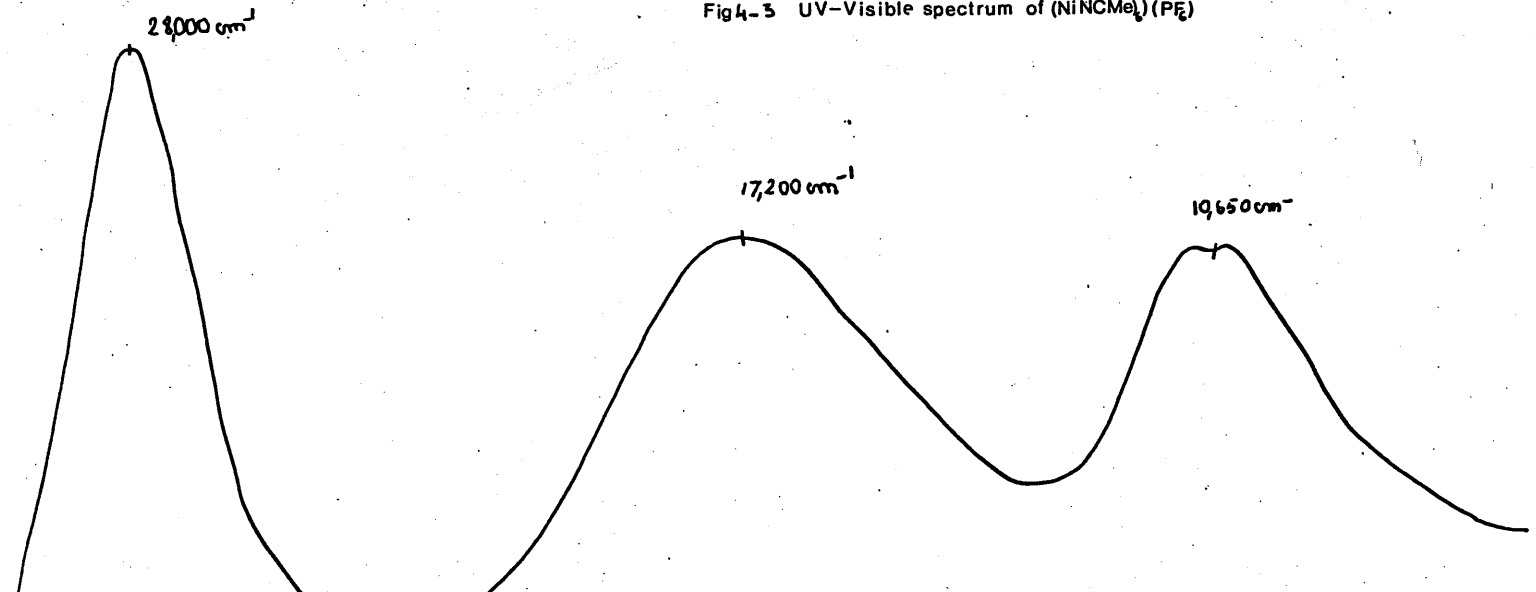

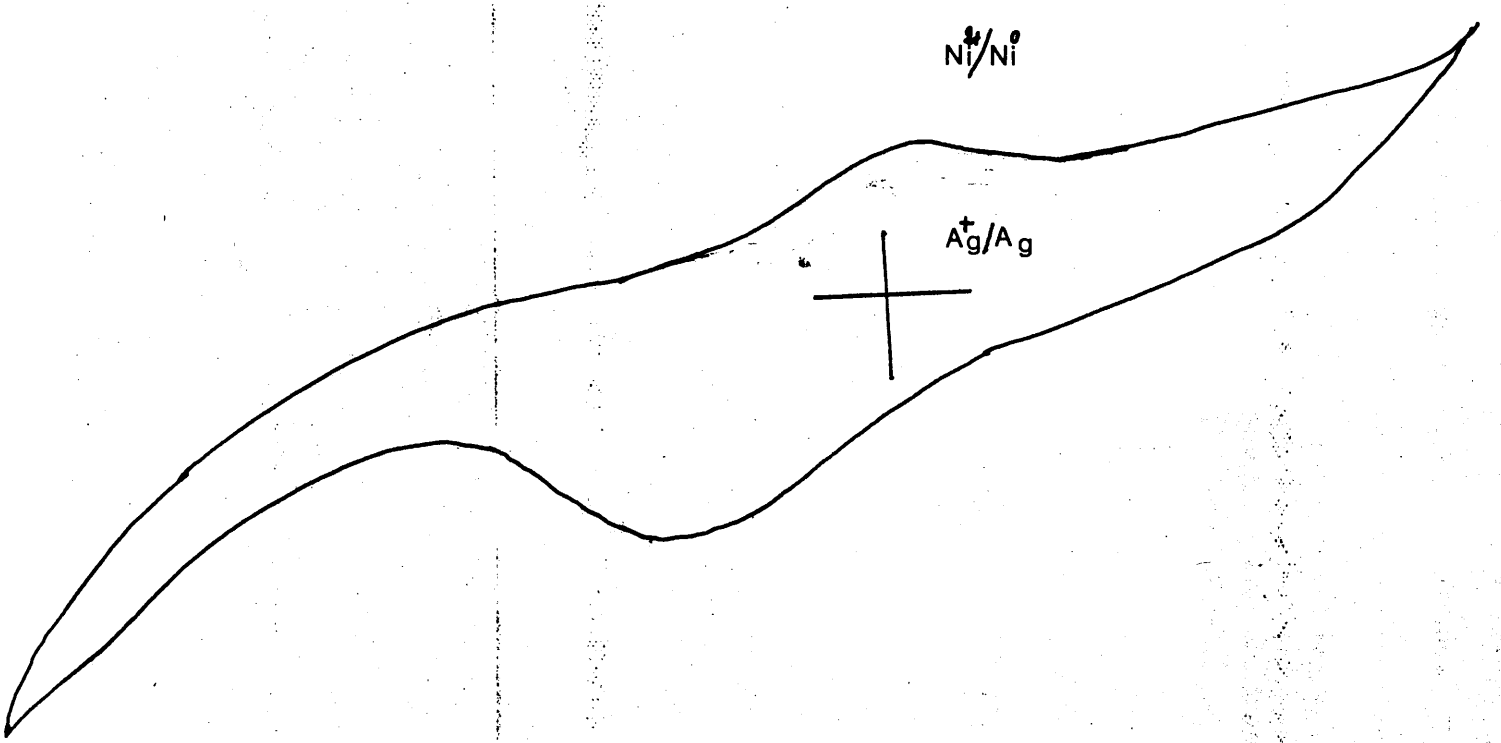

Fig 4.4 C-V of $(Ni(NCMe_6)X(PF_6)_2$ solution

ν_3 frequency of PF_6^- ion and also the band at 555 cm^{-1} is assigned to ν_4 (PF_6^-).

The solution of nickel hexafluorophosphate in acetonitrile is purple in accord with the geometry of the complex. Since ligand field theory predicts a fourfold splitting of the d-orbital energy levels in an octahedral field, we should expect to find d-d transition energies represented by three absorption bands. The electronic spectrum of $[Ni(NCMe)_6][PF_6]_2$ shows the presence of these bands at the following frequencies: ν_1 10650 cm^{-1}, ν_2 17200 cm^{-1} and ν_3 28000 cm^{-1}.

The magnitudes of the ligand field splitting parameter and the Racah parameter are deduced from the expressions of the three transitions observed and are Δ = 10650 cm^{-1}, B' = 884 cm^{-1}, respectively. These results may be compared with those obtained for the absorption of solvated $[Ni(NCMe)_6]^{2+}$ with tungsten hexafluoride as the counter anion. Those now reported are found to parallel them exactly.

Cyclic voltammetry of $[Ni(NCMe)_6][PF_6]_2$ in acetonitrile was also performed. The voltammogram obtained features only a quasi-reversible wave at $E_{\frac{1}{2}}$ = 0.32V vs. Ag^+/Ag. This is attributed to the couple Ni^{2+}/Ni and is in agreement with the value determined for Ni(II) hexafluorotungstate(V) salts.

Oxidation of Nickel by MoF_6

A previously evacuated and flamed out reaction vessel was loaded with nickel metal (powder purity 99.99%). After re-evacuation of the flask acetonitrile and MoF_6 were added by vacuum distillation at 77K. On warming up to room temperature the solution mixture was

colourless. No reaction seemed to occur even after overnight shaking. The same reaction as described above was performed again but using a large excess of MoF_6, the molar ratio being $Ni:MoF_6$, 1:20. After two hours shaking, polymerisation of the solvent occurred but no reaction between Ni and MoF_6 was evident.

Reaction of nickel with MoF_6 in presence of pyridine

Because pyridine is a better σ-donor than acetonitrile it would probably stabilise the nickel(II) if it is added. When pyridine (1 ml) was added to a mixture of nickel metal, MoF_6 and CH_3CN on warming to 296K, a yellow product was formed, accompanied by release of white fumes, probably hydrogen fluoride gas, and the reaction was appreciably exothermic. When stored at room temperature the yellow product turned red-brown. Because of its colour it was first believed that a Ni(III) salt had been prepared but subsequent atomic absorption analysis has shown that the salt prepared contains no nickel at all. Further, microanalysis indicates that the complex formed is $MoF_5.2py$.

Found: C, 34.1; H, 2.8; F, 27.4; Mo, 27.45; N, 7.8.

$C_{10}H_{10}F_5MoN_2$ requires C, 34.3; H, 2.9; F, 27.2; Mo, 25.5; N, 8.0%.

The same reaction was performed in absence of nickel and resulted in the formation of a yellow product identified as $MoF_5.2py$.

The infrared spectrum of $MoF_5.2py$ was compared to that of free pyridine[76,77] and the following assignments were made.

Table 45. Infrared and Raman spectra of $MoF_5 \cdot 2py$

Frequency (cm)	Assignement
1610	py. comb. ($\nu_1+\nu_6$)
1378	coord. py
1355	coord. py
1250	overtone
1218	coord. py
1160	coord. py
1070	coord. py
1032	coord. py
1020	coord. py
625	MoF_6^- (in)
679	MoF_6^- (Raman)
570	py.

Coordinated pyridine is usually readily distinguishable from the free base by the presence of a weak band between 1235 and 1250 cm^{-1} and which is observed in the present case at 1250 cm^{-1}. It is also distinguished by a shift in the strong 1578 cm^{-1} band to 1610 cm^{-1} also shown in the present case. This band appears with a shoulder in the spectrum of the free base which is not present in the spectrum of coordinated pyridine. The spectrum of free pyridine presents a group of five bands between 990 and 1217 cm^{-1}. In the spectrum of $MoF_5.2py$ the same group of five bands appears at the following frequencies: 1020, 1032, 1070, 1160 and 1218 cm^{-1}. These bands are accompanied with splittings, the origin of which is very uncertain. An extra moderate band at 1250 cm^{-1} is either an overtone or a combination band which has become infrared active. A weak band at 1355 cm^{-1} and a medium band at 1378 cm^{-1} are also assigned to coordinated pyridine. A strong band at 1610 cm^{-1} is assigned to a combination band ($\nu_1+\nu_6$) which is enhanced by Fermi resonance with the vibration ν_8.

The infrared and Raman spectra of the adduct show a band at 625 cm^{-1} and 679 cm^{-1}, respectively, which can be reasonably assigned to a ν_3 vibration of the MoF_6^- anion. The structure of the adduct is hence suggested to be the following, $MoF_6^- - MoF_4Py_4^+$. The readiness with which the reduction reaction occurs can easily be explained by the capacity of the anion to accommodate new electrons in its empty orbitals and also the ability of pyridine to donate a lone pair of electrons.

Reaction of clean nickel metal with MoF_6

The failure of MoF_6 to oxidise nickel metal is presumably due to its inability to react with the oxide film on the metal surface. Passivation of metals by oxide films is a well-documented phenomenon and the layer can be removed in some cases by chemical methods. Since NO^+ oxidises nickel in acetonitrile this treatment was applied to the metal. For this purpose a three-limb reaction vessel (Fig. 4.1) was used. Nickel foil was loaded into limb A in the presence of $NOPF_6$. Acetonitrile (5 ml) was added by vacuum distillation. The reaction mixture was warmed to room temperature and shaken overnight. The purple solution formed was tipped into limb B of the flask and fresh acetonitrile was distilled into limb A. This was used to wash off the nickel foil which remained. The washing was repeated four times using fresh acetonitrile each time. Limb B was then sealed off. Fresh acetonitrile (6 ml) and MoF_6 were then added into limb A. After warming to room temperature, the solution was shaken for two hours. A purple solution formed after shaking and by removal of the volatile material a very small amount of purple product was isolated. This most probably results from the oxidation of clean nickel metal with MoF_6. The yield of the reaction was too small for its characterization but its infrared spectrum showed the presence of the anion MoF_6^- and coordinated acetonitrile.

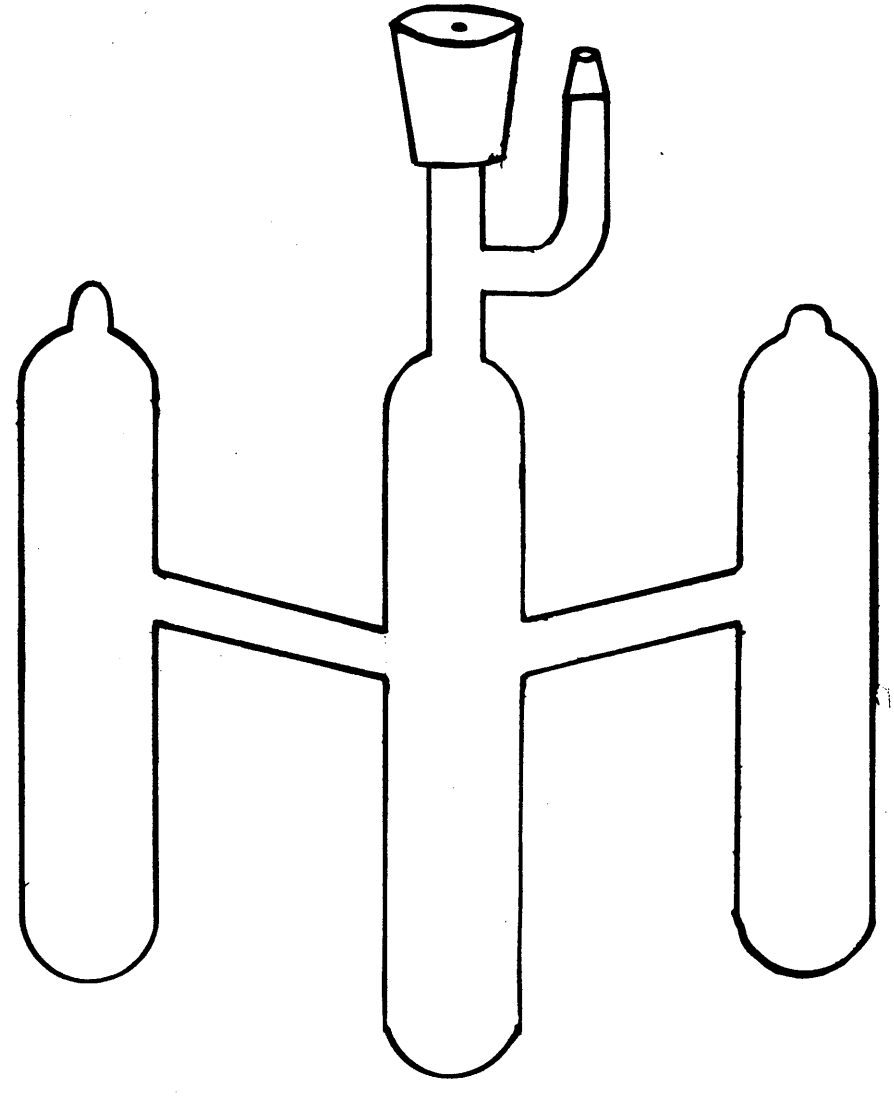

FIG THREE LIMBS REACTION VESSEL

Oxidation of an evaporated nickel film with MoF_6

As a possible way of improving the reaction, a nickel film was prepared under vacuum, as described in Chapter II. Acetonitrile and MoF_6 were added by vacuum distillation at 77K and allowed to warm to 298K. After a few minutes shaking the thick deposit of the nickel film started to peel off in thin flakes while the solution gradually became purple. The solution was left to settle for 1/2 hour and was then decanted into the empty side of the reaction vessel. The solvent was removed by back distillation using liquid nitrogen as coolant; a purple solid was isolated.

The U.V.-visible spectrum of the solid in acetonitrile contained three peaks at ν_{max} 10300 cm^{-1}, ν_{max} 16670 cm^{-1} and ν_{max} 27030 cm^{-1}, respectively. These bands are assigned to the following transitions:

$$^3A_{2g}(F) \longrightarrow {}^3T_{2g}(F)$$

$$^3A_{2g}(P) \longrightarrow {}^3T_{1g}(F)$$

$$^3A_{2g}(F) \longrightarrow {}^3T_{1g}(P)$$

The assignments of these transitions have been made by comparison with the solution spectrum of $[Ni(NCMe)_6]^{2+}$ where WF_6^- and PF_6^- are the counter anions. The frequencies and band widths are in good agreement with the predictions based on the Orgel diagram.

The magnitude of the ligand field splitting parameter and the Racah parameter had also been determined using the same method as shown earlier for the $[Ni(NCMe)_6][WF_6]_2$ case. Δ_o is calculated to be 10300 cm^{-1} and B' 853 cm^{-1}, which represents 82% of the value

Table 4.5 Spectral parameters for octahedral Ni(II) complexes

NiL_6^{2+}	$^3T_{2g}$	$^3T_{2g}$	$^3T_{1g}$	B	Ref.
$(Ni(py_6))^{2+}$	10150	16500	27000	862	79
$(Ni(NH_3)_6)^{2+}$	10750	17500	28100	823	80
$(Ni(H_2O)_6)^{2+}$	8500	13800	25300	930	81
$(Ni(MeCN)_6)^{2+}$	10650	17200	20000	863	This work
$(Ni(MeOH)_6)^{2+}$	8430	14225	25000	915	78
$(Ni(MeCN)_6)^{2+}$	10700	17400	27810	855	63
$(Ni(DMSO)_6)^{2+}$	7730	12970	24040	921	82

$NH_3 \approx MeCN > py > H_2O > MeOH > DMSO$

of the Racah parameter for the free ion. A good agreement is found between the value of Δ_o and B' derived experimentally in this work and the values reported in the literature for $[Ni(NCMe)_6]^{2+}$.[38] Comparison of these values with relevant NiL_6^{2+} (Table 4-5) L = py, NH_3, H_2O, MeOH, DMSO; places acetonitrile ligand towards the stronger end of the spectrochemical series, the order being DMSO < MeOH < H_2O < Py < MeCN ≈ NH_3. This order is the same as that derived from cobalt(II) spectra and work performed by others.

The infrared spectrum of nickel hexafluoromolybdate(V) in acetonitrile has been recorded in the region 200-4000 cm^{-1}, where the presence of the anion MoF_6^- and coordination of acetonitrile have been established. The strong band at 630 cm^{-1} is assigned to the ν_3 frequency of the hexafluoromolybdate(V) ion. Comparison of the infrared spectrum of free acetonitrile with the spectrum recorded in this work gives evidence of coordination of acetonitrile from shifts in frequency of its absorption bands. Two bands at 2300 cm^{-1} and 2325 cm^{-1} are assigned to the C≡N fundamental stretch and a combination of the C-C stretching mode and the CH_3 deformation, respectively. A band at 1035 cm^{-1} is assigned to a CH_3 rocking and a band at 945 cm^{-1} is assigned to a C-C stretching mode.

Further analysis of the complex $[Ni(NCMe)_6][MoF_6]_2$ was not performed because the yield of the reaction was insufficient, despite the improvement registered when using an evaporated nickel film.

Table 4-6: Infrared spectrum of solid $(Ni(NCMe)_6)(MoF_6)_2$

Frequency (cm^{-1})	Assignement
2325	comb CH_3CN (A_1)
2300	C≡N stretch (A_1)
1035	CH rock (ν_7)(E)
945	C-C stretch (ν_4) (A_1)
630	MoF_6^-
515	C-C≡N bend (ν_8) (E)

Reaction of WF_6 with evaporated nickel film

An evaporated nickel film was prepared as previously described in Chapter II. Acetonitrile and tungsten hexafluoride were vacuum distilled at 77K into the empty side of the reaction vessel, and left to warm up to room temperature.

Oxidation of nickel film by WF_6 was being performed in a gas phase. After two hours no reaction between the nickel film and WF_6 was evident. However, a white salt was growing on the upper part of the nickel wire near the spot welding connecting the nickel wire to the tungsten electrodes. This part of the nickel wire, where the white salt was growing, apparently did not take part in the evaporation process, and probably retained its oxide layer. This is on the basis that while all the nickel wire was "red" during the evaporation process, this same part was not; hence its temperature was below that necessary for a deoxidation and an evaporation process to proceed.

The spot weldings were covered with 2 mm ϕ glass tubing and a new vacuum evaporated nickel film was prepared. After addition of WF_6 and acetonitrile the reaction mixture was shaken for a few hours but no reaction occurred. The solution mixture was then removed by vacuum distillation and the reaction vessel was opened to allow air in. After re-evacuation of the reaction vessel the mixture, WF_6 and acetonitrile, was back distilled. A purple salt was isolated after overnight shaking and was identified as $[Ni(NcMe)_6][WF_6]_2$ complex. This series of experiments show that WF_6 reacts easily with massive nickel but it does not react with an evaporated nickel film supposably free from its oxide layer. If, after making the nickel film under vacuum, the

reaction vessel is opened to air before performing the reaction, WF_6 reacts with the nickel film Opposite behaviour was shown by molybdenum hexafluoride which reacts with vacuum evaporated nickel film but does not react with massive nickel, although MoF_6 is thermodynamically a stronger oxidising agent. This behaviour of nickel metal towards the hexafluorides of molybdenum and tungsten is unexpected, and as a consequence , the reaction of tungsten hexafluoride with evaporated nickel film was performed again and monitored by the use of ^{18}F-labelled tungsten hexafluoride. The reaction is described below and was performed with the help of M.F. Ghorab, a fellow student.

Reaction between ^{18}F-labelled WF_6 and an evaporated nickel film

The reaction between ^{18}F-labelled WF_6 and Ni was followed using a double-limb reaction vessel made of Pyrex glass and fitted with P.T.F.E. glass stop cock (Fig. 4.4). One limb was coated with nickel film prepared under vacuum and the other contained WF_5 ^{18}F and CH_3CN.

WF_5 ^{28}F was prepared by ^{18}F exchange reaction (1h, 313K) between WF_6 and ^{18}F-labelled CsF, which had been prepared by neutron irradiation (1/2h) of Li_2CO_3 according to the nuclear reaction

$$^{7}Li\ (n,\alpha)\ T \quad \text{followed by} \quad T\ (o,n)\ ^{18}F$$

then

$$Li\ ^{18}F + H_2SO_4\ [conc] \xrightarrow{t^\circ} H\ ^{18}F$$

$$CsOH + H\ ^{18}F \longrightarrow Cs\ ^{18}F$$

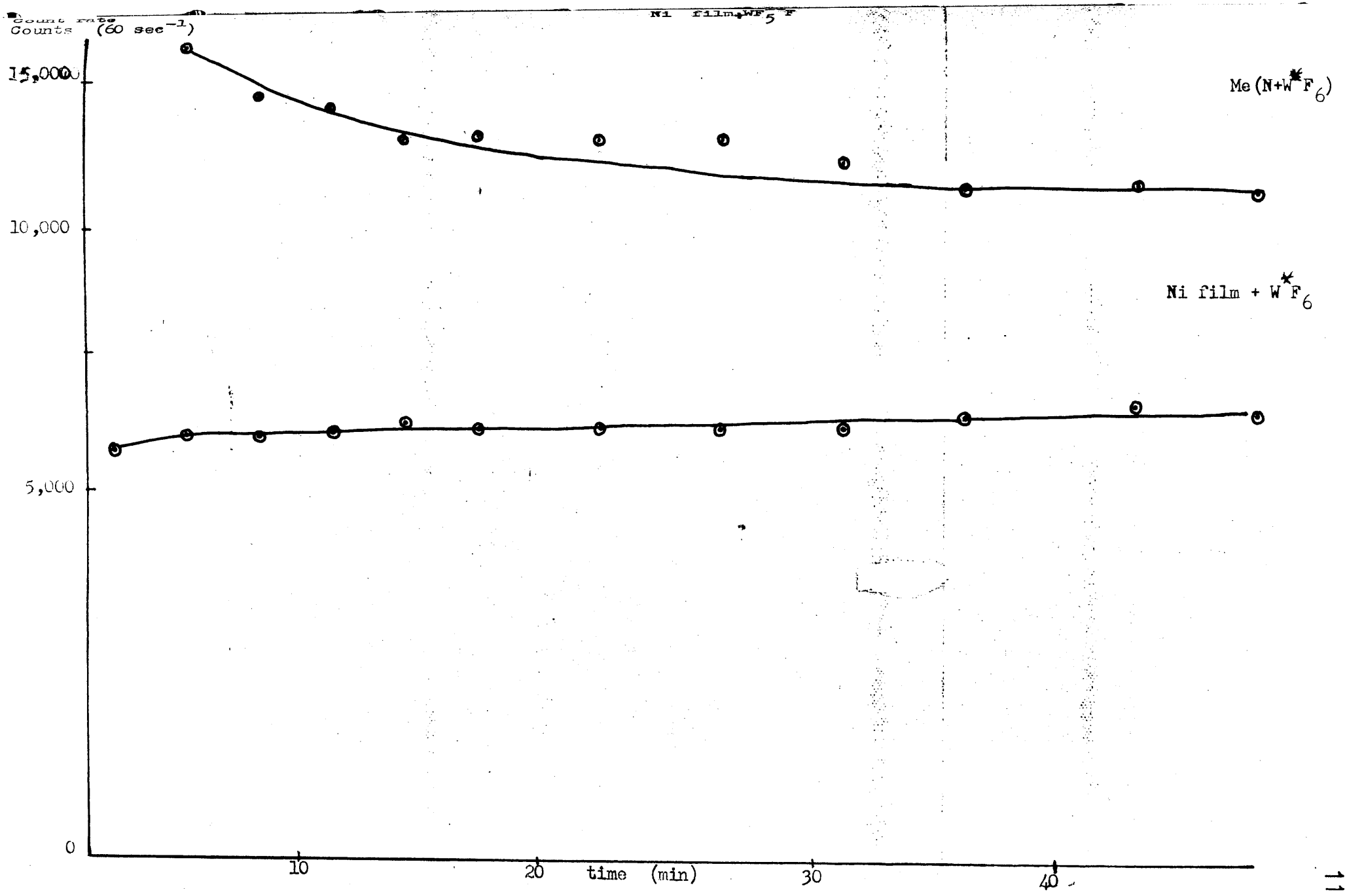
Ni film + WF5 F
Count rate
Counts (60 sec^{-1})
15,000
10,000
5,000
0
10
20
30
40
time (min)
Me (N+W*F6)
Ni film + W*F6

Once transferred into the reaction vessel the sample of WF_5 ^{18}F (0.93 mmol) was allowed to warm up to room temperature and the reaction followed in time by counting alternately the ^{18}F activity ($t_{1/2}$ = 110 min, E = 0.51 MeV) in the two limbs using a well scintillation counter. After one hour of reaction WF_5 ^{18}F was transferred into another counting vessel; its count rate was 146199 count.min^{-1} (all count rates were corrected for background and decay). The count rate of the nickel after reaction was 294 count.min^{-1}, well above that of the background (14 count.min^{-1}), showing that there was a small uptake of WF_5 ^{18}F by the nickel film (Fig. 4.6).

This experiment shows that WF_6 is adsorbed on nickel but no further reaction takes place in absence of an oxide film. WF_6 can oxidise Ni metal but the reaction is not observed in absence of NiO, for kinetic reasons.

Oxidation of Ni by UF_6

A previously flamed out reaction vessel was loaded with nickel metal. After re-evacuation of the flask CH_3CN (5 m) and UF_6 were added by vacuum distillation at 77K. The mixture was allowed to warm up to room temperature, but no reaction took place even after prolonged shaking and with a variety of mole ratios. The reaction was also performed using a vacuum evaporated nickel film. In this case also no reaction took place.

Conclusion

Nickel metal was reacted with UF_6, MoF_6, WF_6 and NO^+. No reaction occurs with UF_6 but nickel is oxidised by NO^+ ion. MoF_6 reacts only with clean nickel film but it is inert in the presence of NiO. WF_6 does, however, react with massive nickel in solution and in the gas phase, but it does not react with clean nickel. Presence of nickel oxide is thus necessary to catalyse the reaction between Ni and WF_6. The results reported in this chapter will be further discussed in Chapter VI.

CHAPTER V

Oxidation of Zinc by MoF_6, WF_6 and NO^+ in Acetonitrile

INTRODUCTION

Zinc metal is generally not regarded as a transition element because it does not form compounds in which the d-electrons are involved. The metal does, however, share some of the properties of the transition elements. Zinc is softer and has a lower melting point than the transition metals; it is also more electropositive. It has the ability to form complexes, in particular, with ammonia, amines, halide ions, and cyanide. The element shows the same behaviour as its neighbours towards the hexafluorides of transition metals, e.g. MoF_6 and WF_6. For this reason, zinc metal was included in this study, in addition to cobalt and nickel, to determine its chemical reactivity towards the hexafluorides of uranium, molybdenum and tungsten, and the nitrosonium ion.

Some general properties of zinc are given in Table (5.1). The element has two s-electrons outside the filled d-shell, and the divalent state is its only known oxidation state. The +1 state is suggested to exist as an intermediate in the reduction of Zn^{2+}, but it is not stable in aqueous solutions.

Zinc forms halides that are mostly ionic. It reacts with oxygen at high temperature, producing the oxide ZnO. Zn^{2+} tends to form stronger bonds with F and O than with Cℓ, P, and S ligands, i.e. it is a class A (or hard) acid.

Previous work has shown that zinc metal reacts rapidly with both MoF_6 and WF_6 in acetonitrile.[3] The salts isolated were formulated, on the basis of their microanalysis and vibrational spectra, as

Table 5-1 Some physical properties of zinc metal

Atomic weight (Mg/ g mol^{-1})	65.37
Crystal structure	Hexagonal close packed.
Atomic radius (A)	1.33
Principal oxidation number	+2
Ionic radii (A)	
Ionization energies (Ei/ev)	9.394 , 17.964
Electron affinity (Ee/ev)	-
Electronegativity	1.6
Density (/kgm^{-3})	7140
Melting point((Tm/K)	692.6
Boiling point (Tb/K)	1180
Specific latent heat offusion fusion (χ/Jkg^{-1})	10 X 10^{+4}
Specific heat capacity (Cp /Jkg^{-1})	385

$[Zn(MeCN)_5][MoF_6]_2$ and $[Zn(MeCN)_6][WF_6]_2$, respectively.

5.2 EXPERIMENTAL

Zinc metal, powder purity 99.99%, was used as supplied (Goodfellow Metals Limited).

Acetonitrile (Rathburn Chemicals Ltd.) was purified as described in Chapter II and was stored in an argon atmosphere glove box (Lintott Engineering).

MoF_6 (Ozark Mahoning), WF_6 (Ozark Mahoning) and UF_6 (British Nuclear Fuels Ltd.) were purified by low temperature trap to trap distillation over activated sodium fluoride. The hexafluorides were stored over activated sodium fluoride in specially designed breakseal flasks to avoid contamination by moisture and oxygen.

$NOPF_6$ (Fluorochem Ltd.) was used as supplied and stored in a dry-atmosphere glove box.

All glassware was carefully flamed out before use, with a gas/oxygen torch. Reactions and preparation of samples for analysis were performed on a conventional high-vacuum system or in the dry box.

5.3 RESULTS

5.3a Oxidation of Zinc by NO^+ in CH_3CN

The oxidation reaction of zinc by the nitrosonium ion is seemingly not reported in the literature. The reaction was performed in this study using zinc metal and $NOPF_6$. The process of the reaction is basically the same as already described in the oxidation reaction of

Table 5-2 : Vibrational spectrum of $(Zn(NCMe)_6)(PF_6)_2$

Frequency (cm^{-1})	Assignement
2325	comb. CH_3CN ($\nu_2+\nu_1$)(A_1)
2300	C≡N stretch (ν_3)(A_1)
1045	CH_3 rock (ν_7)(A_1)
940	C-C stretch (ν_4)(A_1)
850	T_{1u} PF_6
560	T_{1u} PF_6

cobalt metal by NO^+ (Chapter III, section 3.5). The reaction is spontaneous, producing a milky white solution. A white solid was isolated and it is assumed to be solvated Zn(II) present as $[Zn(NCMe)_6]^{2+}$ with PF_6^- as a counter anion. The Raman spectrum of the white solid has not been recorded but its infrared spectrum gives evidence of coordinated acetonitrile and presence of the PF_6^- anion.

A sharp band at ν_{max} = 850 cm^{-1} is assigned to ν_3 frequency of PF_6^- and an intense band at ν_{max} = 560 cm^{-1} is assigned to $\nu_4(PF_6^-)$. A medium band at 405 cm^{-1} is assigned to a C-C≡N bond of coordinated acetonitrile and a sharp band at 940 cm^{-1} is a C-C stretching mode. The C≡N fundamental stretch is indicated by a sharp band at 2300 cm^{-1} and the band at 2325 cm^{-1} is assigned to a C-C stretch and the CH_3 deformation.

5.3b Oxidation of Zn by MoF_6 and WF_6 in CH_3CN

Oxidation of zinc by MoF_6 and WF_6 is reported in the literature. The reaction was performed as follows: A flamed out reaction vessel was loaded with zinc powder. After re-evacuation of the vessel, acetonitrile (5 ml) and MF_6 (M=W,Mo) were added by vacuum distillation at 77K. The solution mixture was warmed up to room temperature. The oxidation of zinc metal by MF_6 (M=Mo,W) was instantaneous, producing a creamy solution. A white solid was isolated in both cases. By reference to previous work these were formulated as $[Zn(NCMe)_5][MoF_6]_2$ and $[Zn(NCMe)_6][WF_6]_2$.

Table 5-3: Vibrational spectrum of $(Zn(NCMe)_6)(WF_6)_2$

Frequency (cm^{-1})		Assignement
Infrared	Raman	
2325		Comb CH_3CN ($\nu_2+\nu_4$) (A_1)
2300		C≡N stretch (ν_3) (A_1)
940	940	C=C stretch (ν_4) (A_1)
600	-	$\nu_3 WF_6^-$
	671	WF_6^-
	700	WF_7^-
705		WF_7^-

Table 5-4 : Vibrational spectrum of solid $(Zn(NCMe)_6)(MoF_6)_2$

Frequency (cm^{-1})	Assignement
2325	Comb CH_3CN ($\nu_2+\nu_1$) (A)
2300	C≡N stretch (ν_3) (A)
940	C–C stretch (ν_4) (A)
630	MoF_6^-

The infrared and Raman spectra of the solids indicated the presence of a band assigned to the ν_3 (MF_6^-) anion (ν_{max} 600 cm^{-1} for WF_6^- and ν_{max} 630 cm^{-1} for MoF_6^- anion). Coordination of acetonitrile is evident from shifts in frequencies of its C≡N stretch and combination bands occurring at 2300 cm^{-1} and 2325 cm^{-1}, respectively. A band at 940 cm^{-1} is assigned to a C-C stretch mode of CH_3CN.

5.3c Oxidation of zinc by UF_6

Uranium hexafluoride did not oxidise zinc metal even when using a large excess of the oxidant (mole ratio Zn:UF_6, 1:10). A yellow colour quickly developed on addition of UF_6 to the mixture of zinc and acetonitrile. The colour turned to green due to reduction of uranium hexafluoride by acetonitrile. This was followed by solvent polymerisation. No compound was produced from this reaction even after prolonged shaking.

5.4 CONCLUSION

Like the metals of the first row transition series (except nickel) zinc is easily oxidised by both molybdenum and tungsten hexafluoride and the nitrosonium ion. However, it does not react with uranium hexafluoride, the stronger oxidising agent of the group. The reaction of zinc with NO^+ and MF_6 (M=W,Mo) occurs at room temperature, producing white solids. These are characterised by their infrared and Raman spectra, which indicate the presence of coordinated acetonitrile and the anion MF_6^- (M=P,W,Mo).

DISCUSSION

The oxidation of metals has been the subject of a considerable number of studies, both theoretical and experimental. These have been in large measure determined by the need to find the best conditions for using metals in oxidizing atmospheres and hence understand one of the most fundamental aspects of the reactivity of metals.

The present work was aimed to study the oxidation reactions of the transition metals, cobalt and nickel, and their reactivity towards the hexafluorides of second and third row transition elements. Previous workers have carried out, in this department, a detailed investigation of the elements, vanadium,[83] iron,[83] copper,[71] silver[71] and gold,[71] with the hexafluorides of molybdenum and tungsten. A full description of the behaviour of the metals, cobalt and nickel, towards WF_6 and MoF_6 in acetonitrile medium is given in Chapters III and IV of this thesis.

Cobalt and massive nickel are oxidized by WF_6 in CH_3CN producing $[Me(CH_3CN)_6][WF_6]_2$ salts (Me=Co,Ni)

$$Me + WF_6 \xrightarrow{CH_3CN} [Me(CH_3CN)_6]^{2+} + 2WF_6^-$$

MoF_6 readily oxidizes cobalt and zinc but it does not oxidize massive nickel, although it is thermodynamically a stronger oxidizing agent than WF_6. Cobalt and nickel are known to be similar metals and there was apparently no reasonable explanation for the unexpected behaviour of MoF_6 and WF_6 towards massive nickel metal. A comparative study of the physical and chemical properties of cobalt and nickel has been undertaken in the hope of determining a reason for this behaviour.

Cobalt and nickel are typical metals with high melting and boiling points, thus large values for their cohesive energies are indicated The crystals of both metals consist of compact structures in which each atom has 12 close neighbours, thus giving comparatively high densities to the metals.[87] The crystal structure of cobalt is either hexagonal close packed (hcp) or face centered cubic (fcc), depending on temperature, while nickel has a face centered cubic crystal structure only.[48] It should be noted that the environment of a surface atom is very different from that of an atom situated in the interior of the crystal.[90] In particular, in the case of an f.c.c. metal, the number of nearest neighbours is reduced from 12 to 9, 8 or 6 for (111), (100) and (110) faces, respectively. For this reason, surface atoms usually show a very considerable reactivity towards foreign atoms or molecules; free orbitals are available for bonding, thus giving to the atoms at the surface bonding capabilities which are not exhibited by atoms in the bulk of the solid. Despite the uniqueness and complexity of the electronic character of the surface, it is often assumed that there is some resemblance in the properties of bulk and surface atoms. This is specially reflected by Pauling's valance bond theory and its definition of the metallic state.[88]

Pauling's valence bond theory is an empirical approach which considers that metal bonds resemble ordinary covalent bonds, where all or most of the outer electrons of the metal atom take part in bond formation. In his concept, Pauling considers that metallic properties are based on the possession of some or all of the atoms in a given metal of a free orbital, "the metallic orbital", in addition to the orbitals required for bonding and non-bonding electrons, permitting in this way uninhibited resonance of valence bonds.

Although the number of electrons in the d-shell increases with increasing atomic number in the series Mn, Fe, Co, and Ni, the bond length of these metals is practically the same and all elements have the same metallic valency of 6. As an explanation to their experimental observations it was suggested that while some 3d-orbitals may hybridise with 4s- and 4p-orbitals to give bonding orbitals, other 3d-orbitals may be unsuitable for bond formation (atomic orbitals). On this basis the following electronic representation is derived for both cobalt and nickel:

Cobalt : nine electrons outside the argon core

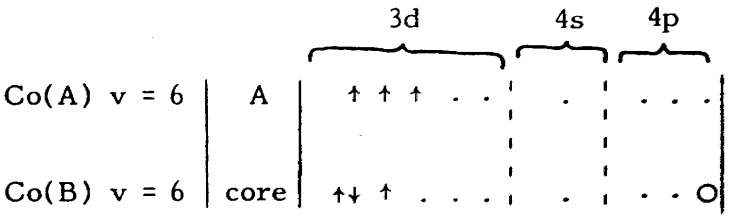

↑↓ ; atomic electrons

. ; valence electrons (electrons occupying bonding orbitals)

O ; metallic orbitals.

The saturation moment of 1.71 magnetons indicates resonance between the two forms of electronic states in the ratio 35:65.

Nickel : ten electrons outside the argon core

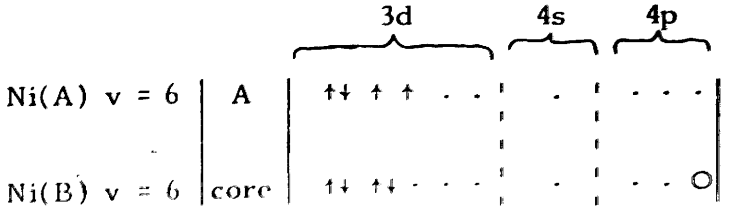

The saturation moment of 0.6 magnetons corresponds to resonance in the ratio 30:70.

Taking into consideration the above determined electronic structure of metals it becomes possible to calculate the "percentage d-character" of the metallic bonds. The percentage d-character is a factor that gives an indication of bond strength. It was calculated for the elements of the first transition series and the following values were obtained.

Element	V	Cr	Mn	Fe	Co	Ni	Cu
Valency	5	6.3	6.4	5.78	6	6	5.5
Percentage d-character	35	39	40.1	39.7	39.5	40.0	36

Nickel has the highest value of percentage d-character and hence a stronger metallic bonding. However the differences within the series of elements Fe, Co and Ni are very small and do not correlate well with the very different behaviour observed towards MoF_6 and WF_6. A further objection to this line of argument is that Pauling's assumption of localized bonding between metal atoms is unrealistic, although conceptually simple. A treatment of the bonding in terms of band theory would be more satisfactory but it is beyond the scope of the present study. However, it is tentatively concluded that the very different behaviour of Co and Ni towards oxidation by hexafluorides is not explicable merely in terms of differences in metallic bonding.

All metals, except gold, are unstable at ordinary temperature, and in the presence of oxygen and become covered with a film of oxide. The covalency between the cation and the anion increases on going to the right of the Periodic Table in the order MnO, FeO, CoO and NiO.[14]

The resistance of a metal to oxidation is usually related to its affinity for oxygen and it depends fundamentally on the properties of the oxide film formed. For example, aluminium, which is a metal with a very high affinity for oxygen, owes its inertness in an oxidizing environment to the remarkable protective qualities of the very thin layer of alumina protecting it from the corrosive atmosphere. Similarly, in the compact form, nickel becomes very stable to air and water, perhaps because it is covered by a layer of oxide. In contrast nickel powder is pyrophoric.[14]

We can suppose that a layer of oxide would constitute a barrier between the metal and the oxidizing agent, and this would explain the inertness shown by MoF_6 towards massive nickel. Taking into account this supposition, a chemically cleaned nickel metal was reacted with MoF_6 in CH_3CN, producing small yields of $[Ni(NCMe)_6][MoF_6]_2$. To improve the reaction, a vacuum evaporated nickel film was prepared, reducing further the concentration of surface impurities and metal oxide to a tolerable level. It was fascinating to see that the assumption made earlier appears to be correct. A noticeable improvement in the reaction was recorded, thus confirming that the relative inertness of MoF_6 towards massive nickel is in major part due to the presence of an oxide layer on the metallic surface.

On the other hand, tungsten hexafluoride, which reacts easily with massive nickel in both solution and gas phase, did not react with a vacuum evaporated nickel film. The reaction occurs easily if the evaporated

nickel film is exposed to air before reacting it with WF_6. A similar reaction was performed using a vacuum evaporated nickel film and monitored by the use of WF_5-^{18}F. This experiment shows that WF_6 is adsorbed on the metallic surface, but the reaction was not observed probably for kinetic reasons.

The results of oxidation of nickel metal with WF_6 and MoF_6 can be interpreted in terms of electron transfer occurring between the oxide layer and the oxidizing agent. In the following, we attempt to understand why the NiO behaves differently from the oxides of other 3d-transition metals.

NiO is isomorphous like CoO and has a sodium chloride lattice. The internuclear distances are, respectively:[90] FeO: 3.03Å; CoO: 3.01Å; NiO: 2.95Å.

The trivalent state of cobalt is extremely unstable in the simple ion and its salts, but in the complexes it is more stable than the divalent state. Approximately equal proportions of Co^{2+}, Co^{3+} and Fe^{2+}, Fe^{3+} are present in their respective metal oxides, but in the nickel oxide layer few Ni^{3+} ions are present relative to the large concentration of Ni^{2+} ions.[89]

The oxides of first-row transition metals can be grouped into two fairly distinct classes: 1) labile oxides which react quickly (within the time of mixing) e.g. cobalt and iron oxides; 2) inert oxides, which react only slowly, e.g. nickel oxide.

The reactivity of the oxides can be closely linked with the electronic configuration of the ion. Cobalt oxide contains both Co^{2+} (d^7) and Co^{3+} (d^6, high spin) ions, and similarly iron oxide contains, in

similar proportions, Fe^{2+} (d^6, high spin) and Fe^{3+} (d^5), which tend to stabilise their electronic configuration. Nickel oxide is predominantly inert Ni^{2+} (d^8), hence an electronic transfer is less likely to occur. Add to this the stronger bonding between the Ni^{2+} and O^{2+} and it then becomes a difficult task for MoF_6 to break the metal framework and react with metallic nickel.

WF_6 is known to be a strong Lewis acid. This is particularly well demonstrated by its fluoride ion transfer reaction to form WF_7^-. WF_6 can then participate in an electron transfer with the nickel oxide forming a Lewis acid-Lewis base adduct, which also acts as a catalyst in the oxidation of metallic nickel. The process of the reaction can be visualised by the following scheme:

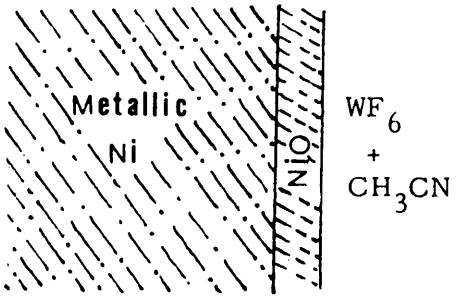

$$NiO + WF_6 \longrightarrow WF_6.O^{2-} + Ni^{2+}$$

$$Ni^{2+} + CH_3CN \longrightarrow [Ni(CH_3CN)_6]^{2+}$$

$$Ni^0_{(solv)} + WF_{6(solv)} \longrightarrow [Ni(CH_3CN)_6]^{2+} + 2WF_6^- \longrightarrow$$

$$\longrightarrow [Ni(CH_3CN)_6][WF_6]_2$$

The process of reaction is different for MoF_6, which does not react with the nickel oxide.

$$NiO + MoF_6 \xrightarrow{CH_3CN} \text{no reaction}$$

The metal being more strongly bonded to the oxygen in the case of nickel, than in the case of iron and cobalt, hence MoF_6 can not break the Ni-O bond which constitutes a barrier between the bulk of the metal and the oxidizing agent. It is, however, thermodynamically strong enough to react with metallic nickel.

$$Ni^0 + MoF_6 \xrightarrow{CH_3CN} [Ni(CH_3CN)_6]^{2+} + 2MoF_6^-$$

CONCLUSION

This work shows that the previously established trend of oxidizing abilities of MoF_6 and WF_6 towards first row transition metals is verified. However, kinetic factors appear to be as important as thermodynamic factors in the conduction of the oxidation process.

REFERENCES

1. F.H. Jardine, Adv. Inorg. Chem. and Radiochem., 1975, 17, 115.
2. L.H. Jones, J. Chem. Phys., 1958, 29, 463; K.L. Chen and R.T. Iwamoto, Inorg. Nucl. Chem. Lett., 1968, 4, 499.
3. A. Prescott, D.W.A. Sharp and J.M. Winfield, J. Chem. Soc., Dalton Trans., 1975, , 936.
4. A.C. Baxter, J.H. Cameron, A. McAuley, F.M. McLaren and J.M. Winfield, J. Fluorine Chem., 1977, 10, 289.
5. J.M. Winfield, J. Fluorine Chem., 1984, 25, 91.
6. R.A. Walton, Quart. Rev. Chem. Soc., 1965, 19, 126.
7. B.M. Storhoff and H.C. Lewis, Coord. Chem. Rev., 1977, 23, 1.
8. J. Reedijk and W.L. Groeneveld, Rec. Rav. Cheim., 1968, 87, 513.
9. T.A. O'Donnell, J. Chem. Soc., 1956, 4681.
10. O. Ruff and A. Heinzlemann, Z. anorg. allgem. Chem., 1911, 72, 63.

11a. H.J. Emeléus and V. Gutmann, J. Chem. Soc., 1949, 2979.

b. H.J. Emeléus and V. Gutmann, J. Chem. Soc., 1950, 2115.

12. J.H. Canterford and R. Colton, "Halides of transition elements", Wiley Interscience, London, 1968.
13. D. Brown, "Halides of the Lanthanides and Actinides", Wiley Interscience Publication, London, 1968.
14. F.A. Cotton and G. Wilkinson, "Advanced Inorganic Chemistry", Fourth Edition, Wiley Interscience, London, 1980.
15. J.H. Levy, J.C. Taylor and A.B. Waugh, J. Fluorine Chem., 1983, 23 (29).

16. I.D. Webb and E.R. Bernstein, J. Am. Chem. Soc., 1978, 100, 483.

17. L.N. Sidorov, A. Ya. Borshehevsky, E.B. Rudny and V.D. Butsky, J. Chem. Phys., 1982, 71, 145.

18. B.P. Mathur, E.W. Rothe and G.P. Reck, J. Chem. Phys., 1977, 67, 377.

19. R.N. Compton, P.W. Reinharott and C.D. Cooper, J. Chem. Phys., 1978, 68, 2023.

20. B.M. George and J.L. Beauchamp, Chem. Phys., 1979, 36, 345.

21. M.K. Murphy and J.L. Beauchamp, J. Am. Chem. Soc., 1977, 99, 4992.

22. J.C. Haartz and D.H. McDaniel, J. Am. Chem. Soc., 1973, 95, 8562; R.N. Compton, J. Chem. Phys., 1977, 66, 4478.

23. J. Burgess and R.D. Peacock, J. Fluorine Chem., 1977, 10, 479.

24. N. Bartlett, Angew. Chem., Int. Ed. Engl., 1968, 7, 433.

25. L.N. Sidorov, E.V. Skokan, M.I. Nikitin and I.D. Sorokin, Internat. J. Mass Spectrum Ion Phys., 1980, 35, 215.

26a. A.T. Pyatenko, A.V. Gusarov and L.N. Ghorokov, Russ. J. Phys. Chem., 1982, 56, 1164.

b. A.T. Pyatenko, A.V. Gusarov and L.N. Ghorokov, Russ. J. Phys. Chem., 1984, 58, 1.

27. N.V. Sidgwick, "The chemical elements and their compounds", Oxford University Press, 1950, Vol. 2, 1034, 1072.

28. G.M. Anderson, J. Iqbal, D.W.A. Sharp, J.M. Winfield, J.H. Cameron and A.G. McLeod, J. Fluorine Chem., 1984, 24, 303.

29. T.A. O'Donnell, D.F. Stewart, Inorg. Chem., 1966, 5, 1434.

30. B.L. Allwood, S.E. Fuller, P.C.Y.K. Ning, A.M.Z. Slawin, J.F. Stoddart and D.J. Williams, J. Chem. Soc., Chem. Commun., 1984, 1356.

31. N. Bartlett and D.H. Lohmann, J. Chem. Soc., 1964, 619.

32. T.A. O'Donnell, D.F. Stewart and P. Wilson, Inorg. Chem., 1966, 5, 1438.

33. B. Frlec and M.H. Hyman, Inorg. Chem., 1967, 6, 2233.

34. G.B. Hargreaves and R.D. Peacock, J. Chem. Soc., 1957, 4212; 1958, 3776.

35. J.A. Berry, A. Prescott, D.W.A. Sharp and J.M. Winfield, J. Fluorine Chem., 1977, 10 247.

36. A. Prescott, D.W.A. Sharp and J.M. Winfield, J. Chem. Soc., Dalton Trans., 1975, 934.

37. D. Nicholls, "Complexes and first row transition elements", The Macmillan Press Ltd., London, 1974.

38. A.B.P. Lever, "Inorganic electronic spectroscopy", Elsevier Science Publishing Company, Oxford, 1984.

39. H.H. Bauer, G.D. Christian and J.E. O'Reilly, "Instrumental Analysis", Allyn and Bacon, Inc., London, 1978.

40. F.A. Cotton, "Chemical applicaitons of group theory", 2nd edition, Wiley Interscience, London, 1970.

41. J. Heinze, Angew. Chem., 1984, 23, 831.

42. T. Sawyer, L. Roberts, "Experimental electrochemistry for chemists", Wiley Interscience, London, 1974.

43. D.R. Crow, Principles and Applications of Electrochemistry", 2nd Edition, Chapman and Hall Ltd., London, 1979.

44. J.R. Geichman, E.A. Smith and P.R. Ogle, Inorg. Chem., 1963, 2, 1012.

45. J. Shamir and J.G. Malm, J. Inorg. Nucl. Chem. Supplement, 1976, 107.

46. S.J. Gregg and K.S.W. Sing, "Adsorption, surface area and porosity", Academic Press, London and New York, 1967.

47. B.G. Linsen, "Physical and Chemical Aspects of Adsorbents and Catalysts", Academic Press, London, 1970.

48. R. Tennent, "Science Data Book", C. Nicholls and Company, Manchester, 1971.

49. L. McGhee and J.M. Winfield, Unpublished work, Glasgow University.

50. J. Donohue, "The structure of the elements", Wiley Interscience, New York, London, 1974.

51. A. Glassner, U.S. Atomic Energy Commission Report ANL.5770.

52. F.D. Rassini et al., "Selected Values of Chemical Thermodynamic Properties", U.S. National Bureau of Standards Circular No. 500, Government Printing Office, Washington, D.C., 1952.

53. H.H. Claassen, J. Chem. Phys., 30, 968 (1959).

54. B. Weinstock, Chem. Eng. News, 42, N28, 86 (1964).

55. J.H. Canterford, R. Colton and T.A. O Donnell, Rev. Pure and Appl. Chem., 1967, 17, 123.

56. M. Stanley Whittingham and A.J. Jacobsen (Ed.). "Intercalation Chem.", Article by N. Bartlett and B. McQuillan, p.19, Academic Press, London, 1982.

57. G.M. Anderson, J.H. Cameron, A.G. Lappin, J.M. Winfield and A. McAuley, Polyhedron, 1982, 1, 467.

58. G.A. Heath, G.T. Hefter, T.W. Boyle, G.D. Desjardins and D.W.A. Sharp, J. Fluorine Chem., 1978, 11, 399.

59. A.M. Bond, I. Irvine and T.A. O'Donnell, Inorg. Chem., 1975, 14, 2408; Inorg. Chem., 1977, 16, 841.

60. J.A. Berry, R.T. Poole, A. Prescott, D.W.A. Sharp and J.M. Winfield, J.C.S. Dalton Trans., 1976, 272.

61. J.S. Griffith, "The Theory of Transition Metal Ions", University Press, Cambridge, 1961.

62. R.L. Carlin, "Transition Metal Chem., 1965, 1, 1.

63. B.J. Hathaway and D.G. Holah, J. Chem. Soc., 1964, 2400.

64. Venlatesarlu, J. Chem. Phys., 1951, 19, 293.

65. W.C. Jones and W.E. Ball, J. Chem. Soc. (A), (1968) 1849.

66. J. Ferguson, D.L. Wood and K. Knox, J. Chem. Phys., 1963, 39, 881.

67. C.J. Jorgensen, Adv. Chem. Phys., 1963, 5, 33.

68. R.A. Palmer and T.S. Piper, Inorg. Chem., 1966, 5, 864.

69. J.A. Berry, Ph.D. Thesis, Glasgow University, 1976.

70. W. Manch, W. Conard Fernelius, J. Chem. Education, 1961, 38, 192.

71. J. Iqbal, Ph.D. Thesis, Glasgow University, 1985.

72. B. Cox, D.W.A. Sharp and A.G. Sharpe, J. Chem. Soc., 1956, 1212.

73. G.B. Hargreaves and R.D. Peacock, J. Chem. Soc., 1958, 2170.

74. N.S. Nikolaev and V.F. Sekhoverkhov, Doklady Akad. Nauk. U.S.S.R., 1961, 136, 621.

75. H.C. Clark and H.J. Emeléus, J. Chem. Soc., 1957, 4778.

76. C.H. Kline, J.R. and J. Turkevitch, J. Chem. Phys., 1944, 12, No.7.

77. N.S. Gill, R.H. Nutall, D.E. Scaife and D.W.A. Sharp, J. Inorg. Nucl. Chem., 1961, 18, 79.

78. V. Imhof and R.S. Drago, Inorg. Chem., 1965, 4, 427.

79. C.K. Jorgensen, Acta Chem. Scand., 1956, 10, 887.

80. C.K. Jorgensen, Acta Chem. Scand., 1955, 9, 1362.

81. A. Bose and R. Chatterjee, Proc. Phys. Soc., 1963, 83, 512.

82. D.W. Meek, R.S. Drago, and T.S. Piper, Inorg. Chem., 1962, 1, 285.

83. J.H. Cameron, Ph.D. Thesis, Glasgow University, 1980.

84. G.W. Ewing, Instrumental Methods of Chemical Analysis, McGraw-Hill Book Company, U.S.A., 1975, 4th edition.

85. C. Joy, W. Fraser, D.W.A. Sharp, G. Webb and J.M. Winfield, J. Chem. Soc., Dalton Trans., 1972, , 2226.

86. A.W. Adamson, "Physical Chemistry of Surfaces", Fourth edition, Wiley Interscience Publications, New York, 1982.

87. N.B. Hannay, "Treatise on Solid State Chemistry", Vol. 1, "The Chemical Structure of Solids", Plenum Press, New York, London, 1973.

88. M.McD. Baker and G.I. Jenkins, Advances in Catalysis, Vol. VII, King's College, London, England, 1955.

89. N.B. Hannay, "Treatise on Solid State Chemistry", Vol. 2, "Defects in Solids", Plenum Press, New York-London, 1973.

90. T.N. Rodhin and G. Ertl, "The nature of the surface chemical bond", North Holland Publishing Co., Amsterdam-New York, Oxford, 1979.